AMINOPHOSPHINE COMPLEXES.

A thesis submitted to the University of Glasgow in fulfilment of the requirements for the degree of

DOCTOR Of PHILOSOPHY

by

MARCUS KWAKU DEH, B.Sc.

Department of Chemistry

University of Glasgow,

GLASGOW.

August, 1977.

ProQuest LLC.
789 East Eisenhower Parkway
P.O. Box 1346
Ann Arbor, MI 48106 – 1346

"IT IS STILL A BEAUTIFUL WORLD".

TO

MY PARENTS AND ALL MY CHEMISTRY TUTORS.

Acknowledgements.

I wish to express my deepest gratitude to my supervisor, Professor D.W.A. Sharp for his interest, patience and encouragement throughout this work.

The author also recognizes the assistance which he has received from many members of staff and research student colleagues.

I also wish to thank Drs. R. Keat and D.S. Rycroft for n.m.r. facilities, Mrs. McConnel of Strathclyde University for far i.r. facilities and Dr. MacSween of Paisley College of Technology for his help.

The financial support received in the form of a Demonstratorship in Chemistry from the University of Glasgow is gratefully acknowledged.

Abreviations.

The following abreviations will be used in this thesis:

w	weak
v	very
s	strong
sh	shoulder
m	medium
b	broad
def.	deformation
Py	Pyridine, 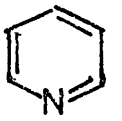
terp	terpyridine 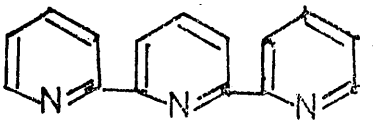
α-pic	α-picoline 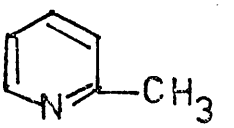
$Py_3P(X)$	tris(2-pyridyl)phosphine (Sulphide)(Oxide) 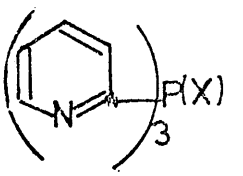
T.BP	trigonal bipyramid
Triarsine	$Me_2As[CH_2]_3AsMe.[CH_2]_3.AsMe_2$

ABSTRACT.

Aminophosphine complexes with the empirical formulae $MX_2P(NMe_2)_3$ (M = Zn, Hg, X = Cl, Br, I; M = Cd, X = Cl), $MX_2 2P(NMe_2)_3$ (M=Hg, X=Cl,Br,I; M = Zn, Cd, X = Cl) and tris(2-pyridyl)phosphine complexes MX_2Py_3P (M = Zn, Hg, X = Cl,Br, I) and $MX_2(Py_3P)_2$ (M=Pt, X=Cl) have been reinvestigated. The mode of co-ordination in the complexes were studied using i.r., Raman and n.m.r. (^1H, ^{31}P, ^{13}C, ^{199}Hg) spectroscopy. The new complexes $HgCl_2PhP(NMe_2)_2$, $PtI_2(Py_3P)_2$ and MX_2Py_3PS (M = Zn, Hg, X=Cl,Br,I) were prepared and studied.

I.r. spectra in the P-N region indicate that the $MX_2P(NMe_2)_3$ and $MX_2 2P(NMe_2)_3$ complexes are co-ordinated through the phosphorus atoms.

Far i.r. spectra (400-40 cm^{-1}) indicate that the $MX_2P(NMe_2)_3$ complexes are dimeric with bridging halogens. The $MX_2 2P(NMe_2)_3$ complexes show one or two metal-halogen stretching frequencies consistent with M(II) ions in pseudo-tetrahedral environments.

Assignments are made for dimeric trans-symmetrical cis-symmetrical and unsymmetrical species in $CDCl_3$ solution of $ZnCl_2P(NMe_2)_3$ on the basis of ^1H, ^{31}P, and ^{13}C n.m.r. spectra.

Variable temperature ^1H n.m.r. studies on $HgX_2 2P(NMe_2)_3$ indicate a fast exchange of phosphorus ligands. The order of the rate of phosphorus ligand exchange is

$$I > Br > Cl$$

$^1H - \{^{199}Hg\}$ INDOR spectrum of $HgCl_2P(NMe_2)_3$ indicate one phosphine ligand bonded to Hg(II). ^{199}Hg decoupling experiments on the ^1H spectrum of $HgCl_2 2P(NMe_2)_3$ indicate two phosphine ligands bonded to Hg(II).

One-bond ^{199}Hg-^{31}P nuclear spin coupling constants for $HgX_2P(NMe_2)_3$ (X=Cl, Br), $HgCl_2 2P(NMe_2)_3$ and $HgCl_2PhP(NMe_2)_2$ are in the range of directly bonded ^{199}Hg-^{31}P couplings.

I.r. Spectra in the regions 1600-1550 and 700-600 cm^{-1} indicate that in the ZnX_2Py_3P and ZnX_2Py_3PS complexes the three pyridyl nitrogen atoms are co-ordinated to Zn(II).

I.r. Spectra in the P⟶S region indicate the presence of Hg-S bonds in the HgX_2Py_3PS complexes. Far i.r. Spectra (400-40 cm^{-1}) indicate that ZnX_2Py_3P and ZnX_2Py_3PS are dimeric with Zn(II) in 6-co-ordinate pseudo-octahedral environments. HgX_2Py_3PS complexes are also dimeric with Hg(II) in pseudo-tetrahedral environments.

A trans-symmetrical structure is proposed for HgX_2Py_3PS and HgX_2Py_3P complexes.

The one bond ^{13}C-^{31}P nuclear spin coupling constants for HgX_2Py_3P complexes in DMSO-d_6 solution increased relative to the free ligand denoting a substantial change in phosphorus hybridization on co-ordination of phosphorus and hence the presence of a Hg-P bond.

Two very strong absorptions at 324 and 300 cm^{-1} for $PtCl_2(Py_3P)_2$ are correlated with Pt-Cl stretches for a cis-Pt(II) halide complex.

$^1J_{(^{195}Pt-^{31}P)}$ for $PtCl_2(Py_3P)_2$ is consistent with the presence of a Pt-P bond.

TABLE OF CONTENTS.

LIST OF TABLES AND FIGURES.

LIST OF TABLES (CONT)

INTRODUCTION

ZINC, CADMIUM AND MERCURY.
HISTORICAL, USES AND TOXICOLOGY.

The use of zinc as an alloy with copper to make brass was known even before the earliest civilization but its importance as a metal became known in Europe at about 1500 A.D.

One of the largest modern uses of zinc is in galvanizing. The low melting point of zinc coupled with its higher position in the electrochemical series relative to iron makes it effective in protecting iron and steel against rust when used as a metal coating[1].

Zinc is an important constituent in the growth of many plants and animals. It is found in a number of metalloproteins and enzymes. However, large amounts cause mallaise, dizziness, vomitting and purging[2]. The low toxicity of zinc is probably due to the fact that it is rapidly eliminated from the body.

Cadmium[3] was discovered in 1817. Its major sources are from zinc ores.

Cadmium is also used as a metal coating from iron and steel against corrosion. Although it is less electropositive than zinc, it has a familiar action.

Cadmium is one of the most toxic of metals. Cadmium depresses growth and reduces protein and fat digestion, causes hypertension and cardiovascular problems. It accumulates in the kidney, liver and reproductive organs[2].

Mercury[4] was one of the first metals known to man. The alchemists took a great interest in it and tried to convert it into silver or gold. Aquinas studied the solutions of metals in mercury and called them amalgams.

The only naturally occurring ore of mercury is the red cinnabar, mercury (II) sulphide, from which practically all the metal is obtained by pyrolysis.

Tremendous interest has been developed in the presence of mercury in the environment, including the biological food chain. Mercury salts are highly toxic. Mercury is retained by the liver, kidney, brain, heart, lungs and muscle tissues. It complexes with - SH groups, thus interfering with enzyme processes[2].

Zinc, cadmium and mercury follow copper, silver and gold in the Periodic Table and have two s electrons outside filled d shells, and therefore are not transition elements in view of what is known of their present chemistry. However, they show similarity to the transition elements in their complex formation with such ligands as amines, cyanides, ammonia, halide ions and phosphines.

Unlike copper, silver and gold in which one or two 'd' electrons can be lost to give ions or complexes in the (II) and (III) oxidation states, zinc, cadmium and mercury have very high third ionization potentials (the energy required, in electron volts, to remove an electron from the filled 'd' orbital) and hence the divalent state is important for these elements. Mercury is unique in this respect in that the univalent state, the mercury (I) ion, Hg_2^{2+}, is also stable in neutral or acidic solutions.

NICKEL PALLADIUM AND PLATINUM. HISTORICAL, USES AND TOXICOLOGY.

The first pure nickel metal was isolated in 1804 by Richter. Nickel occurs naturally in silicate type ores as sulphides and oxides.

Nickel has numerous uses commercially, for example, in situations where corrosion resistance is of major importance such as in stainless steels. Copper-nickel alloys, because of their resistance to corrosion, are used widely especially in marine environments[4].

The importance of nickel in biological systems has recently been documented[2]. It is involved in the structural stability of biological macromolecules. It is also known to cause cancer of the respiratory system[5].

Palladium[4] was first discovered in 1803 by Wollaston who named it palladium after the asteroid Pallas.

Palladium (and platinum) is used in the petroleum industry for the reforming of cracked petroleum fractions thus upgrading the octane rating of gasoline.

Palladium is known[2] to produce acute damage to the liver and kidney cells.

The first report on platinum[4] was by the English physician William Brownrigg in 1750.

Finely divided platinum finds use as a dehydrogenation and hydrogenation catalyst in organic chemistry and in numerous other ways[4].

There are at present no data available as to the toxicity of platinum compounds. However, some platinum compounds are known to be potentially active against cancer[6].

For the transition elements, the energy involved in the removal of successive 'd' electrons is comparable to the extra energy gained in the formation of extra bonds. This fact can be connected with their variable

valency[7].

Nickel displays the oxidation states - 1, 0, +1, +2, +3, +4 but the +2 state is the most common.

The commonest oxidation state for both palladium and platinum is the (II) state while the (Iv) state is stable for both elements.

STEREOCHEMISTRY OF ZINC, CADMIUM AND MERCURY COMPOUNDS.

The stereochemistry of transition metal complexes is determined by ligand field stabilisation energy effects. This is the "splitting" of the 5d orbitals (i.e. d_{xy}, d_{xz}, d_{yz}, $d_{(x^2-y^2)}$ and d_{z^2} of the metal ion in the complex, which were originally of equal energy in the "free" metal ion, into doubly degenerate and triply degenerate energy levels effected by the preferential distribution of the d electrons in the 5d orbitals according to Aufbau, Pauli exclusion principles and Hund's rule such that the orbitals along the axis of the ligands are raised in energy while those directed away from the ligands are lowered in energy relative to the 5d orbital energies in the hypothetical isolated metal ion. The difference in energy, ΔE, between the two sets of energy levels being the ligand field stabilisation energy since such distribution of the d electrons results in minimum repulsion between the d electrons and the electron clouds of the ligands. Because of the complete d shells the stereochemistry of zinc and cadmium compounds is determined only by electrostatic forces, covalent bonding forces and ionic size[8].

Most neutral monodentate ligands can be considered as dipolar. For such ligands, complex formation in solution involves work done against electrostatic forces of repulsion between the ligands to bring them together to co-ordinate, An extra energy term, the lattice energy, arising from the electrostatic interaction between the metal ion and the ligand is involved in order to isolate the complex in the solid state.

Covalent bonding forces may be of two kinds :

(1) interaction between electron pairs in the bonds of the molecule, that is, bond pair-bond pair interactions (this increases with increase in the degree of covalency) and (2) that due to weak interactions between the molecules.

TABLE I

STEREOCHEMISTRY OF SOME ZINC, CADMIUM AND MERCURY COMPOUNDS.

CO-ORDINATION NUMBER	GEOMETRY	EXAMPLE	REF.
2	linear	$Zn(CH_3)_2$	9
2	linear	$Hg(CH_3)_2$	10
4	tetrahedral	$ZnCl_4^{2-}$	11
4	pseudo-tetrahedral	Py_2ZnX_2 X=Cl,Br,I	12
4	tetrahedral	$Zn\ Br_4^{2-}$	13
4	pseudo-tetrahedral	$(Me_4N)HgBr_3$	14
5	Distorted trigonal-pyramidal	[(amine)Zn $(S_2CNMe_2)_2$]	15
5	Distorted trigonal-pyramidal	[(amine)Cd$(S_2$ $CNMe_2)_2$]	15
5	trigonal bipyramidal	$Hg_2NH\ Br_2$	16
6	octahedral	[$Hg(C_5H_5NO)_6$ $(ClO_4)_2$]	17

For size considerations the optimum ratio, radius of central ion: radius of ligand ion, below which the ligands cannot be accommodated, is important. Zinc, cadmium and mercury are large enough to have co-ordination numbers of four, five and six in their complexes. Table 1 shows the preferred co-ordination numbers in some Group IIB metal complexes.

The preferred co-ordination number (the number of nearest neighbours to the given atom irrespective of the bonding between them) of an atom in a compound is determined by several other factors, the most important of which are :

(i) the oxidation state of the metal.

(ii) the nature of the ligand.

(iii) the type of bond (especially if double bonding occurs).

(iv) steric effects.

These factors have been discussed in some depth by Nyholm[7]. One suggestion was that the more polarizable the ligand (ease to distortion of the electron clouds and hence more transfer of negative charge onto the metal ion) the less the co-ordination number. This explains the preferred co-ordination number of six by zinc towards water molecules as in $Zn(H_2O)_6^{2+}$ while for the more polarizable chloride ion, Cl^-, the co-ordination number is four as in $ZnCl_4^{2-}$ ion.

The literature describes two main types of complexes of Lewis base ligands containing Group VB donor atoms with Group IIB metal halides. The MX_2L_2 types have been assigned tetrahedral monomeric stereochemistries while the $(MX_2L)_2$ types the dimeric and halogen-bridged structures[18][19]-[22] although other types have also been described. Most of the investigations on the mode of bonding in these complexes have centred on the use of i.r. spectroscopy and assignments of metal-phosphorus, ν(M-P), metal-halogen, ν(M-X), have been proposed [19]-[23].

Mannet al[18] investigated a large number of cadmium (II) and mercury (II) halide complexes with tertiary phosphines of the type LMX_2 (M=Cd(II), Hg(II), X = Cl, Br, I) and L_2CdX_2, L = Et_3P(AS). The molecular formula of the L_2 $(CdX_2)_2$ were confirmed from molecular weight measurements in organic solvents. Three isomeric forms have been suggested for the compound $(Et_3P)_2$ $(Cd\ Br_2)_2$.

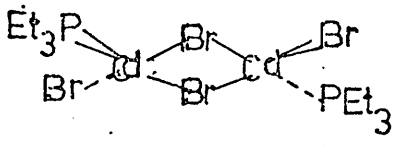

I trans-symmetrical

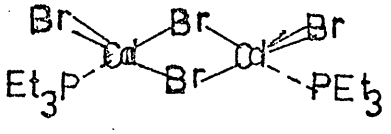

II cis-symmetrical

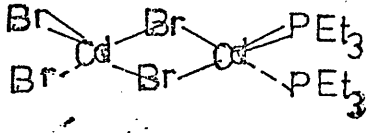

III Unsymmetrical

Crystallographic data of $(CdBr_2)_2$ $(Et_3P)_2$ was interpreted to indicate that it has a centre of ymmetry and therefore has the trans-symmetrical structure (I), also that the cadmium atoms are in tetrahedral environments. In the complexes $(Ph_3P)_2$ HgX_2, the tetrahedral environment of mercury

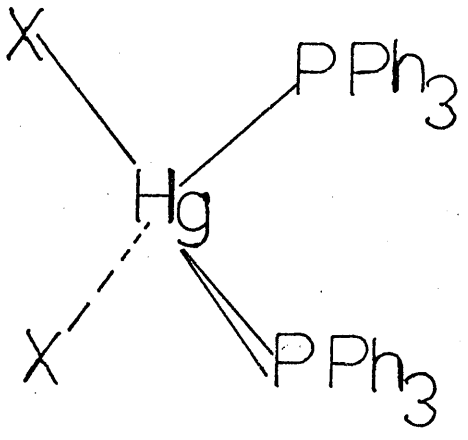

has been assumed by a comparison with the known structure $(Et_3AS)_2\ HgI_2$ [18].

A recent x-ray crystal structural determination [24] of the complexes R_3PHgCl_2 (R = Ph Me, Et) were interpreted to indicate that $Ph_3P\ HgCl_2$ contains discrete chlorine-bridged dimers while Me_3PHgCl_2 contains a zig-zag arrangement of $(Me_3P, HgCl)^+$ cations linked together by chloride anions. Et_3PHgCl_2 has been considered to consist of a chain like arrangement of monomeric Et_3P, $HgCl_2$ units linked together by relatively long intermolecular Hg-Cl interactions. In $Me_3P\ HgCl_2$ and $Et_3P\ HgCl_2$, the mercury atoms are in a five-co-ordinate trigonal bipyramidal environments.

Thus the possible wide variety of stereochemistries that these types of complexes can exhibit depends on the nature of the ligand.

Octahedral polymeric adducts, for example, $CdCl_2\ (NH_3)_2$, $HgBr_2(NH_3)_2$ and $Cd\ Br_2(C_6H_5N)_2$ are also known [25]-[29] as shown below (Fig.1)

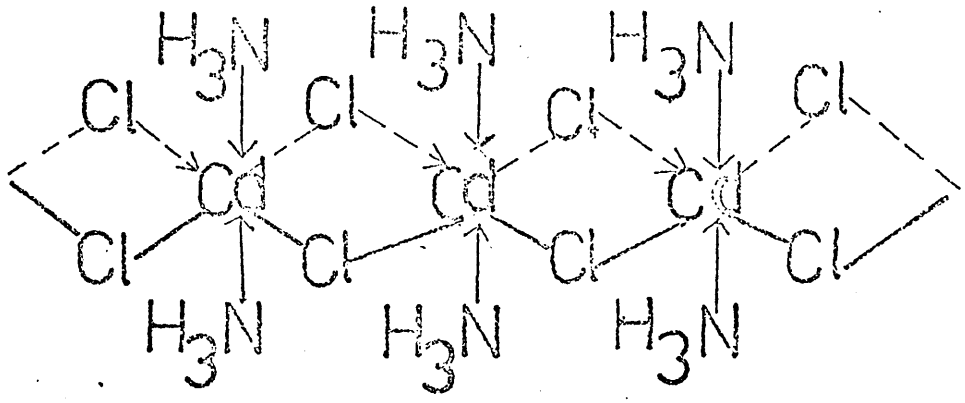

Fig. 1

The tetrahedral environment for cadmium (II) in $(Ph_3P)_2\ CdX_2$ (X=Cl,Br,I) had been suggested on the basis of the known crystal structure of $[Cd\ (NH_3)_4][ReO_4]$[18].

STEREOCHEMISTRY OF NICKEL, PALLADIUM AND PLATINUM COMPOUNDS.

Nickel (II) forms spin-free (containing two unpaired electrons) four-co-ordinate and six co-ordinate octahedral complexes [30]. The octahedral complexes are formed by a large number of electronegative ligands such as water and ammonia. The square-planar four co-ordinate complexes are formed by ligands which can provide large crystal field stabilization energies, and also by ligands which have the ability to form π bonds. The tetrahedral complexes can either be spin-free or spin-paired although the majority of known compounds in the solid state are spin-free irrespective of the ligand field.

The majority of the complexes formed by palladium (II) and platinum (II) are of the square-planar type although in solution solvent molecules may occupy vacant octahedral sites [31]. Table 2 shows a few of the numerous complexes formed by nickel, palladium and platinum.

TABLE 2

OXIDATION STATES AND STEREOCHEMISTRIES OF SOME NICKEL, PALLADIUM AND PLATINUM COMPOUNDS.

OXIDATION STATE	CO-ORDINATION NUMBER	GEOMETRY	EXAMPLE	REF
Ni^{o}	4	Tetrahedral	$(PF_3)_4Ni$	32
Ni^{I} , d^9	4	pseudo-tetrahedral	$Ni(PPh_3)_3X$ (X=Cl,Br,I)	33
Ni^{II} , d^8	4	Square Planar	$NiBr_2P(Et_3)_2$	34
	4	Distorted tetrahedral	$NiBr_2(PPh_3)_2$	35
	5	Square pyramidal	$NiBr_2$Triarsine	36
	6	Octahedral	$[\{Ni(\alpha\text{-pic})_6\}(ClO_4)_2]$	37
Ni^{III} , d^7	5	TBP	$NiBr_3(PMe_2Ph)_2$	38
Pd^{II} , d^8	4	Square Planar	$PdCl_2[(Ph)_2PNC_2H_5P(Ph)_2]$	39
Pt (II) , d^8	4	Square Planar	trans-Py_2PtCl_2	40

DONOR AND ACCEPTOR PROPERTIES OF LIGANDS AND METALS.

Metals have been qualitatively classified[41] into those having Class "A" or "Class B" character. Class A elements (eg Zn^{2+}), form their most stable complexes with ligands in which the co-ordinating atom is a first row element (N,O, F) rather than those of analogous ligands in which the electron donor is a second row element (P,S,Cl). Class B elements form their most stable complexes with P, S and Cl or the subsequent ligand atoms in the family of these elements. The third group of electron acceptor elements (eg Cd^{2+}) have a border line behaviour. Among the most pronounced Class B acceptors are Cu(I), Pd(II), Ag(I), Pt(II) and Hg(II).

Pearson[42] gave an alternative classification of metal ion-ligand interactions. Metal ions which are small often have high charge (hence high charge to radius ratios) and have no valence shell electrons that are easily polarized or removed; such ions are known as "hard acids" (e.g. Li^{+}, Mg^{2+}). These are effective in electrostatic bonding and display class A behaviour. Metal ions which are large, of low charge, or have valence-shell electrons that are easily polarized are "soft acids". The latter form covalent bonds effectively and display Class B behaviour (e.g. Cu^{+}, Ag^{+}, Cd^{2+}, Hg^{2+}, Pd^{2+}, Pt^{2+}, Hg^{+}), while borderline behaviour is shown by the third group (e.g. Zn^{2+}, Ni^{2+}, Cu^{2+}).

Ligands have similarly been classified into those that are "hard" (non-polarizable) and those that are "soft" (polarizable). "Hard bases" have non-polarizable valence shell electrons and are effective in forming electrostatic bonds (e.g. H_2O, Cl^{-}, NH_3). "Soft bases" are effective in forming covalent bonds (e.g. R_2S, R_3P, R_3As), with some borderline cases (e.g. pyridine). The generalisation is that soft acids form most stable complexes with soft bases and hard acids with hard bases. A quantitative interpretation of these qualitative classifications has been given[43] in whic

the authors correlated the magnitude of the donor-acceptor interactions with the electronic properties of the metal ions and ligands.

AMINOPHOSPHINES OR TERTIARY PHOSPHINES AS LIGANDS.

Aminophosphines are phosphorus compounds in which the phosphorus is directly bonded to nitrogen. Much attention is being given to their study in recent years, probably because they serve as potential ligands, and some of their complexes are useful polymerization catalysts[44]. Tris(dimethylamino)phosphine, $P(NMe_2)_3$, is known to impart flame retardant and ion-exchange properties to cotton fabrics[45].

Phosphorus has the outer shell electronic configuration ($3s^2 3p^3$), and from Hund's rule the bonding electrons of phosphorus (III) are represented by $3p_x^1$, $3p_y^1$, $3p_z^1$, then the lone pair is located in the 3s orbital. However, Vilkov[46] and co-workers suggested from electron diffraction studies on tris(dimethylamino)phosphine that the phosphorus atom is Sp^3 hybridised. There is some controversy about the structure of tris(dimethylamino)phosphine[47]. Electron diffraction study[46] on tris(dimethylamino)phosphine was interpreted to indicate that the nitrogen atoms are Sp^2 hybridised. Thus the nitrogen non-bonding lone pair must reside in the $2p_z$ orbital. Therefore in aminophosphines there is the possibility that either nitrogen or phosphorus can function as the donor sites in adducts and complexes. Also there is the possibility of delocalization of the nitrogen lone pair into the 3d orbital of phosphorus to form a $2p(N)\rightarrow 3d(P)_{\pi}$ bond; this could reduce interaction of the nitrogen lone pair with the sigma bond framework since bonding electron pairs and non-bonding electron pairs inter-repel differently, the order of repulsion being given by[48] bonding $\longleftrightarrow$ bonding $<$ bonding $\longleftrightarrow$ non-bonding $<$ non-bonding $\longleftrightarrow$ non-bonding. As an aid to understanding the mode of bonding in aminophosphines structural determinations[46][49][50] and theoretical calculation of geometric parameters have been presented[51].

A recent photoelectron spectrum of tris(dimethylamino)phosphine was

interpreted[52] to indicate that the molecule has a Cs symmetry with two of the nitrogen lone pairs interacting in a sigma manner while the remaining nitrogen lone pair interacts in a π fashion with the phosphorus lone pair.

The geometry and electronic structure of $P(NMe_2)_3$ has been determined[51] by the $CNDO/_2$ method. The result indicates the near planarity of the molecules $P(NMe_2)_3$ (NPN = 118°). This contrasts with the experimentally determined angle of 96.5° in the vapour state by Vilkov[46]. However, Dorschner and Kaufmann[51] criticised this later value on steric grounds as it equals the FPF angle observed in PF_3 (FPF= 96.3°)[50] in which steric effects of the fluorine atoms on the bond angle is expected to be less demanding than steric crowding due to the N-dimethyl groups in $P(NMe_2)_3$

The strength of a base is defined[53] in terms of the protonated base. Thus the base strength is a measure of the bonding between a base and a proton and therefore a measure of the sigma bonding ability of that base. The calculation[51] was used to show that in tris(dimethylamino)phosphine the phosphorus atom is more basic than the nitrogen atoms and will function as the donor centre. The weaker basicity of the nitrogen atoms in tris-(dimethylamino)phosphine relative to the phosphorus atom was rationalised in terms of $2p(N)_\pi \longrightarrow 3d\ (P)_\pi$ bonding. The calculation[51] also indicates that in $XP\ (NMe_2)_3$ (X= O, S, Se) the nitrogen atom remains less basic than the oxygen and sulphur atoms, and the latter function as the donor centres as observed experimentally[54]-[55].

There is some evidence[56][57] that the phosphoryl link, PO, and other similar types of links (eg. P-S, P-Se) do have some pi character. For a large number of X_3PO compounds including $(Et\ O)_3PO$ the average bond length r(P-O), X_3PO, is 1.46 ± 0.03A°, which is much shorter than other types of P-O link for which the average is 1.62 ± 0.05A°[57].

For a tetra co-ordinate phosphorus as in X_3PO with Sp^3 hybridised sigma orbitals, four of the valence electrons are involved in sigma bonding with the ligand orbitals while the fifth odd electron occupies one of the 3d orbitals. The oxygen atom in P - O is Sp^2 hybridised with two lone pairs occupying non-bonding orbitals. A simple valence bond description of bonding in the phosphoryl link is given below (Fig.2).

Fig.2. Valence Bond Description of PO link (57)

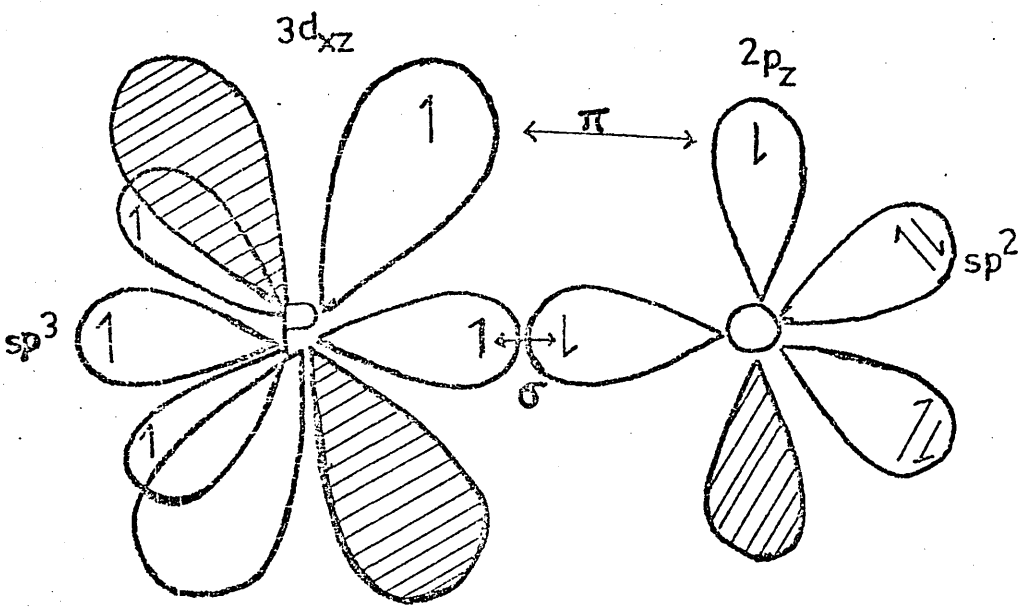

It has been suggested (57) that of the five 3d orbitals, the $3d_{xz}$ has the minimum interaction of the sigma bond frame work and is the one

which is involved in the $2P_{\pi} \longrightarrow 3d_{\pi}$ bonding.

In the $XP(NMe_2)_3$ series[51] the involvement of the phosphorus 3d orbitals in the P-X bonds (X = O, S, Se) effects a negligible $p(N)_{\pi} \longrightarrow d(P)_{\pi}$ electron transfer.

Studies on other aminophosphines also suggested that the P-N bond has a pi component[58][59]. An x-ray diffraction study[49] shows that the bicyclic aminophosphine OP (NMe $CH_2)_3$CMe has the structure

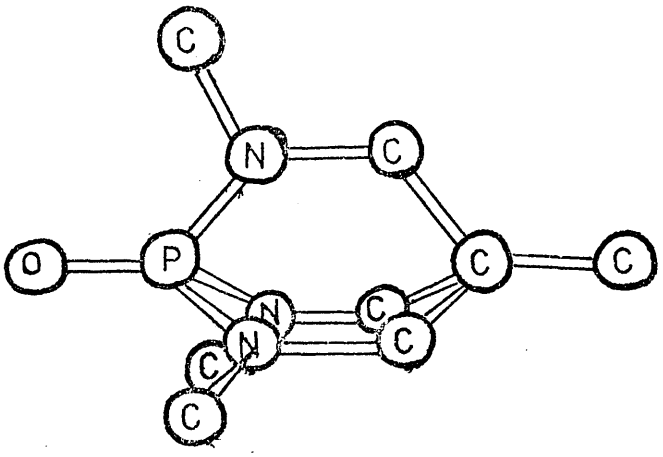

and that the nitrogen atoms are near planar. This has been attributed partly to a donor $2p(N) \longrightarrow 3d(P)$ pi bonding and partly to the steric interactions of the nitrogen methyl groups with the methylene hydrogens. The P-N bond length of 1.558A° in OP (NMe $CH_2)_3$ CMe is very short compared with the single P-N bond length of 1.77A°[50] in

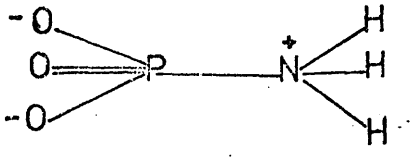

an indication of a pi component in the P-N bond.

The solid state structure of PF_2 (NMe_2)[50] has the planar framework

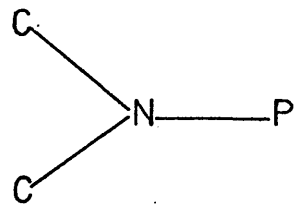

The environment about the nitrogen atom would be pyramidal if the lone pairs were exerting their full stereochemical influence. The presence of 2p(N)⟶ 3d(P) pi bonding in PF_2NMe_2 is further indicated by the fact that the P-N bond length, r (P-N) = 1.628A°, is very short compared to the single bond length of 1.77A° quoted above.

The use of n.m.r., i.r. and hydrolytic data showed that in the chloramination and alkylation of many nitrogen-phosphorus compounds, the point of attack is always the phosphorus rather than the nitrogen atoms[61].

It has also been shown from structural studies that $P_\pi \longrightarrow d_\pi$ bonding is greater between first and second row elements than between two second row elements. For example nitrogen has a planar environment in H_2NPF_2[62] but the H_2PP fragment is not planar in H_2PPF_2[63]. Also while the heavy atoms in trisilylamine, $(SiH_3)_3N$, are planar those in trisilylphosphine are not[64].

The delocalization of the nitrogen lone pair in $P_\pi \longrightarrow d_\pi$ bonding has been invoked to account for the lower basicity than expected in trisilylamine[65].

Relatively little work has been done on the co-ordination chemistry of aminophosphines with Zinc (II), cadmium (II) and mercury (II) halides

and with nickel (II), palladium (II) and platinum halides although numerous transition metal carbonyl complexes have been described [66]-[70].

X-ray crystal structure of the boron adduct, $(CH_3)_2NPF_2B_4H_8$ [71] indicates that the phosphorus, nitrogen and the two carbon atoms are essentially coplanar but there is a considerable shortening of P-N, $r(P-N) = 1.593A^o$ and P-F, $r(P-F) = 1.594A^o$ bond lengths compared to the free ligand values of $r(P-N) = 1.628A^o$ and $r(P-F) = 1.610A^o$ respectively.

An increase in the FPF angle is observed in the adduct, $\widehat{FPF} = 96.5(3)^o$ compared to the free ligand value, $\widehat{FPF} = 91.5(3)^o$.

Clemens, Sisler and Brey[72] studied the reaction of $(CH_3)_2$ NP $(CH_3)_2$ with Al $(C_2H_5)_3$. They reported that a phosphorus-aluminium bond was formed when the reagents were directly combined but that the structure changed to give nitrogen-aluminium bond when the adduct was heated.

Co-ordination through the phosphorus atom in $P(NMe_2)_3$ with the boron hydrides BH_3, $B(H)(CH_2CH_3)_2$ has been observed experimentally. ^{11}B, ^1H and ^{31}P n.m.r. studies indicate phosphorus-boron bonding[73][74]. However, BCl_3, BF_3[75] and PCl_3[76] attack the nitrogen atom and dissociate the P-N bond:

$$P(NMe_2)_3 \xrightarrow{BX_3 (X=F,\ Cl)} Me_2NBX_2 + PX_3$$

Parry and Schultz [77] described 1:1 adduct of $P(NMe_2)_3$ with $AlCl_3$. The adduct $AlCl_3P(NMe_2)_3$ has been shown to be dimeric in methylene chloride solution with the initial structure

$$\left[(Me_2N)_3\ P - P\ (N\ Me_2\ )_2 \right]^+ \left[NR_2(AlCl_3)_2 \right]^-$$

Noth and Vetter[78] studied the complexes $CdI_2P(NMe_2)_3$, $CdI_22P(NMe_2)_3$ $HgI_2P(NMe_2)_3$ and $HgI_22P(NMe_2)_3$. From molecular weight studies and by

comparison with x-ray crystal structure of other dimeric phosphine complexes of cadmium (II) and mercury (II) reported by Mann et al[18] they suggested that (1) $CdI_2P(NMe_2)_3$ exists in solution as undissociated binuclear complex

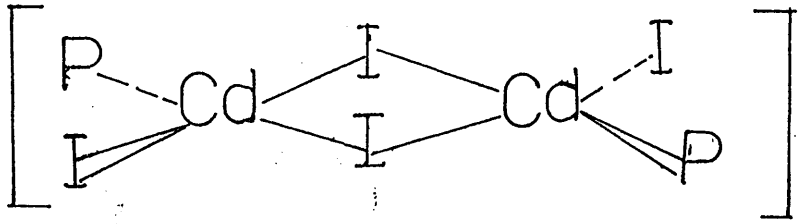

(2) Co-ordination is through the phosphorus atom. Some of the other reported aminophosphine complexes are shown in Table 3 below.

TABLE 3

Aminophosphine complexes with some Metal Halides.

Compound	Suggested mode of bonding	Method of Investigation	Ref
trans-$PtCl_2 2P(NMe_2)_3$	P	n.m.r.	79
trans-$PtI_2 2P(NMe_2)_3$	P	i.r.	66
trans-$PdCl_2 2P(NMe_2)_3$	P	i.r.	66
trans-$PdI_2 2P(NMe_2)_3$	P	i.r.	66
$ZnCl_2Et_2NP(Ph)_2$	P or N	Conductivity	80
$CdCl_2Et_2NP(Ph)_2$	P or N	Conductivity	80
$PhP(NR_2)_2HgI_2$ (R=Me, Et, Pr)	P	Ref 18	59

Cruickshank[81] studied zinc (II) cadmium (II) and mercury (II) halide complexes with $P(NMe_2)_3$. He formulated them as 1 : 1 dimeric and 1 : 2 monomeric complexes on the basis of molecular weight measurements which were close to dimeric and monomeric values respectively. The experimentally observed molecular weights are shown in Table 4 below :

TABLE 4

Molecular Weight Data for Some Aminophosphine Complexes[81]

Compound	Solvent	Molecular Weights Observed	Calculated
$[ZnCl_2P(NMe_2)_3]_2$	C_6H_6	629	600
$[ZnBr_2P(NMe_2)_3]_2$	C_6H_6	809	777
$[ZnI_2P(NMe_2)_3]_2$	C_6H_6	997	965
$[HgCl_2P(NMe_2)_3]_2$	$CHCl_3$	837	869
$[HgBr_2P(NMe_2)_3]_2$	$CHCl_3$	1068	1048
$[HgI_2P(NMe_2)_3]_2$	$CHCl_3$	1267	1235
$HgCl_2 2P(NMe_2)_3$	Cryoscopic	579	598
$HgBr_2 2P(NMe_2)_3$	Cryoscopic	653	687
$HgI_2 2P(NMe_2)_3$	Cryoscopic	704	781
$ZnCl_2 2P(NMe_2)_3$	Cryoscopic	536	463
$CdCl_2 2P(NMe_2)_3$	Cryoscopic	576	510

I.r. and n.m.r. evidence were used to deduce that co-ordination was through the phosphorus atom in these complexes. The 1 : 1 and 1 : 2 complexes were also suggested to be dimeric with bridging halogens and monomeric with C_{2v} symmetry for the MP_2X_2 skeleton respectively from far i.r. spectra[81].

Low molar conductivities, Λ_M, (Λ_M = 0.7 ohm^{-1} $mole^{-1}$ cm^{-2}) were obtained[81] for the 1 : 1 complexes of $P(NMe_2)_3$ with zinc (II) and cadmium (II) halides in benzene solutions and for 1 : 1 mercury (II) halides in

chloroform solutions (Λ_M=0.2 ohm^{-1} $mole^{-1}$ cm^{-2}). These results were interpreted[81] to indicate the existence of binuclear undissociated complexes in solution.

In conclusion, present evidence seems to suggest that the P-N bond in aminophosphines has a pi component, and that P ⟶ d pi bonding between filled 2P orbital of nitrogen and the empty 3d orbital of phosphorus gives the phosphorus atom a greater electron density than the nitrogen atom and makes it a stronger electron donor relative to the nitrogen atom.

However, the possibility of bonding through nitrogen cannot be ruled out.

Complexes with tris(2-pyridyl)phospine and tris-(2 pyridyl)phospine sulphide.

With relevance to the present work, the known complexes of tris (2-pyridyl)phosphine and other pyridyl derivatives are shown in Table 5 below.

TABLE 5

Some complexes of tris(2-pyridyl)phosphine and Derivatives.

Compound	Suggested bonded atom	Method of investigation	Ref
ZnX_2 ()$_3$ P (X=Cl,Br, I)	tri-dentate through N	i.r.	81
HgX_2 ()$_3$ P (X=Cl, Br,I)	P	i.r.	81
$PtCl_2$2 ()$_3$ P	P	i.r.	81
$PdCl_2$2 ()$_3$ P	P	i.r.	81
Zn()$_3$ P $(ClO_4)_2$	tri-dentate	polarography	82
Zn()$_3$ P $(NO_3)_2$	through	polarography	
	N	polarography	82
NiX_2 ()CH(P Ph_2)$_2$ X= Cl,Br,I	N	i.r.	83
Ni2()$_3$N $(ClO_4)_2$	tri-dentate through pyridyl nitrogens	x-ray powder difraction; solid state and solution i.r.	84

The HgX_2 ()$_3$ P complexes were assigned dimeric halogen-bridged structures on the basis of i.r. spectra.

Low molar conductivities,

Λ_M, (Λ_M = 10 - 16 ohm^{-1} mole^{-1} cm^{-2})

were obtained[81] for the HgX_2 ()$_3$P complexes in dimethyl-formamide (DMF) solutions (10^{-3}M). These results were interpreted to indicate the existence of molecular complexes in solution by comparison with literature values for ionic pyridylamine complexes in similar solvents (10^{-3}M) as shown in the Table below -

Solvent	Range of Values, Λ_M	electrolyte
Me No_2	105[85]	A^{2+} B^{2-}
Me No_2	144 - 210 [85][84][86]	C^{2+} $2X^-$
DMF	60-99[87]	A^{2+} B^{2-}
DMF	142 - 180 [87][84][86]	C^{2+} $2X^-$
Me No_2	75-95[88]	D^+ E^-

The ZnX_2 ()$_3$P complexes were assigned the ionic structures

$$\left[M\ 2\ (\ \text{  }\ )_3\ P \right]^{2+} \quad \left[\ MX_4\ \right]^{2-}$$

on the basis of

(i) Conductivity measurements in nitromethane solution (10^{-3}M, Λ_M = 94-108 ohm^{-1} mole^{-1} cm^{-1}).

(ii) the possibility of existence of the $(MX_4)^{2-}$ ions were also suggested from metal-halogen stretching frequencies in the far i.r. spectra.

No complexes of tris(2-pyridyl)phosphine sulphide have been described in the literature; however complexes of triphenylphosphine sulphide

(Selenide) are known. The crystal structure of $HgCl_2Ph_3PSe$[89] was interpreted to indicate that it consists of discrete chlorine-bridged molecules (I) with the mercury atoms in a distorted tetrahedral configuration, with the bonding through the selenium atom.

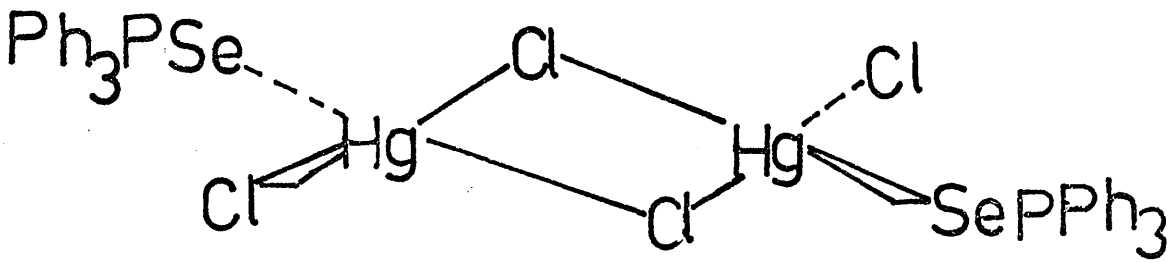

(I)

CHAPTER ONE

EXPERIMENTAL TECHNIQUES

EXPERIMENTAL TECHNIQUES.

Introduction.

In the present study extensive use has been made of nuclear magnetic resonance (n.m.r.) infrared (i.r.) and Raman spectroscopy. These and other relevant aspects of the experimental techniques will be briefly discussed.

Nuclear Magnetic Resonance.(90)

Isotopes of elements with either odd atomic number (odd number of protons in the nucleus) or odd mass number (odd total number of protons and neutrons) for example ^{1}H, ^{19}F, ^{31}P have a magnetic moment μ.

An isolated nucleus with a magnetic moment μ placed in a static magnetic field Bo has 2I + 1 orientations of the Spin I in the field direction and Bo is considered to be along the z-axis of the laboratory co-ordinate system. Since the nuclear magnet also possesses an angular momentum it precesses about Bo with angular velocity, ν, given by

$$\nu = \frac{\gamma B_0}{2\pi}$$

where $\gamma = \frac{\mu}{I\hbar}$ is the magnetogyric ratio of the nucleus, $\hbar = \frac{h}{2\pi}$ where h is Planck's constant.

For a nucleus with $m_I = \pm 1/2$, there are two orientations in the field directions corresponding to

(a) alignment against the field ($m_I = +1/2$), i.e. the higher energy situation

(b) alignment with the field ($m_I = -1/2$) the lower energy situation

The difference in energy between the two energy levels is given by

$$\triangle E = h\nu$$

Before the sample containing the nuclei, for example protons, is irradiated in a magnetic field, the protons will have populated the two states of slightly different energy according to a Boltzmann distribution and there will be a slight excess of nuclei in the lower energy level. If an alternating electromagnetic radiation is applied to the sample along

the x-axis, an energy, $\triangle E$, will be absorbed by the nuclei if the frequency of the irradiation is the same as the Larmor precession frequency of the nucleus and this leads to the promotion of nuclei from the lower to the higher energy level. This is the nuclear magnetic resonance effect.

In order that absorption of energy by nuclei should continue in a nuclear magnetic resonance experiment, there must always be an excess of nuclei in the ground state. This excess is maintained by the release of energy, $\triangle E$, to the environment by the nuclei in the excited state. This transfer of energy from the spin system to the environment (termed the lattice) is called spin-lattice relaxation. The life time of the excited state is measured by the spin-lattice relaxation time T_1.

The method just described where a very weak radiofrequency is applied continuously to the sample and the energy absorbed is measured as a function of field/frequency is called the continuous wave method, the resonance condition can be achieved by either varying the frequency and maintaining the field constant (frequency sweep) or by varying the field and maintaining the frequency constant (field sweep). The spectrum thus obtained is a function of frequency. In these procedures, we excite the resonance position of only one nucleus at a time.

^1H n.m.r. for all complexes were recorded as saturated solutions in $CDCl_3$ using 5 ml n.m.r. tubes on a Jeol C-60-HL n.m.r. instrument at 60 MHz operating frequency and a field strength of 14 Kilogauss.

In the case of $ZnBr_2P(NMe_2)_3$ and $ZnCl_2P(NMe_2)_3$ where poor resolution made assignments difficult an additional 220 MHz spectrum was recorded by PMC U., Harwell.

^{31}P n.m.r. were recorded either on a Varian XL - 100 instrument operating on a field strength of 23, 490 gauss at 40.5 MHz operating frequency or on a Jeol C-60-HL instrument.

Variable temperature ^{1}H n.m.r. were run on a Varian HA-100 instrument. The mercury-199 internuclear double resonance (INDOR) spectrum was recorded on a Jeol C-60-HL instrument fitted with a frequency synthesizer Schomandl ND 100M and amplifier JNM-SD-NC[91].

Chemical Shifts[92]

The field at which bare nucleus absorbs electromagnetic radiation is changed when electrons surround the nucleus. An applied magnetic field induces the electrons to circulate and the magnetic field, B_1, thus produced opposes the applied magnetic field at the nucleus. Thus for the resonance condition for an isolated nucleus

$$\nu = \frac{\gamma}{2\pi} B_o$$

to operate for a nucleus in a bond, a greater field, $(Bo + B_1)$, must be applied. The nucleus is then said to be shielded by the electrons. As chemically different nuclei of the same element in molecules are in electronically different environments, they are shielded differentially and hence absorb electromagnetic radiation at different regions of the spectrum at constant applied magnetic fields. It is this feature that makes n.m.r. spectroscopy invaluable to chemists for structural determination. For comparative purposes the chemical shift is often given by a field independent parameter, δ, in parts per million, (ppm), where

$$-\delta = \frac{H_s - H_r}{H_r} \times 10^6$$

and H_s and H_r are the magnetic fields at which the sample and reference compounds give n.m.r. signals.

The ^{31}p chemical shifts for the three doublets of $ZnX_2P(NMe_2)_3$ (X=Cl, Br,I) were determined on XL-100 instrument by the double resonance method[93].

The range of chemical shifts will be discussed under the n.m.r. of the respective nuclei.

Convention for Chemical Shifts.

Chemical shifts in this work are given as positive downfield of the following reference compounds :

^{1}H : TMS ($(CH_3)_4Si$)

^{13}C : TMS

^{31}P : H_3PO_4 (85%)

^{199}Hg : $(CH_3)_2Hg$

The Nuclear Spin-Spin Coupling Constant[94]

This is exemplified by the electron mediated interaction between two directly bonded nuclei as in ^{13}C - ^{1}H coupling. The interaction of the proton nuclear moment with the electron spin in such that an antiparallel alignment of the nuclear and electron spins is effected (diagram below)

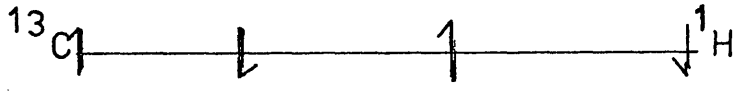

The antiparallel alignment of the other electron in the ^{13}C - ^{1}H bond is governed by the Pauli exclusion principle. The interaction of the latter electron with the ^{13}C nucleus again produces an antiparallel orientation. Thus the coupling constant is a measure of the ability of the spin orientation of one nucleus to affect (via the electrons in the bond) the energy of another nucleus, and so produces a splitting in the spectrum of that nucleus. If for antiparallel orientation of spins the energy of the system is minimum, then the coupling constant is defined to be positive. The model just described predicts that all one bond couplings will be positive; this however is found experimentally not to be correct and more complex theories have been developed to accommodate this fact.

The range and magnitude of coupling constants will be discussed under the n.m.r. spectra of the respective complexes.

^{199}Hg - ^{31}P coupling constants were determined from the ^{1}H spectrum by the double resonance method[93].

Fourier Transform Spectroscopy[95]

In a magnetic resonance experiment the sensitivity of a nucleus is measured in terms of the strength of the signals. This depends upon the relative number of upward and downward transitions between the two almost equally populated energy levels. From the resonance condition

$$\nu = \frac{\gamma}{2\pi} B_0 \qquad \left(\gamma = \frac{\mu}{I\hbar}\right)$$

nuclei with low magnetic moments (e.g. ^{13}C, μ = 0.79 Bohr magnetons) and hence low values of consequently have small values of $\Delta\bar{c}$. Such nuclei have the population difference of nuclei in the two energy levels even smaller than for nuclei with higher values of μ(e.g. ^{1}H, μ = 2.79 Bohr magnetons) at the same field strength Bo. Coupl ed with the low μ value, ^{13}C has low natural abundance (1.1% compared with 100% for ^{1}H) thus increasing the difficulty of detection by a factor of hundred.

One method of enhancing the sensitivity is to use super-conducting magnets[96] which give very strong magnetic field strengths. The sensitivity can also be increased by the method of time averaging[97] and by the use of pulsed Fourier transform methods.

The advantage of pulsed Fourier transform n.m.r. over continuous wave n.m.r. is that in the former information about the resonance position of all the nuclei of one type in the sample is obtained simultaneously while in the latter this information is obtained one at a time.

^{13}C n.m.r. spectra of $P(NMe_2)_3$ complexes were run as saturated solutions in $CDCl_3$ at room temperature (ca 298°K) with TMS at Oppm on a Varian XL-100 pulsed Fourier transform instrument with complete proton decoupling. The operating frequency is 25.2 MHz.

Infrared and Raman Spectroscopy.

There are great advantages in applying both infrared and Raman techniques to the same compound. In particular, for compounds with a centre of symmetry the vibrational frequencies can be completely assigned if both techniques are used. Most metal-ligand stretching vibrations occur below 600 cm^{-1} and can be found in the far infrared region. Raman spectroscopy is also ideally suited for studying such vibrations since it can be extended as low as 10 cm^{-1} the limit being 0 cm^{-1} which is the frequency of the exciting line. Raman spectroscopy offers additional advantage over infrared as water is an excellent solvent because its polarizability changes little during vibration. Consequently the Raman scattering is very weak.

Raman Spectroscopy[98]

The Raman effect is essentially a scattering phenomenon; the frequency of the scattered light is analysed. In a normal Raman spectrum the exciting frequency is such that it is not strongly absorbed by the sample. When the radiation is absorbed by the sample it is called fluorescence. When it is scattered by the molecules of the sample it is called Rayleigh scattering. Raman (1928) discovered that the scattered radiation has either the same frequency, ν_0, as the incident radiation (Rayleigh scattering) or different frequencies (Raman scattering). When the high energy protons of the monochromatic radiation interact with the molecules of the sample, they are raised to a highly energetic unstable state. The Rayleigh scattering is due to those molecules which return to the ground state by emitting the same energy ν_0 as the incident radiation. Some of the molecules come to rest at a vibration level, ν_x by emitting energy of lower frequency, $\nu_0 - \Delta\nu$ called a Stokes line; a few molecules initially in a higher vibrational state emit energy at a higher frequency, $\nu_0 + \Delta\nu$ (anti-Stokes lines) by returning to the ground state. The anti-Stokes lines

are weak at room temperature and are not normally observed (Fig.3)

Fig 3.

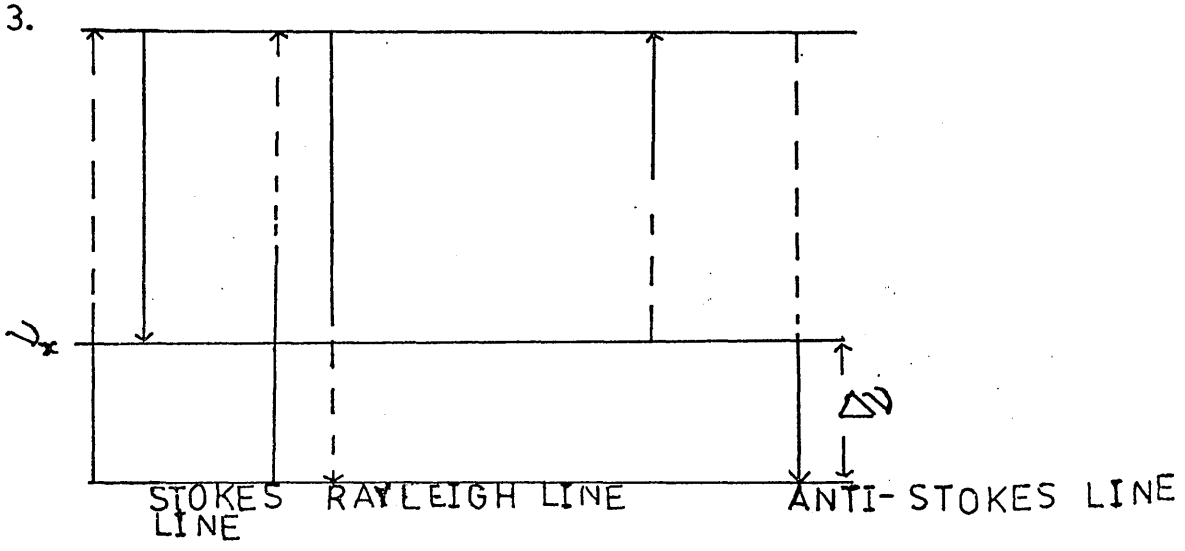

The Raman frequency shift, ($\Delta\nu$), is the difference in frequency between the incident radiation (Rayleigh line) and the Raman scattered radiation. These displacements correspond to the frequencies of vibration of the molecule.

The electric field of the electromagnetic radiation induces an oscillating dipole moment μ in the molecule which is proportional to the polarizability α (ease of electron cloud movement in an electric field) of the molecule, that is

$$\mu = \alpha E$$

where E is the electric field.

Therefore for a molecule to absorb energy and to show a Raman effect, there must be a change in the polarizability of the molecule while for infrared activity, the dipole moment must change. For centro-symmetric molecules a vibration which is active in the Raman is inactive in the infrared and vice versa.

In addition the polarization of the emitted light can be measured by analyser and designated as polarized or depolarized. For symmetric

vibrations of the molecule the light is polarized and for asymmetric vibrations it is depolarised.

For Raman active transitions, the selection rules are that the vibrational quantum number, ν, of a mode must change by $\Delta\nu = \pm 1$ and the rotational quantum number, J, must change by $\Delta J = 0, \pm 2$ where the zero corresponds to the Rayleigh scattering and the ± 2 corresponds to the Raman transitions.

Raman spectra were run either as liquids or polycrystalline solids in sealed cylindrical Raman tubes on a Spex Ramalog 4 instrument fitted with Coherent radiation 52G ion lasers (Kr^+ and Ar^+).

Infrared Spectroscopy[99]

Infrared spectra can be divided into three regions: the near infrared (12000-4000 cm^{-1}), the mid-infrared (4000-200 cm^{-1}) and the far infrared (200-10 cm^{-1}) and the latter is concerned mainly with the pure rotation spectra of molecules.

The concept of "group frequencies" is one of the most powerful tools used in the determination of molecular structure by vibrational spectroscopy. In many molecules vibrations tend to affect mainly one bond or a set of like bonds (i.e. a group) with the rest of the molecule moving only marginally in order to preserve the centre of gravity of the molecule. The vibrations can be resolved into a set of independent motions called normal modes. For a molecule possessing N atoms each of the N atoms can be described in terms of three cartesian co-ordinates. The total number of degrees of freedom is therefore 3N. For a non-linear molecule, the total number of normal vibrations is 3 N-6 and 3 N-5 for a linear molecule. The degeneracy, symmetry and spectral activity of the normal modes can be deduced by mathematical group theory. Thus the vibrations in the molecule which give

rise to each spectral band can be assigned. The group frequencies can also be identified by correlation of the observed absorption bands with published infrared spectra of similar classes of compounds. The probability of infrared transition between two energy levels is given by

$$\mu_{nm} = \int \psi_n^* \mu \psi_m \, d\tau$$

where ψ_m, ψ_n are the upper and lower vibrational wave functions and μ is the electric dipole moment. If the molecule has a permanent dipole moment then the bond length will change as the molecule vibrates. Consequently μ will change.

Infrared spectra 4000-200 cm^{-1} were run as Nujol and fluorolube or hexachlorobutadiene mulls on a Perkin Elmer SP 225 infrared grating spectrophotometer.

Far infrared spectra were measured as polythene discs using a Fourier transform interferometer FS - 720 fitted with a recording wave analyser and a Fourier transform computer FTC - 100/7.

CHEMICALS.

Dry Solvents.

Petroleum ether (40-60°), chloroform (analytical grade), anhydrous diethyl ether, Tetrahydrofuran, Benzene, ethanol, were all purified and dried by published methods[100]. Anhydrous dimethylamine and phenyl dichlorophosphine were obtained commercially.

Anhydrous Metal halides.

Anhydrous zinc chloride and anhydrous zinc iodide were obtained commercially from organic/inorganic Chemical Corporation, California, U.S.A.

Anhydrous cadmium chloride was obtained[101] by treating the commercial grade $CdCl_2\ 2H_2O$ with thionyl chloride which had been freshly purified by distillation with triphenylphosphite and dried over potassium hydroxide pellets in a Vacuum desiccator for 12 hours.

Anhydrous zinc bromide was obtained by heating the commercial grade zinc bromide at 150° under Vacuum.

Mercury (II) chloride, mercury (II) bromide and mercury (II) iodide were all of analytical grade quality.

Platinum (II) chloride was obtained from Johnson Mathey Chemicals, London.

Copper (I) chloride was prepared by the method of Keller and Wycoff[102].

The analytical data for the anhydrous metal halides prepared are as follows:

$ZnBr_2$ (Found,%Br; = 70.7, calc 70.9;); $CdCl_2$ (Found Cl; 38.3, calc, 38.7); Cu(1)Cl (Found, Cl; 35.8, calc. 35.9).

Platinum iodide Monohydrate, PtI_2H_2O

This was prepared by the method of Watt and Cude[103].

Preparation of tris(dimethylamino)phosphine.[104]

A petroleum ether solution of phosphorus trichloride (50.4 ml, 0.57 mole) was added dropwise to anhydrous dimethylamine (250 ml, 3.8 moles) dissolved in petroleum ether (bp 40-60°) at -73°.

$$PCl_3 + 6Me_2NH \longrightarrow (Me_2N)_3P + 3Me_2\overset{+}{N}H_2Cl^-$$

The reaction mixture was stirred mechanically during the addition and then overnight under nitrogen, washed with dry petroleum ether and the washings added to the filtrate the petroleum ether was removed in a rotary evaporator to yield a pale straw coloured product which on vacuum distillation yielded a colourless liquid (bp 28° / 0.3mm). Yield ca. 30 gm (38%) based on phosphorus trichloride. Because of the hygroscopic nature of the product precautions against moisture were taken during the preparation. The criteria for purity will be discussed under i.r. and n.m.r. spectra of the product.

Bis(dimethylamino)phenyl phosphine.

This was prepared by the method of Ewart et al [59] from anhydrous dimethylamine and phenyldichlorophosphine. The latter was purified by Vacuum distillation before use. The purity will be discussed under the i.r. and n.m.r. spectra of the product.

Preparation of Aminophosphine Complexes.

The compounds were prepared[81] following similar procedures of handling reactants and solvents in a Lintott dry atmosphere box filled with dry nitrogen.

$HgX_2\ P(NMe_2)_3$ and $HgX_2\ 2P(NMe_2)_3$ (X=Cl, Br, I)

For example, tris(dimethylamino)phosphine (1.625 gm, 0.01 mole) previously dried over molecular sieves (4A) was dissolved in chloroform (30-40 ml). Mercury (II) chloride (2.7152 gm, 0.01 mole) was added to the tris(dimethylamino)phosphine solution. The mixture was magnetically stirred until complete dissolution had taken place to give a clear colourless solution. The complex was isolated by pouring the solution into dry petroleum ether (bp 40-60°). The precipitate was filtered, washed several times with dry petroleum ether, dried first under dry nitrogen and then under Vacuum to give a white solid product.

Yield ca. 4.3 gm.

The $HgX_2\ 2P(NMe_2)_3$ complexes were similarly prepared by using stoichiometric quantities.

$ZnX_2P(NMe_2)_3$ (X = Cl, Br, I)

In a typical reaction Zn (II) iodide (3.192 gm, 0.01 mole) was suspended in a dry benzene (100 ml). Tris(dimethylamino)phosphine (1.625 gm, 0.01 mole) was added dropwise to the suspension. The mixture was stirred magnetically while refluxing until complete dissolution took place with precautions taken against moisture. The complex was precipitated by filtering the solution into petroleum ether (bp 40-60°). The white precipitate was filtered, washed several times with dry petroleum ether and dried in a stream of dry nitrogen in a Lintott dry box. The complex looses the ligand if an attempt is made to dry it under Vacuum. Yield ca. 4.8 gm (99.6%)

$Cd\ Cl_2\ P(NMe_2)_3$

Anhydrous cadmium (II) chloride (1.833 gm, 0.01 mole) and tris(dimethylamino)phosphine (1.625 gm, 0.01 mole) were mechanically shaken (ca 6 hrs) in dry tetrahydrofuran (100 ml). The complex was isolated by filtering

the solution into dry petroleum ether (bp 40-60°) when it precipitates. The white product was filtered and dried in a dry atmosphere box under nitrogen.

$Zn\ Cl_2\ 2P(NMe_2)_3$

Zinc (II) chloride (0.6825 gm, 0.005 mole) and tris(dimethylamino) phosphine (1.625 gm, 0.01 mole) were shaken (overnight) together in dry benzene (100 ml) in a reaction vessel fitted with Rotaflo stopcocks until complete dissolution had taken place. The solvent was removed on a Vacuum line to give colourless crystals of the product (2.3075 gm).

$Cd\ Cl_2\ 2P(NMe_2)_3$

Tris(dimethylamino)phosphine (3.25 gm, 0.02 mole) was dissolved in dry benzene (40 ml) and cadmium (II) chloride (1.833 gm, 0.01 mole) was added to the benzene solution in a reaction vessel fitted with Rotaflo stopcocks. The reactants were mechanically shaken (overnight) until complete dissolution had taken place to give a clear colourless solution. The solvent was removed on a Vacuum line to give a colourless product (5.08 gm).

Bis(dimethylamino)phenyl phosphine Mercury (II) Chloride

$Hg\ Cl_2\ Ph\ P(N\ Me_2)_2$

A solution of bis(dimethylamino)phenyl phosphine (1.960 gm, 0.01 mole) in anhydrous methanol (40 ml) was added dropwise to a magnetically stirred solution of Hg(II) chloride (2.715 gm, 0.01 mole) in anhydrous methanol (200 ml). The white crystalline product was filtered washed with methanol (yield 4.5 gm) and then recrystallised from dry acetone (yield 3.4 gm).

Elemental Analysis.

The analytical results are shown in Tables 6 and 7. The elemental analysis shows only the ligand to metal ratio in the complexes but does not indicate if they are dimeric.

The 1 : 1 complex of tris(dimethylamino) phosphine with cadmium(II) chloride does not give a consistent elemental analysis for all different samples of the same complex prepared. This is probably because the complex decomposed readily at room temperature. It is uncertain whether this complex has the formulation $\left[CdCl_2\ P(NMe_2)_3 \right]_2$ as proposed by Cruickshank[81] since he gave metal and halogen analysis only which were not supported by a molecular weight measurement. This complex was insoluble in all organic solvents tested except chloroform, in which it has only very low solubility. Attempts were made to obtain single crystals of this complex from tetrahydrofuran solutions but with no success.

Elemental analyses were done by Mrs. W. Harkness and her staff of the Chemistry Department, Glasgow University.

Elemental analyses for $ZnBr_2P(NMe_2)_3$ and $ZnI_2P(NMe_2)_3$ were done by Alfred Bernhardt, Elbach, West Germany.

Molecular Weights.

Attempts were made to determine the molecular weights of the complexes by mass spectrometry but they gave no parent ions.

Experimental Difficulties.

All the Zinc (II), cadmium (II) and mercury (II) halide complexes with tris(dimethylamino)phosphine and the mercury (II) chloride complex with bis(dimethylamino)phenyl phosphine decompossed at room temperature. The zinc complexes turned into a damp mass after some weeks even if kept in a dry box. The cadmium and mercury complexes decomposed after some weeks

even if kept in a refrigerator and did not yield satisfactory analysis. The bis(dimethylamino)phenyl phosphine complex decomposed after a few days to a black solid.

We did not get all the ^{13}C data as we would have liked because of instrumental difficulties.

TABLE 6

Analytical Data for Zinc, Cadmium and Mercury Halide Complexes with $P(NMe_2)_3$

	Found %						Calculated %					
Compound	C	H	N	P	Hal	Metal	C	H	N	P	Hal	Metal
$HgCl_2P(NMe_2)_3$	16.4	4.2	9.0	7	16.4		16.5	4.2	9.7	7.1	16.3	
$Hg\ Br_2P(NMe_2)_3$	13.4	3.4	8.1	6.1	30.7		13.8	3.5	8.0	5.9	30.5	
$HgI_2P(NMe_2)_3$	11.9	3.1	7.2	4.9	40.8		11.7	2.9	6.8	5.0	40.4	
$Hg\ Br_2 2P(NMe_2)_3$	20.8	5.0	11.8	8.8	23.8		21.0	5.3	12.2	9.0	23.3	
$HgCl_2\ 2P(NMe_2)_3$	24.4	5.8	13.1	10.4	11.8		24.1	6.1	14.1	10.4	11.9	
$HgI_2\ 2P(NMe_2)_3$	18.1	4.1	10.3	7.9	32.0		18.4	4.6	10.8	8.0	32.6	
$CdCl_2P(NMe_2)_3$	20.4	5.4			20.6		20.8	5.2			20.5	
$CdCl_2\ 2P(NMe_2)_3$	28.2	6.9	16.0				28.3	7.1	16.5			
$ZnCl_2P(NMe_2)_3$	21.9	6.2	14.1				21.8	6.0	14.0			
$ZnBr_2P(NMe_2)_3$	18.4	4.7	10.7	7.9	41.3	16.5	18.6	4.6	10.8	8.0	41.2	16.9
$ZnI_2P(NMe_2)_3$	14.8	3.9	8.6	6.3	52.7		14.9	3.7	8.7	6.4	52.6	
$ZnCl_2\ 2P(NMe_2)_3$	31.0	17.9	7.7				31.2	18.2	7.8			
$P\ t\ Cl_2 2P(NMe_2)_3$	24.4	6.0	13.9		12.0		24.3	6.1	14.2		12.0	

TABLE 7

Analytical Data for Bisdimethyl Aminophenyl Phosphine Complex with Mercury (11) Chloride

	Found %						Calculated %					
Compound	C	H	N	P	Hal	Metal	C	H	N	P	Hal	Metal
$HgCl_2PhP(NMe_2)_2$	25.7	3.6	5.9	6.4			25.7	3.7	6.0	6.6		

CHAPTER TWO

INFRARED AND RAMAN SPECTRA OF AMINOPHOSPHINE COMPLEXES.

TABLE 8

IR AND RAMAN SPECTRA (4000-400 cm^{-1}) OF $P(NMe_2)_3$ COMPLEXES.

VIBRATION		ν CH	CH_3 def		CH_3 rock	CH_3 rock	ν_{C-N}	ν_{P-N}	ν_{P-N}
	IR	2790 w	1464 v s	1408 sh	-	1200 vs	1056 vs	964 vs 900 sh	688 s
$P(NMe_2)_3$	R	2793 s	-		-	-	-	965 w	659 ms
$ZnCl_2P(NMe_2)_3$	IR	2800 wb	1464 ms		1300 vsb	1184 sb	1068 ms	980 w	720 712 (s)
$ZnBr_2P(NMe_2)_3$	IR	2800 sh	1460 vsb		1292 ms	1164 sb	1064 w	975 sb	(762 674) (722) (vs)
$ZnI_2P(NMe_2)_3$	IR	2805 ms	1465 s		1060 s	1170 ms	1060 s	977 ms	(714 708) vs
$ZnCl_2 2P(NMe_2)_3$	IR	2800 sh	1472 vsb		1280 vsb	1192 vsb	1060 vs	952 vsb	(752 712 672) ((ms) (vs) (vs)
$CdCl_2P(NMe_2)_3$	IR	2770 bs	1460 vs		1370 ms	-	1060 vsb	876 vs	720 vs
$CdCl_2 2P(NMe_2)_3$	IR	2790 ms	1470 vs		1300 vs	1120 vs	1064 ms	828 vs	(732 672) (vs vsb)
$HgCl_2P(NMe_2)_3$	IR	2795 vs	1456 vs		1280 vs	1180 vs	1048 vs	972 vs	734 726 666 vs vs vs
	R	-	1448 bw		-	-	-	985 vs	677 vs

TABLE 8 CONT

VIBRATION		ν_{CH}	CH_3 def.	CH_3 rock	CH_3 rock	ν_{C-N}	ν_{P-N}	ν_{P-N}
	IR	2800 s	1460 vs	1288 vs	1172 vs	1064 vs	(976 970) (sb s)	730 668 vs vs
$HgBr_2P(NMe_2)_3$	R	2870 wb	-	-	-	-	992 bw	740 676 bw ms
$HgI_2P(NMe_2)_3$	IR	2880 s	1450 vs	1284 1256 vs sh	1172 vs	1060 vs	(972 952) (vs s)	728 720 664 vs vs vs
	IR	2800 sh	1460 vs	1288 vs	1172 vs	1060 vs	976 vs	736 730 668 vs vs vs
$HgCl_2P(NMe_2)_3$	R	2790 vs	-	-	-	-	-	-
$HgBr_2{}^2P(NMe_2)_3$	IR	2790 s sh	1448 vs	1284 vs	1184 vs	1064 vs	976 vs	724 664 vs vs
$HgI_2{}^2P(NMe_2)_3$	IR	2790 s,sh	1448 vs	1278 vs	1172 vs	1052 vs	960 vs	716 660 vs vs
$PtCl_2{}^2P(NMe_2)_3$	IR	2790 vssh	1456 vs	1280 vs	1184 vs	1062 vs	(976 952) (vs vs)	(716 692 652) (vs vs vs)
$Hg(SCN)_2P(NMe_2)_3$	IR	2830 vssh	1465 vsb	1295 vs	1185 vs	1070 vs	985 vs	760 670 vs vs

TABLE 9

IR P-N FREQUENCY SHIFTS, $\Delta\nu$ P-N, AND C-N FREQUENCY SHIFTS $\Delta\nu$ C-N IN $P(NMe_2)_3$ COMPLEXES.

	$\Delta\nu$ C-N cm^{-1}	$\Delta\nu$ P-N cm^{-1}	
COMPOUND	RELATIVE TO $^{-1}\nu$C-N AT 1056 cm^{-1}	RELATIVE TO $^{-1}\nu$P-N AT 964 cm^{-1}	RELATIVE TO $^{-1}\nu$P-N AT 688 cm^{-1}
$ZnCl_2P(NMe_2)_3$	+ 12	+ 16	+ 32, + 24
$ZnBr_2P(NMe_2)_3$	+ 8	+ 11	+ 74, + 34, - 14
$ZnI_2P(NMe_2)_3$	+ 4	+ 13	+ 26, + 20
$ZnCl_22P(NMe_2)_3$	+ 4	- 12	+ 64, + 24, - 16
$CdCl_2P(NMe_2)_3$	+ 4	- 88	+ 32
$CdCl_22P(NMe_2)_3$	+ 8	- 76	+ 44, - 16
$HgCl_2P(NMe_2)_3$	- 8	+ 8	+ 46, + 38, - 22
$HgBr_2P(NMe_2)_3$	+ 8	+ 12, + 6	+ 42, - 20
$HgI_2P(NMe_2)_3$	+ 4	+ 8, - 12	+ 40, + 32
$HgCl_22P(NMe_2)_3$	+ 4	+ 12	+ 48, + 42, - 20
$HgBr_22P(NMe_2)_3$	+ 8	+ 12	+ 36, - 24

TABLE 9 CONT

	Δ νC-N cm^{-1}	Δ νP-N cm^{-1}	
COMPOUND	RELATIVE TO νC-N AT 1056 cm^{-1}	RELATIVE TO νP-N AT 964 cm^{-1}	RELATIVE TO νP-N AT 688 cm^{-1}
$HgI_2 2P(NMe_2)_3$	- 4	- 4	+ 40, + 32, - 24
$PtCl_2 2P(NMe_2)_3$	+ 6	+ 12, - 12	+ 28, + 4, - 36
$Hg(SCN)_2 P(NMe_2)_3$	+ 14	+ 21	+ 72, - 18

TABLE 10

Differences, Δ cm^{-1}, in Raman and Infrared (I.R.) Frequencies in $HgCl_2P(NMe_2)_3$, $HgBr_2P(NMe_2)_3$

COMPOUND Vibration		ν_{CH}	CH_3 def	CH_3 rock	CH_3 rock	ν_{C-N}	ν_{P-N}	ν_{P-N}		
$HgCl_2P(NMe_2)_3$	IR	2795 vs	1456 vs	1280 vs	1180 vs	1048 vs	972 vs	666 vs		
	R	-	1448	-	-	-	985 vs	677 vs		
Δ		-	8	-	-	-	13	11		
$HgBr_2P(NMe_2)_3$	IR	2800 s	1460 vs	1288 vs	1172 vs	1064 vs	970 s	668 vs		
	R	2820 wb	-	-	-	-	992	676		
Δ		20					22	8		
$HgCl_2P(NMe_2)_3$	IR	-	336 ms	280 v,sb	-	175	-	-	100 vs	-
	R	370 w,b	334 w,b	280 m,sb	225 205 w,b	-	168 s	130 w	101 vbs	88 sh
Δ		-	2	0	-	-	-	1		

TABLE 10 Cont.

COMPOUND Vibration		ν_{CH}	CH_3 def	CH_3 rock	CH_3 rock	ν_{C-N}	ν_{P-N}	ν_{P-N}		
$HgBr_2P(NMe_2)_3$	IR		316 vs		208 w	186		114 vs	100 sh	-
	R		-		-	180 w	129 b,sh	-	-	93
Δ			-		-	6	-	-	-	

TABLE 11

INFRARED AND RAMAN SPECTRA OF $PhP(NMe_2)_2$ AND $PhP(NMe_2)HgCl_2$

VIBRATION	$PhP(NMe_2)_2$		$HgCl_2PhP(NMe_2)_2$	
	IR	R	IR	R
CH stretch	3060 (vs)		3030 b,s	
	2971 sh	2945 w,b		2972 w
	2880 vs	2901 w		
	2830 vs	2853 s		
	2785 vs	2830 w		
		2808 s	2760 ms	
Ph-P(?)	1482 vs	1495 (w)	1464 vs	
or	1456 b	1445 w	1438 vs	
CH_3def(?)	1436 vs	1420 w	1408 sh	
CH_3 rock	1288 sh		1280 bw	
	1262 vs			
	1140 s,sh	1176 w	1146 (ms)	
	1116 vs	1129 sh		
		1109 vs	1105 (ms)	1112 w
	1098 vs	1079 vs	1060 ms	1030 w
C-N stretch	1060 vs	1048 vs		
	1028 w	1011 vs	1020 w	1004 vs
		1000 sh		
	976 vs	983 sh	972 vs	
P-N stretch	960 vs		936 sh	
	752 vs		756 ms	
P-N stretch	736 vs		724 vs	
unassigned	708 vs			
	696 vs		696 ms	
	672 vs		680 ms	
	638 vs	643 w		
	620 w	627 w		
Unassigned	546 vs	551 s	548 ms	
	532 sh		530 ms	

TABLE 11 (CONT)

VIBRATION	$PhP(NMe_2)_2$		$HgCl_2PhP(NMe_2)_2$	
	IR	R	IR	R
Unassigned	514 sh			
	444 vs	455 w		
	416 w	344 vw		
	340 w	312 ms		
	224 vs	280 w	280 w	279 ms
		248 w	230 w	

TABLE 12

Far Infrared and Raman Spectra (400-40 cm^{-1}) of $P(NMe_2)_3$ Complexes.

$P(NMe_2)_3$	IR	373 w	350 m	320 m	280 w	252 m	220 m	200 w	186 w	174 w	142 m	124 m	95 m	78 m
	R		338 wb	306 w,b					182 vs	170 sh	151 w			48 w
$ZnCl_2P(NMe_2)_3$	IR		333 v,s,b	300 sh		240 vs,b		200 vs				124 v,s,b,		
$ZnBr_2P(NMe_2)_3$	IR	360 vs	316 vs		248 vs					172 vs		122 vs		88 vs
$ZnI_2P(NMe_2)_3$	IR	355 ms		320 m	250 m		216 ms	200 ms			155 s	122 msb		78 m
$ZnCl_2{}^2P(NMe_2)_3$	IR	360 m	340 sh	305 sh	288 vs					170 w		122 ms		110 ms
$CdCl_2P(NMe_2)_3$	IR	384 ms			278 s		252 m	230 ms	205 m					100 ms
$CdCl_2{}^2P(NMe_2)_3$	IR	365 ms			261 sb		245 s			170 m	132 w		94 s	
$HgCl_2P(NMe_2)_3$	IR		336 ms		280 vsb				175 vsb		168 vsb	100 vs		
	R	370 wb	334 wb		280 ms		225 205 } wb					130 w	101 vs	88 sh

TABLE 12 (CONT)

$HgBr_2P(NMe_2)_3$	IR				316 vs						186 vs			114 vs	100 sh
	R							208 w		186 w			129 bsh	93 sh	80 vs
$HgI_2P(NMe_2)_3$	IR	370 wb	324 wb		284 w							148 w	120 sh	96 vs	
$HgCl_2 2P(NMe_2)_3$	IR	365 w	300 w		280 ms			206 s	190 sh			168 vs	102 wsh	88 s	
	R		311 vs	292 sh		277 w	245 sb	212 w	187 sh				171 ssh	160 vs	137 sh
$HgBr_2 2P(NMe_2)_3$	IR	356 m	322 s		282 w									135 sb	112 w
$HgI_2 2P(NMe_2)_3$	IR	356 wsh	308 w	240 w									108 vs		
$PtCl_2 2P(NMe_2)_3$	IR	356 vs	336 vsb	328 vs	280 vs	216 vs	172 vs							148 sh	112 vs

INFRARED AND RAMAN SPECTRA OF AMINOPHOSPHINE COMPLEXES.

INTRODUCTION

P-N Stretching frequencies.

The frequency range for P-N bond stretching in phosphorus-nitrogen compounds is not well defined.

Chittenden and Thomas[105] calculated the single bond P-N stretching frequency in phosphorus-nitrogen compounds to be at 755 cm^{-1}. However, in a review of numerous results of compounds containing the groupings:

PNH_2, PNHR, (R = alkyl group)

PNR_2 (R = alkyl, aryl, Alk O, Ar O etc)

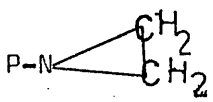

P-N=C, P-N-P,

They[105] found no bands in the region 750-680 cm^{-1} which could be assigned to a P-N stretching frequency and they assigned them to the region 1053-879 cm^{-1}. Payne and Walker [106] assigned ν_{P-N} to the region 920-897 cm^{-1} in compounds of the type

$(Ph_2P)_2$ NR (R = Me, H, Et, Pr^i)

but gave no evidence for the assignment. Larsson[107] studied the hydrolysis of compounds of the type:

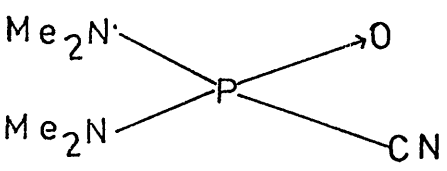

He observed that the decrease in intensity of an absorption band at 730 cm^{-1} was closely paralleled by the amount of dimethylamine liberated. He therefore concluded that this band must be attributed to a vibration of the

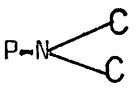

skeleton. As only the P-N bond of this skeleton was broken during the hydrolysis, this supported the assignment of the 730 cm^{-1} band to ν_{P-N}. Burganda[108] assigned two strong i.r. absorptions at 950-935 cm^{-1} to the P-N stretch in $P(NMe_2)_3$ while a weak band at 715 cm^{-1} was attributed to the vibration of the grouping $P-NC_2$ in $P(NMe_2)_3$[108]. An intense band at 600 cm^{-1} was tentatively assigned to the P-N stretch in $P(NMe_2)_3$ but he[108] gave no evidence for all the assignments. Mathis et al[109] noted that in trivalent phosphorus compounds the P-N stretching frequency varied between 1010 cm^{-1} and 790 cm^{-1}. By comparison of the i.r. spectra of the compound 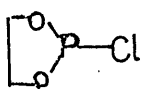

and twenty-three phosphorus-nitrogen compounds including

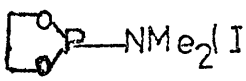 (I), $MeP(NMe_2)_2$ (II), $P(NMe_2)_3$ (III)

They observed only one band at 969 cm^{-1} for (I) while doublets were observed for (II) and (III) at 971-952 cm^{-1} and 951 - 935 cm^{-1} respectively. These they[109] attributed in the case of (I) to a P-N stretching vibration and for (II) and (III) to the symmetric and anti-symmetric stretching frequencies of the PN_2 and PN_3 groupings respectively. The observed[109] variation in P-N stretching frequencies was suggested to depend on overlap of nitrogen lone pair orbitals with empty phosphorus d orbitals in $p_\pi \longrightarrow d_\pi$ bonding. This resulted in increased P-N

stretching frequency. Further they noted[109] that the effect of conjugation of the nitrogen lone pair on P-N frequency was more important than either

(1) the electronegativity of substituents on phosphorus

(2) the possibility of conjugation of the substituent with phosphorus.

The observed increase in P-N stretching frequency was found to correlate well with the barrier to rotation about the P-N bond measured by n.m.r., and the Kinetic rate of exchange with methyl trifluoro acetate[109].

Vidal et al[110][111] assigned the P-N vibration in $(Me_2N)_3PO$ at 735 cm^{-1} to 740 cm^{-1}.

In the present work the maximum frequency shifts to higher frequencies in the $P(NMe_2)_3$ complexes relative to the free ligand value were observed in the regions 1000-800 cm^{-1} and 750-650 cm^{-1}. Thus the P-N stretching frequencies in the two regions were correlated but which of the vibration modes is symmetric or antisymmetric cannot be ascertained.

I. Results and Discussion.

I.r and Raman Spectra of tris(dimethylamino)phosphine Complexes.

Only the absorption frequencies in the complexes which vary significantly from the free ligand values are shown in Table 8. No distinction is made between symmetric and antisymmetric modes.

$P(NMe_2)_3$ is very hygroscopic and was always handled in a dry atmosphere box filled with dry nitrogen. Similarly i.r. mulls were prepared in a dry atmosphere box. The P⟶O vibration occurs as a very strong band at 1208 cm^{-1} in $(Me_2N)_3$ P⟶O and in complexes at 1185 cm^{-1} [112]. The asymmetric C-N stretching vibration in $OP(NMe_2)_3$ also occurs in this region (1195 cm^{-1})[55][108]. However, present i.r. evidence indicates that in

$OP(NMe_2)_3$, $\nu_{P\rightarrow O}$ is at 1208 cm^{-1} (112) 1207(55) or 1210 cm^{-1} (111). The absence of bands in the last three regions seems to indicate the absence of phosphine oxide as an impurity in the $P(NMe_2)_3$ prepared.

No Raman spectra were obtained for the complexes $ZnCl_2P(NMe_2)_3$, $ZnBr_2P(NMe_2)_3$, $ZnI_2P(NMe_2)_3$, $ZnCl_2P(NMe_2)_3$ $CdCl_2P(NMe_2)_3$, $CdCl_22P(NMe_2)_3$, $HgI_2P(NMe_2)_3$, $HgBr_22P(NMe_2)_3$ and $HgI_22P(NMe_2)_3$ because the samples burnt up in the laser beam. Therefore correlation of Raman spectral evidence to phosphorus or nitrogen co-ordination in the complexes will be considered only with reference to $HgCl_2P(NMe_2)_3$, $HgBr_2P(NMe_2)_3$ and $HgCl_22P(NMe_2)_3$.

Mode of co-ordination in tris(dimethylamino)phosphine Complexes -

A Summary of infrared evidence.

Phosphorus or Nitrogen co-ordination

I.R. P-N stretching frequencies. Region 1000-600 cm^{-1}

The P-N stretching frequencies of all the complexes are shown in Table 8. The P-N frequency shifts in all the complexes relative to the unco-ordinated $P(NMe_2)_3$ are shown in Table 9. It can be seen that bands usually, but not always, shift to higher frequencies. These observations will be discussed under P-N stretching frequencies (page 68).

The minimum shifts of the ν_{P-N} bands to higher frequencies for the various complexes are as follows :-

Compound	964 cm^{-1} band	688 cm^{-1} band
ZnX_2 $P(NMe_2)_3$ (X=Cl,Br,)	11	20
$ZnCl_2 2P(NMe_2)_3$		24
$CdCl_2 P(NMe_2)_3$		
$CdCl_2 2P(NMe_2)_3$		32
HgX_2 $P(NMe_2)_3$	8	32
HgX_2 $2P(NMe_2)_3$ (X-Cl,BrI)	12	32
trans- $PtCl_2 2P(NMe_2)_3$	12	4

The trans- Pt $Cl_2 2P(NMe_2)_3$ has been shown to be phosphorus bonded.[113]

The observed shifts in νP-N to higher frequencies may be interpreted as arising from an increase in P-N bond order because of increased delocalization of the nitrogen lone pair into the phosphorus d orbital. This results from the introduction of positive charge on phosphorus on co-ordination of phosphorus to a metal ion. Parry and Schultz[77] observed an increase of about 20 cm^{-1} in the P-N stretching frequency in the complex $(Me_2N)_3P.(Me_2N)_2$ PCl. $AlCl_3$ compared to the free ligand value. This was associated with an increase in the P-N bond strength resulting from delocalization of the nitrogen lone pair in pi bonding with the phosphorus.

I.r studies[111] on the BF_3 and BCl_3 adducts $(Me_2N)_3$ PO.BF_3, $(Me_2N)_3$ PO.BCl_3

have been interpreted to indicate that co-ordination is via the phosphoryl oxygen atoms. The position of the P⟶O stretching frequency in the BF_3 and BCl_3 adducts at 1145 and 1125 cm^{-1} respectively is less than that of the free ligand at 1210 cm^{-1}. Accompanying the decrease in ν PO is also an increase in the frequency of the P-N band located at 740-735 cm^{-1} in the free ligand to 765 cm^{-I} in the adducts. These results have been interpreted as arising from an increase in the dipole of the P⟶O bond upon co-ordination at the oxygen. This effects a concomitant increase in the order of the P-N bond resulting in an increase of its frequency. A similar interpretation[110] has been offered for the observed decrease of between 11-30 cm^{-1} in P⟶O bond stretching frequencies in the complexes $(Me_2N)_3$ $POHgX_2$(C = Cl, Br, I, CN, CF_3COO) relative to the free ligand value and the accompanying increase of 10-20 cm^{-1} in the P-N bond stretching frequencies with respect to its original location at 735 cm^{-1} in the free ligand.

$CdCl_2P(NMe_2)_3$ and $CdCl_2 2P(NMe_2)_3$ show very large νP-N shifts of -88 cm^{-1} and -76 cm^{-1} respectively referred to 964 cm^{-1}.

Phosphorus or Nitrogen Co-ordination (?). Raman Spectra of $HgCl_2P(NMe_2)_3$ $HgBr_2P(NMe_2)_3$ and $HgCl_2 2P(NMe_2)_3$

The P-N bond Raman stretching frequencies in $P(NMe_2)_3$ is observed (Table 8) as weak and moderately strong bands at 965 and 659 cm^{-1} respectively. These bands shift to higher frequencies in the complexes as shown in the Table below.

Raman P-N stretching Frequency shifts, $\Delta\nu_{P-N}$, in some Mercury (II) Halide Complexes with $P(NMe_2)_3$

Compound	$\Delta\nu_{P-N}$ cm^{-1}	
	Relative to ν_{P-N} at 965 cm^{-1}	Relative to ν_{P-N} at 659 cm^{-1}
$HgCl_2$ $P(NMe_2)_3$	+ 20	+ 18
$HgBr_2$ $P(NMe_2)_3$	+ 27	+ 18, + 17
$HgCl_2 2P(NMe_2)_3$		

These frequency shifts may be interpreted as resulting from phosphorus co-ordination as considered earlier. No Raman bands in the P-N region were observed for $HgCl_2 2P(NMe_2)_3$.

Differences in Raman and Infrared Frequencies in $HgCl_2P(NMe_2)_3$, $HgBr_2P(NMe_2)_3$

The differences between i.r. and Raman frequencies (4000-40 cm^{-1}) in $HgCl_2P(NMe_2)_3$, $HgBr_2P(NMe_2)_3$ are shown in Table 10. It is seen that usually, but not always, there are non-coincident absorptions. If in the mixture of possible isomers there are no common i.r. and Raman bands then each component has also no common bands. In the case of coincident absorptions in a mixture it is not possible to distinguish whether the components have non-common absorptions or not. However, because of the possibility of existence of bands too weak to be resolved, no further conclusions can be drawn.

Region 400 -40 cm^{-1}

$MX_2 2P(NMe_2)_3$ (M= Hg, X=Cl, Br,I) show one or two metal-halogen stretching frequencies, ν_{Mx}, (206-108 cm^{-1}) (Table 17 Page 78) ν_{Mx} is at 288 cm^{-1} in $ZnCl_2 2P(NMe_2)_3$ and at 261 and 245 cm^{-1} in

$CdCl_2$ $2P(NMe_2)_3$. These results are consistent with M(II) ions (M = Zn, Cd, Hg) in pseudo-tetrahedral environments. Metal-phosphorus stretching frequencies ν_{MP}, are observed as weak absorptions at 102, 112 cm^{-1} in $HgCl_2 2P(NMe_2)_3$, and $HgBr_2$ $2P(NMe_2)_3$ respectively.

$MX_2P(NMe_2)_3$ (M = Zn, Hg, X = Cl, Br, I) Complexes.

The ratio of bridging metal-halogen stretching vibration, $\nu_b(MX)$, to the terminal metal-halogen stretching vibration is in the range 0.69-0.72 (Cf Zn_2Cl_4, 0.71) indicating bridging halogen atoms in the $MX_2P(NMe_2)_3$ (M = Zn, X= Cl, Br, I) complexes. This ratio is in the range 0.60 to 0.64 in the $HgX_2P(NMe_2)_3$ (X = Cl, Br, I) complexes close to the calculated range (0.57 - 0.62) in the $(Ph_3PHgX_2)_2$ (X = Cl, Br, I) complexes indicating bridging halogen atoms. (Table 19 page 83)

ν_{MP} in $HgCl_2P(NMe_2)_3$ and $HgBr_2P(NMe_2)_3$ are at 100 cm^{-1} respectively.

(Table 19 Page 83)

Each of the absorption regions will now be discussed in detail.

Region 2900-2700 cm^{-1} CH stretching frequencies.

$P(NMe_2)_3$ was found in this work to have multiple i.r. and Raman bands in the region 3000-2790 cm^{-1}. This compares favourably with the multiple absorption observed[114] in the region 3000-2800 cm^{-1} for the methyl groups in N-methylaniline. Most investigations have centred on the low frequency band at 2800 cm^{-1} for diagnostic purposes. Hill and Meakis[114] pointed out that for an alkyl $N(CH_3)_2$ group (e.g. as in isobutyldimethylamine) two absorption bands 2825-2810 and 2765-2725 cm^{-1} are observed in this region. These have been assigned to the symmetric CH stretching frequencies of the CH_3 groups attached to nitrogen. Burganda[108] observed three bands (at 2795, 2840, and 2780 cm^{-1}) in $P(NMe_2)_3$ and assigned them to CH_3 groups.

Braunholtz et al[115] noted that an N-CH_3 group with a lone pair of electrons on the nitrogen has a characteristic CH symmetric stretching frequency in the region 2760-2820 cm^{-1} and that on co-ordination of the nitrogen lone pair a shift to higher frequencies above 2900 cm^{-1} is observed. Thus the strong band in the region 2800 cm^{-1} is absent in quartenary ammonium salts (e.g. dimethylaniline methiodide) but present in free dimethylaniline. It is also absent in dibromo,1, 4-dimethyl-piperazine palladium (II), indicating that both nitrogen atoms in 1,4-dimethyl-piperazine are involved in co-ordination with the palladium atom. Thus Braunholtz et al[115] concluded that "the absence of a band of moderate strength in the region 2800 cm^{-1} is a reliable criterion for the absence of an N-methyl group with a lone pair of electrons".

In dimethylaminodifluorophosphine, Me_2NPF_2, in which the presence of a pi component in the N-P bond has been shown from x-ray structural studies[50] the CH symmetric stretching frequency of the $N(CH_3)_2$ group occurs at 2815 cm^{-1} but disappearance of this band is observed in $Me_2NPF_2.BF_3$ in which the nitrogen atom is co-ordinated to boron[116].

In $P(NMe_2)_3$ the CH stretching frequency occurs at 2790 cm^{-1} and in the Raman spectrum at 2793 cm^{-1} (Table 8). In the zinc (II) halide complexes this band occurs at 2800 cm^{-1}. In the cadmium chloride complexes it is present as a broad and strong band at 2790 cm^{-1}. It is observed in the region 2880-2795 cm^{-1} in the mercury (II) halide complexes. It occurs as a weak broad band at 2870 cm^{-1} and as a very strong band at 2790 cm^{-1} in the Raman spectrum of $HgBr_2P(NMe_2)_3$ and $HgCl_22P(NMe_2)_3$ respectively.

The complex $Hg(SCN)_2P(NMe_2)_3$[117] contains P-Hg bonds as shown later by n.m.r. evidence but its structure in $CDCl_3$ solution is unknown. However, a strong i.r. absorption at 2060 cm^{-1} ascribed to a bridging thiocyanate group[118] indicates that it is probably dimeric in the solid state.

In trans-$PtCl_2P(NMe_2)_3$ which contains Pt-P bonds[113] CH stretching frequency, ν_{CH}, occurs as a shoulder at 2830 cm^{-1} and in $Hg(SCN)_2P(NMe_2)_3$ ν_{CH} is at 2830 cm^{-1} (Table 8).

However, presence of an absorption in the region 2800 cm^{-1} in the complexes does not necessarily indicate a metal-phosphorus bond since a necessary condition for the disappearance of this band is the involvement of all three nitrogen lone pairs of $(Me_2N)_3P$ in bonding. If only <u>one</u> or <u>two</u> of the three nitrogen atoms are co-ordinated this band could still be present.

<u>Region 1500-1100 cm^{-1} :CH_3 deformation frequencies.</u>

Barcelo and Bellanato[119] used data from electron diffraction studies on monomethylamine, dimethylamine and trimethylamine in the assignment of experimentally observed vibrational modes of these molecules. They[119] assumed that

(1) in the replacement of H in ammonia by methyl groups, the ammonia molecule suffers little change;

(2) mono- and dimethylamine have Cs symmetry;

(3) trimethylamine has C_{3V} symmetry.

Thus the absorptions at 1496 and 1404 cm^{-1} were assigned[119] to the symmetric and that at 1466 cm^{-1} to the antisymmetric CH_3 deformation modes in gaseous $(CH_3)_2NH$.

De Bolster and Groenveldt[120] assigned a series of bands observed in the i.r. spectrum of $(Me_2N)_3PO$ in the region 1481-1405 cm^{-1} to the fundamental of the CH deformation mode by comparison with that of dimethylamine[119]. Bellamy[121] made the following correlations for the CH_3 deformation modes in methyl-nitrogen compounds :

CH_3NH_2 : 1462 cm^{-1}, CH_3N_3 : 1417 cm^{-1},

CH_3NC : 1429 cm^{-1}, $(Me_2N)_2$: 1460 cm^{-1}.

By comparison with the results above, the strong i.r. absorption at 1464 cm^{-1} and the shoulders at 1470 cm^{-1} and 1480 cm^{-1} (Table 8) are correlated with the CH_3 deformation modes in $P(NMe_2)_3$. This absorption is present (Table 8) as a shoulder at 1480 cm^{-1} in $ZnCl_2P(NMe_2)_3$ while the other bands in this region in the other Zinc (II)halide complexes show little shift relative to the free ligand value.

In $CdCl_2P(NMe_2)_3$ a shift of 4 cm^{-1} below 1464 cm^{-1} in the free ligand is observed while this absorption is absent in $CdCl_2 2P(NMe_2)_3$.

A shift to frequencies below 1464 cm^{-1} is observed (Table 8) in all the mercury (II) halide complexes with $P(NMe_2)_3$.
Trans-$PtCl_2P(NMe_2)_3$,[79] which has been shown to be phosphorus-bonded, shows a shift of about 8 cm^{-1} below 1464 cm^{-1} while for $Hg(SCN)_2P(NMe_2)_3$[117] a negligible shift is observed (1465 cm^{-1}).

Table 13 shows shifts in the i.r. CH_3 deformation frequencies in the mercury (II) halide complexes.

Table 13

CH_3 Deformation Frequencies, δCH_3,

Shifts in Mercury (II) Halide Complexes with $P(NMe_2)_3$

Compound	δCH_3 cm^{-1}	$\Delta\delta CH_3$ cm^{-1}
$P(NMe_2)_3$	1464 VS	-
$HgCl_2P(NMe_2)_3$	1460 VS	-4
$HgBr_2P(NMe_2)_3$	1460 VS	-4
$HgI_2P(NMe_2)_3$	1450 VS	-14
$HgCl_2 2P(NMe_2)_3$	1460 VS	-4
$HgBr_2 2P(NMe_2)_3$	1448 VS	-16
$HgI_2 2P(NMe_2)_3$	1460 VS	-16

Region 1200-1100 cm^{-1} CH_3 rock frequencies.

CH_3 rock vibrations depend largely on the surroundings. This vibration deforms the N - C - H bond angle and is also sensitive to the electronegativity of the substituent X in $X-CH_3$[122]. For example the appropriate rock frequencies in cm^{-1} are as follows :[122]
$Si-CH_3$ near 800 cm^{-1}, $P-CH_3$, near 880 cm^{-1}, $S-CH_3$ near 960 cm^{-1} and $Cl-CH_3$ near 1016 cm^{-1}. Since the Alred-Rochow electronegativities of the substituents, X, are in the order

$$N > Cl > S > P > Si$$

it is expected that the $N-CH_3$ rock will occur above 1016 cm^{-1}. Barcelo and Bellanato[119] assigned the i.r. bands at 1244 and 1129 cm^{-1} to the symmetric and asymmetric CH_3 rocking modes in CH_3NH_2 and for $(CH_3)_2NH$ this band was assigned[119] at 1155 cm^{-1}. Two i.r. bands observed as a medium shoulder at 1152 cm^{-1} and as a weak shoulder at 1106 cm^{-1} were assigned[120] to the CH_3 rocking modes in $OP(NMe_2)_3$ by comparison with similar systems[119]

From the previous discussion the strong band observed at 1200 cm^{-1} in the i.r. spectrum of $P(NMe_2)_3$ may be correlated with the CH_3 rocking mode.

A new absorption band appears in the region 1370-1270 cm^{-1} in all the complexes. These are correlated with the CH_3 rocking mode. The absorptions at 1370 cm^{-1} in $CdCl_2P(NMe_2)_3$ and $CdCl_2 2P(NMe_2)_3$ occur at highest wave-numbers (cm^{-1}) by about + 70 cm^{-1}. The absorption at 1200 cm^{-1} in free $P(NMe_2)_3$ shifts to lower frequencies in the complexes (ca - 16 to - 80 cm^{-1})

Region 1100-1000 cm^{-1} C-N stretching frequencies.

Mayhood and Harvey[123] made correlations between i.r. absorption frequencies and the presence of dialkylamino groups in fourteen organic esters of phosphorus, containing dimethylamino groups, of the type Me_2NPCl_2, $(Me_2N)_2POCl$, $(Me_2)_2MePO$ etc. They[123] described bands at 1190

and 1064 cm^{-1} as probably arising from the C-N vibration of the - $N(CH_3)_2$ group. They[123] supported their assignment by calculating ν C-N to be at 1178 cm^{-1}. In the assignment of the vibrational frequencies in $P(NMe_2)_3$, Burgada[108] attributed an absorption at 1055 cm^{-1} to the vibration of the C-N bond in the - $N(CH_3)_2$ group. Burg and Sarkis[124] assigned the C-N stretch in $(CF_3)_2P(O)$ - $N(CH_3)_2$ to the region 1079 cm^{-1}. However, no evidence was given. The fundamental C-N vibrations of gaseous dimethylamine and monomethylamine were assigned at 930 and 1044 cm^{-1} respectively[119]. Fleming et al[125] arbitrarily assumed the symmetry C_s for the molecule $(CH_3)_2NPF_2$ and from group theoretical considerations made assignments for the fundamental vibrations in $(CH_3)_2NPF_2$ by comparison with those of dimethylamine, trimethylamine and trifluorophosphine. Thus they assigned the C-N stretch to absorptions at 1191 and 980 cm^{-1}. De Bolster and Groenveldt[120] attempted a complete assignment of the vibrational frequencies in $(Me_2N)_3PO$ by normal co-ordinate analysis and assigned the strong shoulder absorption at 1169 and the medium absorption at 1067 cm^{-1} to the C-N stretching by comparison with similar compounds[108] (123-125).

By comparison with the systems above the absorption observed at 1056 cm^{-1} in $P(NMe_2)_3$ was correlated with the C-N stretch in this work.

An examination of Table 9 indicates that in general there is a shift in the C-N stretch to higher frequencies above 1056 cm^{-1} in all the complexes. Table 9 also indicates that in general $\Delta\nu$(C-N) < $\Delta\nu$(P-N). This is expected since C-N is one bond away from the co-ordinating centre, if phosphorus co-ordination is postulated as discussed earlier.

Region 1000-650 cm^{-1}: P-N stretching frequencies.

The P-N stretching frequencies in $P(NMe_2)_3$ and in the complexes were discussed on page 58 it was noted that in general there was a shift to higher frequencies in the P-N vibrations in the complexes relative to the free ligand values (Tables 8 and 9).

In all the complexes except for $CdCl_2P(NMe_2)_3$, the P-N stretching frequencies in the region 800-600 cm^{-1} were split into multiplets in which some components were shifted towards higher wave numbers while the other components were shifted towards lower wavenumbers (cm^{-1}) compared with the single strong band in $P(NMe_2)_3$. A similar effect occured for some of the bands in the region 964 cm^{-1}. This may be attributed to solid state effects.

P-N in the Zinc (II), cadmium (II) and mercury (II) halide complexes investigated here was previously assigned[81] to the region 750-650 cm^{-1} on the grounds that the bands in this region moved to higher frequencies on co-ordination of the ligand. However, since some of the bands in the regions 1056 and 964 cm^{-1} also moved to higher frequencies on co-ordination of the ligand, shifts in the position of the absorption bands alone are insufficient to make assignments and the magnitude of the shifts to higher frequencies also need to be considered.

II. Infrared and Raman Spectra of Bis(dimethylamino)phenylphosphine and $HgCl_2PhP(NMe_2)_2$

Introduction.

The absorption frequencies in the ligand, $PhP(NMe_2)_2$ and $HgCl_2PhP(NMe_2)_2$ are shown in Table 11. $PhPO(NMe_2)_2$ has strong i.r. and Raman bands at 1193 and 1204 cm^{-1} attributed to the P⟶O stretch [55], while the P⟶O bending mode occurs as a medium band at 461 and 473 cm^{-1} in the i.r. and Raman spectra respectively. Tentative correlations of the absorption bands with the fundamental vibrations are made by comparison with those of bis(dimethylamino)phenylphosphine oxide[55]. No distinction is made here between symmetric and antisymmetric vibrations.

Results and Discussion.

Region 3060-2780 cm^{-1}: CH stretching frequencies.

The absorptions in this region have been correlated with the C-H stretch modes of the group - $N(CH_3)_2$ by comparison with $PhP(O)(NMe_2)_2$ in which νCH is at 2875-2790 cm^{-1} [55] and with other similar compounds[108][114][115]. A shift to low wavenumbers (ca 25-30 cm^{-1}) is observed in the i.r. spectrum of $HgCl_2PhP(NMe_2)_2$ compared to the free ligand values.

Region 1500-1400 cm^{-1}

P-phenyl Ring Vibrations.

Strong bands at 1000 cm^{-1} and between 1450-1425 cm^{-1} have been assigned to phenyl ring vibrations of the P-phenyl group in compounds of the type $C_2H_5Ph(O)(OH)$, $CH_3-C_6H_4P(H)(O)(OH)$[126] by empirical correlations of reference spectra of organophosphorus compounds containing phenyl groups[126]. Corbridge[127] listed a series of compounds (eg Ph_3P, $PhPCl_2$, $PhPEt_2$) in which the medium or strong absorption at 1450-1425 cm^{-1} and a weak absorption at 1010-990 cm^{-1} had been assigned to the planar ring deformation of a

phenyl group attached to a heteroatom. De Bolster[55] assigned the absorptions in the region 1487-1404 cm^{-1} to the CH_3 deformation mode in $PhP(O)(NMe_2)_2$ with no assignment for the aromatic bands. It is suggested that the absorptions in the region 1482-1436 cm^{-1} in $PhP(NMe_2)_2$ could arise from P-Ph or CH_3 vibrations, or a combination of both.

Region 1098-1000 cm^{-1} C-N stretching Frequencies.

The observed absorptions in this region are tentatively correlated with the C-N stretch as discussed earlier[108][120][124][126][127].

Region 1000-600 cm^{-1} P-N stretching Frequencies.

De Bolster[55] assigned the antisymmetric P-N stretch to the medium band at 965 cm^{-1} in $PhP(O)(NMe_2)_2$ and the symmetric stretch to the medium absorption at 729 cm^{-1}.

The absorption in the region 800-600 cm^{-1} in $PhP(NMe_2)_2$ is very complex containing at least seven lines. Therefore these absorptions do not arise from "pure" vibrations but rather involve coupling with other modes. It is suggested that the resonance effect shown below

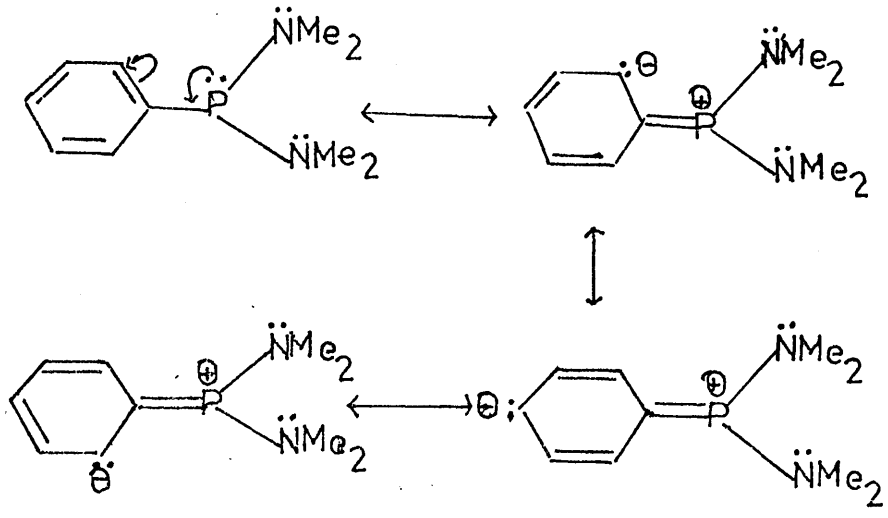

will result in increased delocalization of the nitrogen lone pairs into empty d orbitals of the slightly positively charged phosphorus in $PhP(NMe_2)_2$. It is therefore expected that the P-N stretch in $PhP(NMe_2)_2$ will occur at slightly higher frequencies than in $PhP(O)(NMe_2)_2$ where an empty phosphorus d orbital is involved in $p_\pi \longrightarrow d_\pi$ bonding with the oxygen atom[57]. From the previous discussion on P-N stretching frequencies (105)(106)(109)(110)(111) the very strong absorptions at 976 and 960 cm^{-1} and at 752 and 736 cm^{-1}, are correlated with the P-N stretch in $PhP(NMe_2)_2$.

Complete and unambiguous assignment would be possible only if the structure of $PhP(NMe_2)_2$ were known. From the structure the number of i.r. and Raman active fundamentals could be calculated; the theoretical absorption frequencies in the molecule for the various groups could then be calculated, using force constants from model compounds, and compared with the experimentally observed absorption bands in $PhP(NMe_2)_2$ and in similar compounds.

Phosphorus or nitrogen bonding in $HgCl_2PhP(NMe_2)_2$?

It is not possible to draw any conclusion from the P-N region of the spectrum as to the possibility of phosphorus or nitrogen bonding in the complex.

Infrared and Raman spectrum of $HgCl_2PhP(NMe_2)_2$

No common bands are observed in both the i.r. and Raman spectrum. However, because of the possibility of existence of bands which are too weak to be resolved, no further conclusions can be drawn.

III. Far infrared spectra of tris(dimethylamino)phosphine complexes.

Introduction

Metal-halide stretching Vibrations.

It is often easy to make assignments unequivocably for the metal-halide stretching vibrations because the frequency of the vibration will decrease as the mass of the halogen atom increases. Therefore accurate assignments can be made by comparing spectra of the chlorides, the bromides and the iodides. However, difficulties can arise when the structure of the chlorides, bromides and iodides are different since other effects may counteract the mass effect.

In most cases coupling could occur between the metal-halogen stretching vibrations in the far i.r. and other skeletal modes in the molecule. Therefore the former may not be 'pure' vibrations[128]. Despite this certain valuable and useful correlations are possible.

Some of the factors which determine the position of a metal-halogen stretching vibration, ν_{M-X}, are the following[129]

(i) A larger mass of halogen corresponds to a lower frequency of the ν_{M-X}, for example:[22]

Compound	ν_{M-X} cm^{-1}
$(Ph_3P)_2\ CdCl_2$	268, 261
$(Ph_3P)_2\ Cd\ Br_2$	195, 176,
$(Ph_3P)_2\ Cd\ I_2$	166 145

(ii) Non-bridging halogen atoms yield higher frequencies of $\nu_{t(M-X)}$ than $\nu_{b(M-X)}$ for bridging halogen atoms. For example[128]

Compound	$\nu_{b(MX)cm^{-1}}$ bridging	$\nu_{t(MX)cm^{-1}}$ terminal
$(Al\ Cl_3)_2$ (gas)	340	506
	438	625
	420	606
	301	484
$Zn_2\ Cl_4$	297	435

Metal-halogen stretching vibrations of some Group IIB metal-halide complexes are given in Table 14 below

Table 14

Metal-halide stretching Vibrations of some Zn(II), Cd(II), Pseudo-tetrahedral complexes.

Compound	$\nu_{mx\ cm^{-1}}$	Ref
$ZnCl_2 2(Me_2N)_3PO$	315	120
	285	
$CdCl_2 2(Me_2N)_3PO$	265	120
$CdCl_2(Me_2N)_3PO$	200	120
$ZnBr_2 2(Me_2N)_3PO$	263	120
	227	
$Zn(NH_3)_2Cl_2$	285	128
$Zn(NH_3)_2Br_2$	213	128
$CdCl_2(PPh_3)_2$	268	22
	261	
$ZnCl_2Py_2$	329	12
	291	

Metal-phorphorus stretching Vibrations, ν_{mp}.

Table 15 summarizes the data for some known ν_{mp} vibrations.

Table 15

Summary of Infrared data for some ν_{mp} vibrations, cm^{-1}

Compound	ν_{mp} cm^{-1}	Stereochemistry	Ref.
$(Ph_3P)_2ZnCl_2$	166s	pseudo tetrahedral	22
$(Ph_3P)_2ZnBr_2$	157s	pseudo tetrahedral	22
$(Ph_3P)_2$ ZnI_2	153s	pseudo tetrahedral	22
$(Ph_3P)_2$ $CdCl_2$	136m	pseudo tetrahedral	22
$(Ph_3P)_2$ $CdBr_2$	134m	pseudo tetrahedral	22
$(Ph_3P)_2$ CdI_2	133s	pseudo tetrahedral	22
$(Ph_3P)_2$ $HgCl_2$	137w,108m	pseudo tetrahedral	22
$(Ph_3P)_2$ $HgBr_2$	132w,104w	pseudo tetrahedral	22
$(Ph_3P)_2$ HgI_2	133sh,98vw	pseudo tetrahedral	22
cis-$PtCl_2(PMe_3)_2$	362m	square planar	130
trans-$PtCl_2(PMe_3)_2$	413w	square planar	
	382w	square planar	130

ν_{mp} lies in the range 460-91 cm^{-1}. From the evidence available to date, ν_{mp} is often weak to medium in intensity.

Metal-Nitrogen Stretching Frequencies, ν_{MN}.

Table 16 summarizes data for some literature ν_{MN} assignments. ν_{MN} vibrations are strongly dependent on the mass of the ligands. Thus for most metal-ammine complexes ν_{MN} lies between 277-500 cm^{-1} (12)(131). However, for hexa-ammines of divalent metals ν_{MN} is near 300 cm^{-1} (132). ν_{MN} for metal-pyridine is in the range 200-287 cm^{-1} (12). It is expected that ν_{MN} in $(Me_2N)_3P$ complexes will occur in the range 200-287 cm^{-1}.

In general the metal nitrogen vibration is weak to medium in intensity.

Table 16

Metal-Nitrogen Stretching Frequencies, ν_{MN}, For some Metal (II) Complexes.

Compound	Co-ordination Number	ν_{MN} cm^{-1}	Ref
$Zn(NH_3)_6\ Cl_2$	6	300	133
$Zn(NH_3)_6\ Br_2$	6	294	133
$Zn(NH_3)_6\ I_2$	6	282	133
$Zn\ (NH_3)_2\ Cl_2$	4	421	133
$Zn(NH_3)_2\ Br_2$	4	392	133
$Zn(NH_3)_2\ I_2$	4	414	133
$Cd(NH_3)_6\ Cl_2$	6	298	133
$Cd(NH_3)_6\ Br_2$	6	291	133
$Cd(NH_3)_6\ I_2$	6	277	133
$cis\text{-}Pt(NH_3)_2\ Cl_2$	4	510	134
$cis\text{-}Pt(NH_3)_2\ Br_2$	4	492, 485	134
$trans\text{-}Pt(NH_3)_2\ Cl_2$	4	509	134
$trans\text{-}Pt(NH_3)_2\ Br_2$	4	531, 506	128

Table 16 Cont

Compound	Co-ordination Number	ν MN cm^{-1}	Ref
$ZnCl_2Py_2$	4	218	12
$ZnBr_2Py_2$	4	219	12
ZnI_2Py_2	4	222	12

Results and Discussion.

The i.r. spectra (400-40 cm^{-1}) of the complexes are shown in Table 12.

1:2 Complexes of Zn(II), Cd(II) and Hg(II) Halides.

Metal-Halogen Stretching Frequencies, ν_{MX}.

The number of i.r. active normal modes in MA_2X_2 compounds (A is a monodentate ligand) predicted[55] from group theory for the metal-halogen stretching vibration ν_{MX} are as shown in the Table below.

Stereochemistry	Type	Local Symmetry group	ν_{M-X} i.r. active
Tetrahedral	MX_4	Td	t_2
Pseudo-tetrahedral	MA_2X_2	C_{2v}	$a_1 + b_2$

Thus two M-X vibrational absorptions are characteristic of MA_2X_2 compounds (Table 14 page 73) while those of the type $MX_4^=$ have only one M-X stretching vibration as shown in the Table below.

Anion	ν_{MX} cm^{-1}
$ZnCl_4^=$	298
$CdCl_4^=$	260
$HgCl_4^=$	228
$HgBr_4^=$	169
	46
$HgI_4^=$	118
	41

ν_{MX} in $ZnCl_2 2P(NMe_2)_3$ and $CdCl_2 2P(NMe_2)_3$ are easily assigned as very strong absorptions at 288, 305 cm^{-1} and at 261, 245 cm^{-1} respectively (Table 17) below by comparison with ν_{MX} values in $(Me_2N)_3PO$ complexes[120] Table 14 page 73).

Table 17

Metal-halogen, ν_{M-X}, and Metal phosphorus, ν_{M-P}, Stretching Frequencies of MX_2 L Complexes with $P(NMe_2)_3$

Compound	ν_{MX} cm^{-1}	ν_{M-P} cm^{-1}
$ZnCl_2 2P(NMe_2)_3$	305(s,sh)	
	288 vs	
$CdCl_2 2P(NMe_2)_3$	261 (s,b)	
	245 s	
$HgCl_2 2P(NMe_2)_3$	206 (s)	102 wsh
$HgBr_2 2P(NMe_2)_3$	135 (s,b)	112 w
$HgI_2 2P(NMe_2)_3$	108 (vs)	not observed
$PtCl_2 2P(NMe_2)_3$	336 s	unassigned

The observed ν_{MX} values in $ZnCl_2 2P(NMe_2)_3$, $CdCl_2 2P(NMe_2)_3$, $HgX_2 2P(NMe_2)_3$ (X = Cl, Br, I) (Table 17) are in the region of those assigned[81] for this vibration as follows.

Compound	ν_{MX} cm^{-1}
$ZnCl_2 2P(NMe_2)_3$	305 (s), 290 (s)
$CdCl_2 2P(NMe_2)_3$	260 (s), 245 (s)
$HgCl_2 2P(NMe_2)_3$	205 (s), 190 (s,sh)
$HgBr_2 2P(NMe_2)_3$	136 (s), 130 (s)
$HgI_2 2P(NMe_2)_3$	101 (s)

The ν_{MX} vibration at 101 cm^{-1} in $HgI_2 2P(NMe_2)_3$ [81] could not be confirmed. Instead a very strong absorption at 108 cm^{-1} was correlated with ν_{MX} in $HgI_2 2P(NMe_2)_3$.

An examination of Table 17 indicates that in some cases only one metal-halogen stretching frequency is observed. However, failure to resolve the expected number of skeletal stretching frequencies is not uncommon for pseudo-tetrahedral MA_2X_2 complexes[12].

The pseudo-tetrahedral environment of Cadmium (II) in $CdCl_2 2P(NMe_2)_3$ may be further inferred by comparison with $CdCl_2(PPh_3)_2$, the crystal structure[135] of which was interpreted to indicate that the cadmium atom is in pseudo-tetrahedral environment as predicted from i.r. spectroscopy (ν_{MX} : 268, 261 cm^{-1}).

$PtCl_2 2P(NMe_2)_3$ shows a very strong absorption at 336 cm^{-1} attributable to a Pt-Cl stretching frequency for a trans-platinum (II) square planar complex[66].

Metal-phosphorus stretching Frequencies, ν_{MP}.

The absorptions tentatively assigned here as ν_{MP} (Table 17) are rather weak in intensity. In addition these absorption bands are in the same regions as free ligand absorption bands. Although the ν_{MP} values agree to some extent with those made earlier[81] as follows,

Compound	Mp cm^{-1}
$HgCl_2 2P(NMe_2)_3$	100 w, sh
$HgBr_2 2P(NMe_2)_3$	110 w, sh
$HgI_2 2P(NMe_2)_3$	109 (w,sh)

they cannot be conclusive in themselves as evidence for metal-phosphorus bonding in the complexes.

No mass independent peaks were observed in the spectra of $HgCl_2 2P(NMe_2)_3$ and $HgBr_2 2P(NMe_2)_3$ but ν_{MP} in these complexes were correlated with the absorptions at 102 and 112 cm^{-1} (Table 17) respectively by comparison with ν_{MP} values for $HgX_2(PPh_3)_2$ (X = Cl,Br,I)[22] (Table 15). The weak shoulder absorption at 109 cm^{-1} attributed[81] to ν_{MP} in $HgI_2 2P(NMe_2)_3$ could not be confirmed.

Other bands in i.r. spectrum of 1:2 complexes with $(PNMe_2)_3$

These bands are shown in Table 18. It is seen that some of the bands are either the same or shifted slightly in position relative to the free ligand absorption bands. These have not been given any specific assignments.

Metal-Nitrogen Stretching Vibrations (?).

No bands are observed in the i.r. spectra of 1 : 2 complexes of Hg(II) halides which are dependent on the mass of the halogen apart from $\nu_t(MX)$ which could be correlated with ν_{MN} in these complexes.

Table 18

Other Bands in I.R. Spectrum of 1:2 complexes with $P(NMe_2)_3$

Compound													
$P(NMe_2)_3$	373 w	350 m	320 m	280 w	252 m	220 m	200 w	186 w	174 w	142 w	124 m	95 m	78 m
$ZnCl_2 2P(NMe_2)_3$	360 m	340 sh							170 w		122 ms	110 ms	
$CdCl_2 2P(NMe_2)_3$		365 ms								132 w	120 m	94 m	
$HgCl_2 2P(NMe_2)_3$		365 w	300 w	280 ms					168 vs			102 wsh	88 sh
$HgBr_2 2P(NMe_2)_3$		356 m	322 ms	282 w								112 w	
$HgI_2 2P(NMe_2)_3$		356 wsh	308 w			240 w							
$PtCl_2 2P(NMe_2)_3$		356 vs		280 vs		216 vs			172 vs	148 vs		112 vs	

1:1 Complexes of Zn (II), Cd (II) and Hg (II) halides with $P(NMe_2)_3$

Terminal metal-halogen, ν_t (M-X) and bridging metal-halogen, ν_b (M-X) Vibrations.

Deacon et al[22] studied 1 : 1 complexes with mercury (II) halides of the type $(Ph_3PHgX_2)_2$ (x = Cl, Br, I) in the far i.r. region (400-40 cm^{-1}) One ν_t (M-X) vibration and one ν_b (M-X) stretching vibration both of which were dependent on the mass of the halogen were predicted and found for these compounds from group theoretical treatment. A second but more complex form of the ν_b^1 (M-X) stretch had been predicted[22] for the $(Ph_3PHgX_2)_2$ compounds but this occurred at a lower frequency relative to the ν_b (M-X) considered earlier and was also dependent on the mass of the halogen. The assignments [22] are given in the Table below,

Compound	ν_{M-X} cm^{-1} terminal	ν_{M-X} cm^{-1} bridging	$\frac{\nu_{b(M-X)}}{\nu_t (M-X)}$	ν_b^1 M-X cm^{-1} bridging	ν_{MP} cm^{-1}
$(Ph_3PHgCl_2)_2$	287 s	180 (s)	0.62	97(s),83	152m
$(Ph_3PHgBr_2)_2$	198 s	111 (s)	0.57	60 (sh)	129s
$(Ph_3PHgI_2)_2$	156 (s)	110 m	0.62	50 m	135
		86 m			(m)

For gaseous $(AlCl_3)_2$ the ratio[128]

$$\frac{\nu_{b(MX)\ (dimer)}}{\nu_{t(MX)\ (dimer)}} = 0.68$$

and for Zn_2Cl_4, the ratio is 0.71. For most dimeric transition metal complexes[128] this ratio lies in the range 0.60 to 0.85. The calculated ratios for the $(Ph_3PHgX_2)_2$ compounds also lie in this range.

The crystal structure[24] of $(Ph_3PHgCl_2)_2$ indicates that it is halogen

Table 19

Far i.r. (400 - 40 cm^{-1}) Parameters in MX_2L Complexes

Compound	ν_t (MX) cm^{-1}	ν_b (MX) cm^{-1}	$\frac{\nu_b\ (MX)}{\nu_t\ (MX)}$	ν_{bl} M x cm^{-1} bridging	ν_{M-P}
$ZnCl_2P(NMe_2)_3$	333 sb	240 bs	0.72	124 vs	not observed
$ZnBr_2P(NMe_2)_3$	248 vs	172 ms	0.69	88 vs	not observed
$ZnI_2P(NMe_2)_3$	216 ms	155 s	0.71	78 m	not observed
$CdCl_2P(NMe_2)_3$	278 s				not observed
$HgCl_2P(NMe_2)_3$	280 ms	168 vsb	0.60		100 vs
$HgBr_2P(NMe_2)_3$	186 vs	114 vs	0.61	not observed	100 sh
$HgI_2P(NMe_2)_3$	148 vs	96 vs	0.64	not observed	not observed

bridged and dimeric in agreement with i.r. prediction[22].

In the present work, the ν_t (M-X) and $\nu_{b(M-X)}$ correlations in $MX_2P(NMe_2)_3$ compounds are shown in Table 19.

The calculated $\frac{\nu_{b(MX)}}{\nu_{t(MX)}}$ ratios are in agreement with those considered earlier.

$\nu_{t(MX)}$, $\nu_{b(MX)}$ are very strong absorptions in all the Zn (II), Hg(II) halide complexes. These correlations are in near agreement with those made[81] for the dimeric $MX_2P(NMe_2)_3$ complexes as follows :

Compound	$\nu_{t(MX)}$	$\nu_{b(MX)}$	$\nu_{b'(MX)}$
$ZnCl_2P(NMe_2)_3$	327 (s)	240 (s)	120 (s)
	296 s,sh	225 (s,sh)	
$ZnBr_2P(NMe_2)_3$	259 (s)	190 (s)	95 (msh)
	230 (s)	170 (s)	
$ZnI_2P(NMe_2)_3$	216 (m)	155 (s)	77 (m)
		142 (m,sh)	
$CdCl_2P(NMe_2)_3$	277	205 (m)	100 (s)
	270 (m)	228 (m)	88 w,sh
$HgCl_2P(NMe_2)_3$	282 (s)	168 (s)	88 (w,sh)
		118 (s)	72 (m)
$HgBr_2P(NMe_2)_3$	190 (s)	116 (s)	55 (m,sh)
$HgI_2P(NMe_2)_3$	147 (s)	87 (s)	42 (w)

The medium shoulder absorption at 95 cm^{-1} attributed[81] to $\nu_{b^1(MX)}$ in $ZnBr_2P(NMe_2)_3$ could not be confirmed but rather a very strong absorption at 88 cm^{-1} was correlated with the complex $\nu_{b^1(MX)}$ bridging mode in $ZnBr_2P(NMe_2)_3$. A band in the region 83-97 cm^{-1} was also observed in $(Ph_3P)_2(HgCl_2)_2$[22].

For $CdCl_2P(NMe_2)_3$ only ν_t (M-X) was assigned with some certainty by comparison with the assignments[22] for $CdX_2(PPh_3)_2$ (C=Cl,Br,I).

Metal-phosphorus stretching Vibrations, ν_{MP}.

No absorptions were observed in the spectra of the $ZnX_2P(NMe_2)_3$ complexes which were independent of the mass of the halogen and which could be assigned to ν_{MP}. The absorptions at 170 cm^{-1}, assigned[81] to ν_{MP} in $ZnCl_2P(NMe_2)_3$, $ZnBr_2P(NMe_2)_3$ and at 165 cm^{-1} in $ZnI_2P(NMe_2)_3$ were not observed. A similar phenomenon was observed in $(Ph_3PHgX_2)_2$[22]; that is, no mass independent peaks which could be assigned to ν_{M-P} were observed and only tentative assignments were made for ν_{MP} in these latter compounds (Table 15).

Strong absorptions at 100 cm^{-1} in $HgCl_2P(NMe_2)_3$ and as a shoulder at 100 cm^{-1} in $HgBr_2P(NMe_2)_3$ were independent of the mass of the halogen and may be assigned to ν_{MP} vibrations. No band was observed in this region for $HgI_2P(NMe_2)_3$.

Metal-Nitrogen stretching Vibrations (?)

Apart from ν_t(M-X), ν_b (M-X) and $\nu_{b'}$ (M-X) no mass dependent absorptions were observed in the i.r. (400-40 cm^{-1}) spectra of the $MX_2P(NMe_2)_3$ (M=Zn,Hg, X=Cl,Br,I) complexes which could be assigned to ν_{M-N}.

Raman Spectrum of $HgCl_2P(NMe_2)_3$, $HgBr_2P(NMe_2)_3$

The Raman spectra of these complexes are shown in Table 12. It has not been possible to make any specific assignments for these frequencies but they are rather used to ascertain whether the complexes have a centre of symmetry or not (see page 61).

Table 20

Other Bands in i.r. Spectra (400-40 cm^{-1}) of $MX_2P(NMe_2)_3$ Complexes.

M =Zn, Hg, (X = Cl, Br, I), (M = Cd, X = Cl).

Compound													
$P(NMe_2)_3$	373 w	350 m	320 m	280 w	252 m	220 m	200 w	186 w	174 w	142 m	124 m	95 m	78 m
$ZnCl_2P(NMe_2)_3$			300 sh				200 vs				124 vsb		
$ZnBr_2P(NMe_2)_3$		360 vs	316 vs								122 vs		
$ZnI_2P(NMe_2)_3$	–	355 ms	320 m		250 m		200 ms				122 msb		
$CdCl_2P(NMe_2)_3$		384 ms			252 m	230 ms	205 m					100 ms	
$HgCl_2P(NMe_2)_3$			336 ms						175 vsb				
$HgBr_2P(NMe_2)_3$			316 vs										
$HgI_2P(NMe_2)_3$		356 wsh	308 w		240 w								

CHAPTER THREE

NUCLEAR MAGNETIC RESONANCE SPECTRA OF AMINOPHOSPHINE COMPLEXES.

Table 21

^{1}H and ^{31}P N.M.R. Parameters of Aminiphosphine Complexes

Compound	Solvent	δ_{H} (ppm) (TMS)			$\delta_{^{31}P}$ (ppm)			$^{3}J_{P-H}$ (Hz)			%		
		A	B	C	A	B	C	A	B	C	A	B	C
$P(NMe_2)_3$	neat	2.46			+122.2			8.8					
$HgCl_2P(NMe_2)_3$	$CDCl_3$	2.80			+112.8			12.3					
$HgBr_2P(NMe_2)_3$	$CDCl_3$	2.82			+109.2			11.9					
$HgI_2P(NMe_2)_3$	$CDCl_3$	2.90			+91.2			10.9					
$HgCl_2$2P$(NMe_2)_3$	$CDCl_3$	2.81			+122.9			11.9					
$HgBr_2$2P$(NMe_2)_3$	$CDCl_3$	2.82			+118.2			11.0					
$HgI_2$2P$(NMe_2)_3$	$CDCl_3$	2.84			-			10.4					
$CdCl_2P(NMe_2)_3$	$CDCl_3$	2.68	2.70		-	+29.7	+12.7	10.7	9.2				
$CdCl_2$2P$(NMe_2)_3$	$CDCl_3$	2.80			+105.3			10.0					

Table 21 (Cont'd)

Compound	Solvent	δ_{H} (ppm)(TMS)			$\delta_{^{31}P}$ (ppm)			$^{3}J_{P-H}$ (Hz)			%		
		A	B	C	A	B	C	A	B	C	A	B	C
$ZnCl_2P(NMe_2)_3$	$CDCl_3$	2.67	2.65	2.66	+89.3	+28.3	+15.0	12.1	10.9	12.4	47.0	33.0	20.0
$ZnBr_2P(NMe_2)_3$	$CDCl_3$	2.70	2.67	2.68	+86.5	+39.4	+27.7	10.5	9.5	10.8	72.0	20.0	8.0
$ZnI_2P(NMe_2)_3$	$CDCl_3$	2.82	2.67	2.94	+71.1	+49.0	+45.5	10.2	11.0	9.6	60.0	24.0	16.0
$ZnCl_2 2P(NMe_2)_3$	$CDCl_3$	2.68	2.65	-	+92.9	+27.4	-	8.6	9.7	-			
$PtCl_2 2P(NMe_2)_3$	CH_2Cl_2	2.81	-	-	+89.4	-	-	10.1					
$Hg(SCN)_2P(NMe_2)_3$	$CDCl_3$	2.80	-	-	+115.6			12.6					

Table 22

Variable Temperature 100 MHz ^{1}H n.m.r. Parameters of $ZnI_2P(NMe_2)_3$

Temperature	215°K			243°K			273°K			291°K			308°K		
	A	B	C	A	B	C	A	B	C	A	B	C	A	B	C
$\delta_{H_{ppm}}$	2.76	2.83	2.83	2.75	2.82	2.83	2.73	2.81	2.82	2.75	2.81	2.82	2.75	2.81	2.80
$^{3}J_{PH}$ (Hz)	9.4	10.0	11.0	9.4	10.0	11.0	9.4	10.0	11.0	9.4	10.0	10.8	9.4	10.0	11.0

Table 23

Variable temperature ^1H n.m.r. Parameters of Tris(dimethylamino)phosphine and Complexes with Mercury (II) halides (100 MHz)

	δ_H ppm					$^3J_{(PH)}$ Hz				
	Temperature °K					Temperature °K				
Compound	308°	273	253	233	213	308	273	253	233	213
$P(NMe_2)_3$	2.52				2.53	8.8				9.2
$HgCl_2P(NMe_2)_3$	2.88	2.90	2.90	2.91	2.91	12.2	12.4	12.4	12.4	12.4
$HgBr_2P(NMe_2)_3$	2.90			2.92	2.92	12.2			12.2	12.2
$HgI_2P(NMe_2)_3$	2.92		2.93	2.93	2.94	11.3		11.5	11.4	11.4
$HgCl_2{}_2P(NMe_2)_3$	2.81	2.81	2.81	2.82		11.2	11.9	11.9	12.2	
$HgBr_2{}_2P(NMe_2)_3$	2.82	2.82	2.83	2.83		5	11.8	11.8	11.8	
$HgI_2{}_2P(NMe_2)_3$	2.84	2.80	2.83		2.84	5.3	5.3	10.8		10.4

Table 24

^{1}H and ^{31}P n.m.r. Parameters of $PhP(NMe_2)_2$ and $PhP(NMe_2)_2 HgCl_2$

Compound	Solvent	δ_{H} ppm	$\delta_{^{31}P}$ ppm	$^{3}J_{PH}$ (Hz)	$\Delta_{ppm}\ \delta_{^{31}P}$ (Complex) $-\delta_{^{31}P}$ (Ligand)
$PhP(NMe_2)_2$	$CDCl_3$	2.68	+ 100.7	6.0	-
$HgCl_2PhP(NMe_2)_2$	$CDCl_3$	2.90	+ 110.7	12.5	+ 10

Table 25

^{13}C N.M.R. Parameters for $P(NMe_2)_3$ Complexes

Compound	$\delta_{^{13}C}$ ppm			$^2J_{(^{13}C - ^{31}P)}$ Hz		
	G	E	F	G	E	F
$P(NMe_2)_3$		38.3				
$HgCl_2P(NMe_2)_3$		37.4			+ 8.3	
$HgBr_2P(NMe_2)_3$		37.5			+ 8.0	
$HgI_2P(NMe_2)_3$		37.6			+ 7.4	
$HgCl_2 2P(NMe_2)_3$		37.6			< 6.0	
$HgBr_2 2P(NMe_2)_3$		37.7			<.5.0	
$HgI_2 2P(NMe_2)_3$		37.9			< 2.5	

Table 25 (Cont)

Compound	$\delta_{^{13}C}$ ppm			$^{2}J_{(^{13}C - ^{31}P)}$ Hz		
	G	E	F	G	E	F
$ZnCl_2P(NMe_2)_3$	38.6	37.0	34.0		+ 8.2	6.2
$ZnCl_2P(NMe_2)_3$		37.5	34.9			6.4
$CdCl_2{}^2P(NMe_2)_3$		37.5			< 5.0	
$PtCl_2{}^2P(NMe_2)_3$	38.9			3.5		

Table 26

^{31}P Chemical shifts of $P(NMe_2)_3$ Complexes

		$\delta_{^{31}P}$ ppm			△ ppm		
Complex		A	B	C	A	B	C
$P(NMe_2)_3$		122.2			-		
$HgCl_2P(NMe_2)_3$		112.8			-9.4		
$HgBr_2P(NMe_2)_3$		109.2			-13.0		
$HgI_2P(NMe_2)_3$		91.2			-31.0		
$HgCl_2{}^2P(NMe_2)_3$		122.9			+0.7		
$HgBr_2{}^2P(NMe_2)_3$		118.2			-3.3		
$HgI_2{}^2P(NMe_2)_3$		-			-		

Table 26 Cont

Complex		$\delta_{^{31}P}$ ppm			△ ppm		
		A	B	C	A	B	C
$CdCl_2P(NMe_2)_3$			29.7	12.7	-	-92.5	-109.5
$CdCl_2{}^{2P}(NMe_2)_3$		105.3			-16.9		
$ZnCl_2P(NMe_2)_3$		89.3	28.3	15.0	-32.9	-93.9	-107.2
$ZnBr_2P(NMe_2)_3$		86.5	39.4	27.7	-35.7	-83.3	-94.5
$ZnI_2P(NMe_2)_3$		71.1	49.0	45.5	-51.1	-73.2	-76.7
$ZnCl_2{}^{2P}(NMe_2)_3$		92.9	27.4	-	-29.3	-94.8	
$PtCl_2{}^{2P}(NMe_2)_3$		89.4			-32.8		
$Hg(SCN)_2P(NMe_2)_3$		115.6			-6.6		

Table 27

$^{1}J_{M-P}$, $^{4}J_{Hg-H}$, $^{2}J_{P\ MP}$, δ_{Hg} Parameters in $P(NMe_2)_3$ Complexes

Compound	$^{1}J_{M-P}$ (Hz)	$^{4}J_{M-H}$ (Hz)	$^{2}J_{PMP}$ Hz	δ_{Hg} ppm
$HgCl_2P(NMe_2)_3$	11,258	14.6		-815
$HgBr_2P(NMe_2)_3$	10,362	12.2		-1119
$HgCl_2{}^2P(NMe_2)_3$	7,165	6.0	362	-592
$HgBr_2{}^2P(NMe_2)_3$		5.3		
$HgI_2{}^2P(NMe_2)_3$				
$PtCl_2{}^2P(NMe_2)_3$	3,188	0	755	
$Hg(SCN)_2P(NMe_2)_3$	9,700	14.0		
$HgCl_2PhP(NMe_2)_2$	9,430	14.5		

NUCLEAR MAGNETIC RESONANCE SPECTRA OF AMINOPHOSPHINE COMPLEXES.

Introduction.

Considerable use has been made of n.m.r. spectroscopy in understanding the mode of bonding in organophosphorus compounds and in transition metal phosphine complexes. ^{1}H and ^{31}P n.m.r. has been used mainly hitherto.

Recent papers have indicated the increasing attention being given to the use of ^{13}C n.m.r. and most of these have centred on the measurement of $^{13}C - ^{31}P$ nuclear spin coupling constants.

In the present investigation ^{1}H, ^{31}P, ^{13}C, and ^{199}Hg n.m.r. have been used to some extent. A brief review will now be given of results from n.m.r. investigations on similar classes of compounds.

The ^{1}H chemical shifts of some amino-group containing compounds are as follows(136)

Compound	σ_H ppm	% Conc in CCl_4
Me_3N	2.12	2
$Me_3N\ BH_3$	2.60	5
$(Me_2N)_3\ P$	2.43	neat
$(Me_2N)_3\ PO$	2.60	2%

It is seen that the ^{1}H chemical shift in $Me_3N\ BH_3$ is to low field relative to the free ligand value indicating deshielding of the methyl protons on co-ordination of the nitrogen to boron. Similarly a downfield shift of the methyl protons in $(Me_2N)_3\ PO$ on co-ordination of the phosphorus in $(Me_2N)_3\ P$ is observed. Therefore ^{1}H chemical shifts alone are insufficient for distinguishing between P or N co-ordination in amino-phosphines.

Vidal et al [110] investigated the ^{1}H and ^{31}P n.m.r. spectra of Hg(II) halide complexes $HgX_2 2(Me_2N)_3$ PO (X = Cl, Br, I, CN, CF_3COO). As mentioned earlier co-ordination was shown to be through the oxygen atom in these complexes. These workers [110] detected no change in the ^{1}H chemical shifts (2.47 ppm) compared to the free $(Me_2N)_3PO$ value indicating that there is probably no deshielding of the N-methyl protons.

Only small ^{31}P chemical shift changes on co-ordination were observed in the ^{31}P n.m.r. spectra of the $HgX_2 2 (Me_2N)_3$ PO complexes ($\delta^{31}P$ = + 1.61 to + 5.06 ppm downfield of H_3PO_4) relative to the free ligand value of + 23.0 ppm. The small values of the co-ordination chemical shifts were attributed to weak liquid-metal interactions.

I. Summary of Results.

^{1}H Chemical Shifts.

The ^{1}H n.m.r. of all the tris(dimethylamino)phosphine complexes indicate a downfield shift of all the ^{1}H resonances (2.68 to 2.90 ppm) relative to unco-ordinated $P(NMe_2)_3$ (2.46 ppm) indicating deshielding of the N-methyl protons in the complexes.

^{1}H chemical shift of 2.90 ppm in the methyl region was observed in $HgCl_2PhP(NMe_2)_2$ relative to the free $PhP(NMe_2)_2$ value of 2.68 ppm.

^{31}P Chemical Shifts.

The ^{31}P chemical shift change on co-ordination, Δ, in all the complexes lie in the range 3 to 51 ppm upfield of the ^{31}P chemical shift in the unco-ordinated $P(NMe_2)_3$ ($\delta_{^{31}P}$ = + 122.2 ppm) suggesting shielding of the phosphorus nucleus on phosphorus co-ordination. However for $HgCl_2{}^2P(NMe_2)_3$ Δ is 0.7 ppm downfield of $P(NMe_2)_3$.

^{199}Hg-^{31}P Nuclear Spin Coupling Constants.

For the $HgX_2P(NMe_2)_3$ and $HgCl_2{}^2P(NMe_2)_3$ complexes, the one-bond ^{199}Hg-^{31}P coupling constants $^{1}J_{(^{199}Hg-^{31}P)}$ are in the range 7000-11000 Hz suggesting coupling between directly bonded atoms as in the structure

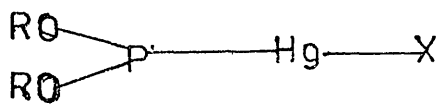

(R = alkyl group, X = Cl, Br) where the ^{199}Hg-^{31}P coupling constants are in the range 7000-1300 Hz (Table 30 page 135).

The n.m.r. spectra of the nuclei in the respective compounds will now be considered in detail.

Results and Discussion.

^1H n.m.r. spectrum of tris(dimethylamino)phosphine.

The ^1H spectrum of $P(NMe_2)_3$ as a neat liquid at ambient temperature (308^oK) is a doublet of 1:1 intensity from coupling of the ^{31}P nucleus ($I = 1/2$) to the eighteen equivalent protons. There are no extra peaks in the methyl region which could be assigned to impurities in $P(NMe_2)_3$.

^1H n.m.r. spectra of $ZnCl_2P(NMe_2)_3$, $ZnBr_2P(NMe_2)_3$ and $ZnI_2P(NMe_2)_3$

Three doublets were observed in the methyl region in the ^1H n.m.r. spectra of $ZnX_2P(NMe_2)_3$ complexes in $CDCl_3$ solution:
a main doublet (A), a low-field doublet (B) and a high field doublet (C).

$ZnCl_2P(NMe_2)_3$

60 MHz (298^oK) ^1H spectrum showed one doublet (δ_H = 2.62 ppm $^3J_{PH}$ = 11.2Hz)
100 MHz (308^oK) showed two pairs of poorly resolved doublets.

220 MHz (295^oK) ^1H spectrum showed three doublets of integrated peak intensities 40: 3:2 (Table 21). The observation of three doublets of unequal intensities at 220 MHz indicated the presence of three species in $CDCl_3$ solution and that at 60 MHz, the chemical shifts of the different species were too close to be resolved. These results will be discussed further under (i) ^1H chemical shifts (page 121)
(ii) ^{31}P chemical shifts (page 123)
(iii) ^1H-^{31}P nuclear spin coupling constants (page 132)

$ZnBr_2P(NMe_2)_3$

60 MHz (298^oK) ^1H spectrum showed a doublet

(δ_H, = 2.66 ppm, $^3J_{(PH)}$ = 10.4 Hz)

Fig4. ^{1}H NMR (220MHz, 295°K) of $ZnBr_2P(NMe_2)_3$

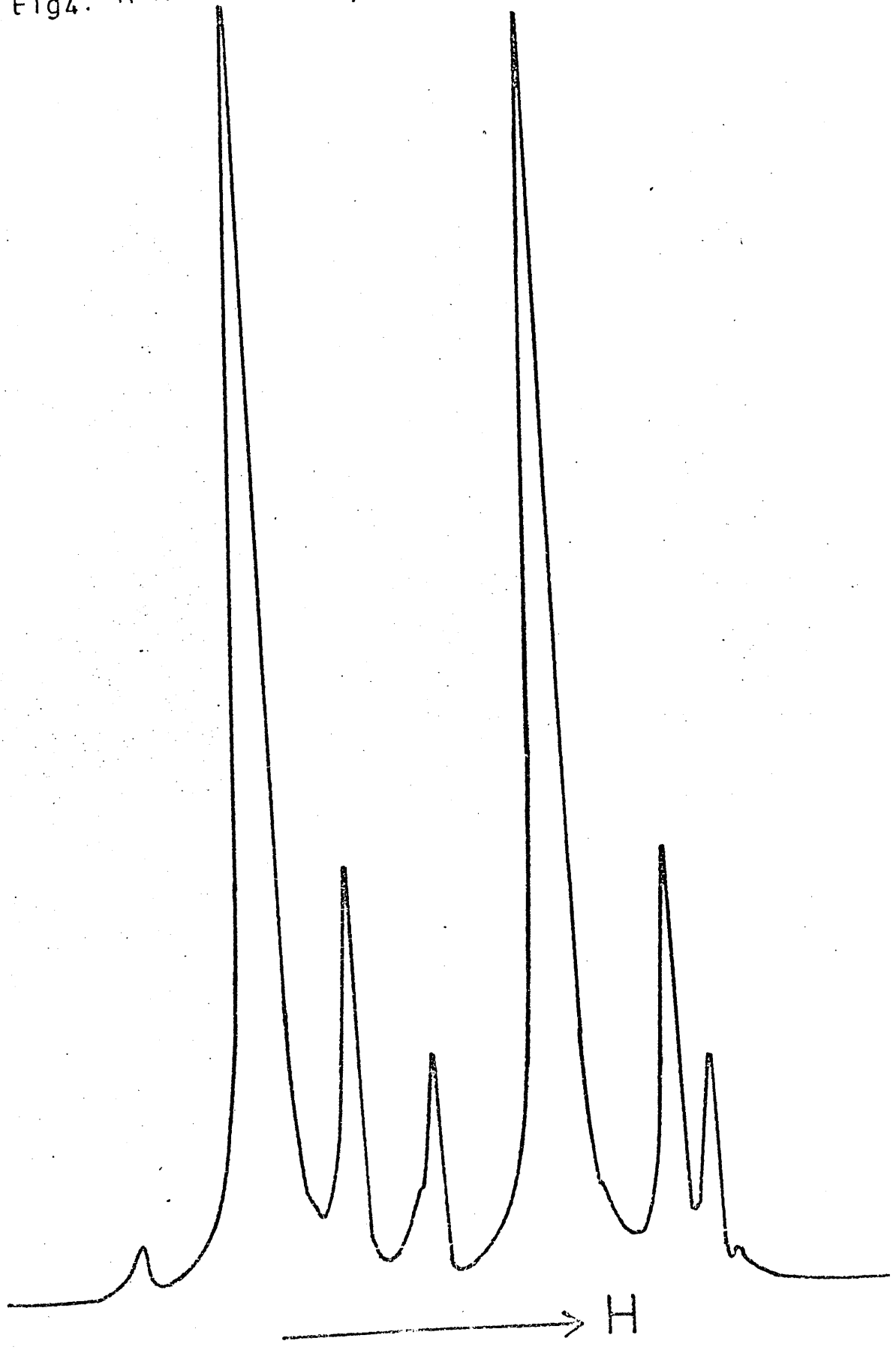

100 MHz (308°K) ^1H spectrum showed three poorly resolved doublets. 220 MHz (295°K) ^1H spectrum (Fig.4) showed three doublets of integrated intensities 40 : 3:1 (Table 21).

$ZnI_2P(NMe_2)_3$

60 MHz (298°K) ^1H spectrum showed two well resolved doublets and a third doublet not so well resolved, all were of unequal peak heights. 100 MHz (308°K) ^1H spectrum showed three doublets of integrated peak intensities 20 : 8:5.

Because $ZnI_2P(NMe_2)_3$ gave a well resolved three doublets in the 100 MHz spectrum at ambient temperature (308°K) it was used to investigate the possible hydrolysis of the product on exposure to air. Exposure of the sample solution (10 min) used for the 100 MHz ^1H n.m.r. as above did not change the nature of the spectrum, i.e. there was no detectable attack at $P(NMe_2)_3$. This indicated that the three doublets observed in the ^1H spectrum of $ZnI_2P(NMe_2)_3$ were probably not hydrolysis products.

In a control experiment, an amount of ZnI_2 and $P(NMe_2)_3$ equivalent to ligand to metal ratio of 1 : 1 were dissolved in $CDCl_3$ at room temperature in a dry box. The ^1H spectrum (90 MHz) indicated two doublets of unequal peak heights (δ_H, 3.04 and 2.84 ppm). This indicated possible formation of a complex at room temperature since ZnI_2 is insoluble in $CDCl_3$.

$CdCl_2P(NMe_2)_3$

100 MHz (308°K) ^1H spectrum showed two doublets of unequal peak heights. A variable temperature (308 to 343°K) ^1H n.m.r. showed two doublets of unequal peak heights but essentially showed no change in the chemical shifts or $^1H - ^{31}P$ coupling constants (Table 21). This indicated the presence of two species in $CDCl_3$ solution.

^{1}H N.M.R. Spectra of Complexes of the General type P_2ML_n.

Trans-$PtCl_2 2P(NMe_2)_3$, $HgX_2 2P(NMe_2)_3$ (X = Cl, Br, I) belong to complexes of the general type P_2ML_n where

(i) M is the metal atom, (M will not be considered in the description of the nuclear spin system).

(ii) L_n represents other ligands in the system and

(iii) P is the phosphorus atom in the ligand in question.

For the $HgX_2 2P(NMe_2)_3$ complexes these belong to the nuclear spin system

$$X_n\ AA^1\ X_n^1$$

where $A = {}^{31}P = A^1$, $X = {}^1H = X^1$

and n = 18

The phosphorus nuclei are magnetically non-equivalent in such systems because $J_{(AX)} \neq J_{AX}^1$. For complexes containing two tris(dimethylamino)-phosphines bonded to a metal atom, information about the coupling between the two phosphorus atoms can be obtained from the ^{1}H n.m.r. Half the X intensity is always in a doublet of separation

$$N = J_{AX} + J_{AX}^1$$

and the position of the other half depends on the relative magnitude of the phosphorus-phosphorus couplings.

If the coupling between the phosphorus atoms is zero a doublet which would look like the doublet observed in complexes with only one tris(dimethylamino)-phosphine, would be expected in the ^{1}H n.m.r. spectrum. The complex $(P(NMe_2)_3)_2\ Ni(CO)_2$ shows this type of ^{1}H spectrum [68].

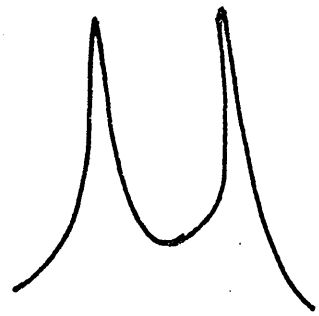

^1H spectrum of $(P(NMe_2)_3)_2\ Ni(CO)_2$

If the coupling between the two phosphorus atoms, $^2J_{PMP}$, is very large in comparison with the phosphorus-hydrogen coupling, $^3J_{(PH)}$ of 8 to 10 Hz, the $X_n\ AA^1X_n^1$ system gives a spectrum similar to that of an A_2X_{2n} system with a coupling half the sum of $J_{(AX)}$ and $J_{(AX)}1$ and a 1:2:1 deceptively simple "triplet" is observed. Thus <u>trans-</u> $PtCl_2 2P(NMe_2)_3$

$$\left[\ \left|{}^3J_{(^{31}P---H)} + 3.{}^5J_{(^{31}P---H)}\right| = 10\ Hz\right.$$

with $^5J_{(^{31}P---^1H)}$ assumed = 0 , and $^2J_{PMP}$ = 755 Hz](Fig.5) shows a "triplet" in the ^1H spectrum whereas only a doublet is observed in the cis-isomer [79]. A deceptively simple"triplet"is observed in the ^1H spectrum of $HgX_2 2P(NMe_2)_3$ (See page 116)

Fig 5 : trans – $PtCl_2\ 2P(NMe_2)_3$, 100MHz (308°K) ^1H NMR

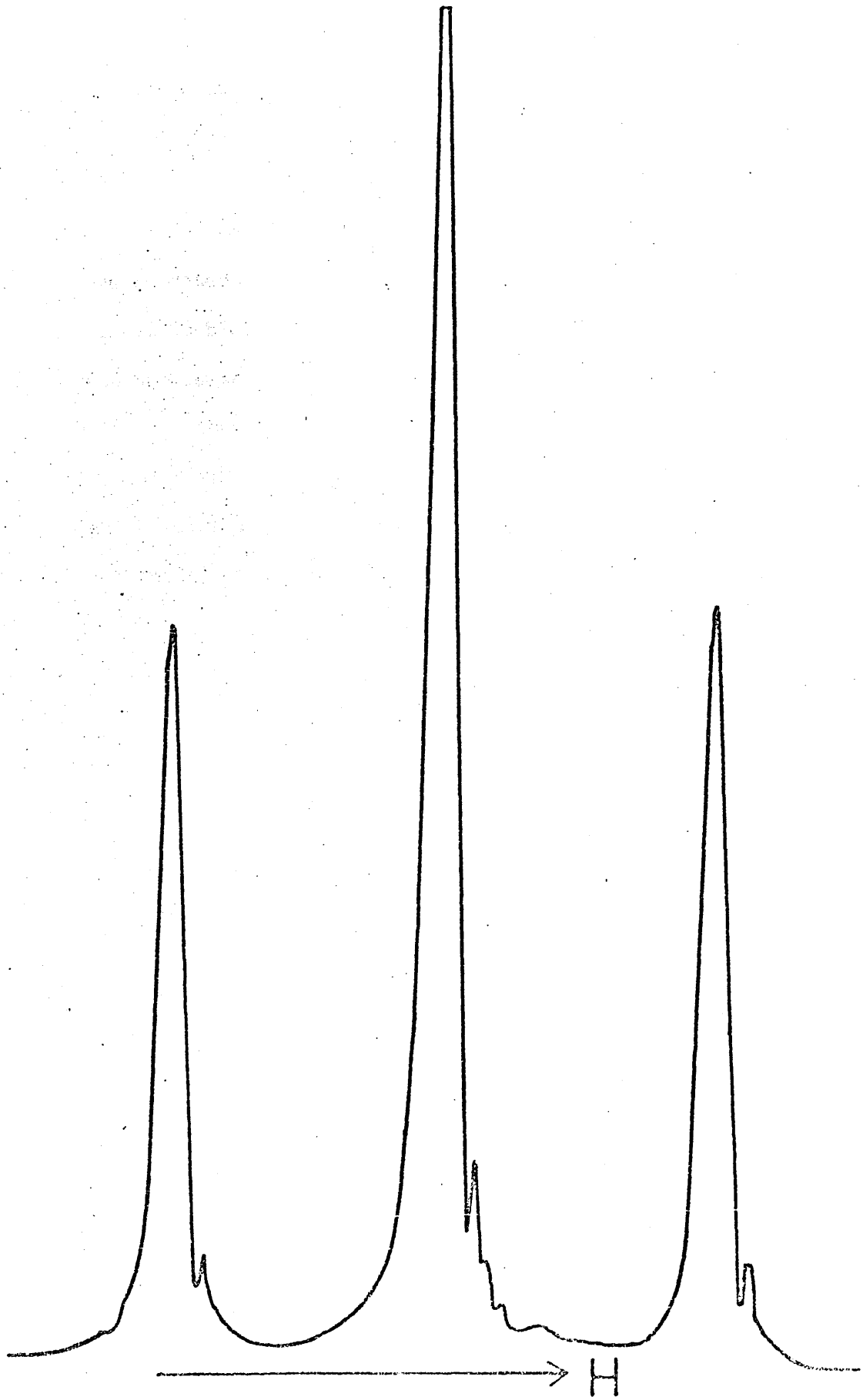

Variable Temperature ^{1}H n.m.r. of $ZnX_2P(NMe_2)_3$, $CdCl_2P(NMe_2)_3$ and $HgX_2P(NMe_2)_3$

The variable temperature ^{1}H n.m.r. of $HgX_2P(NMe_2)_3$ complexes will be discussed on page 108.

Previous 60 MHz ^{1}H n.m.r. investigations [81] on $ZnX_2P(NMe_2)_3$ and $CdCl_2P(NMe_2)_3$ were reported to show two doublets with approximate intensities 1 : 2 while a pair of doublets were observed for the $HgX_2P(NMe_2)_3$ (X= Cl,Br,I) complexes. These showed temperature independence over the range 307° to 343°K. In order to interpret these results the following were some of the possibilities considered:

(1) $P(NMe_2)_3$ might be bidentate through one nitrogen and one phosphorus atom for the 1 : 1 Zn(II) and Cd(II) complexes but monodentate through the phosphorus atom for the Hg(II) complexes.

(ii) The possibility of existence of a mixture of isomers.

The possibility of co-ordination through the nitrogen was ruled out on the grounds that for all the tris(dimethylamino)phosphine complexes the three-bond $^{1}H - ^{31}P$ coupling constants increased relative to the free ligand value. In contrast the system

$$Me_2NPMe_2 \cdot Al(Et)_3$$

has $^{3}J_{PH} = 0$ at 323°K with co-ordination through the nitrogen atom [72].

Because of the poor resolution of $ZnCl_2P(NMe_2)_3$ and $ZnBr_2P(NMe_2)_3$ at 100 MHz variable temperature studies were done only on $ZnI_2P(NMe_2)_3$.

The results (Table 22) indicate that the ^{1}H chemical shifts and $^{1}H - ^{31}P$ coupling constants of each of the doublets are essentially invariant over the temperature range investigated. These suggest that the main cause of the non-equivalence of the N-methyl protons could result from the

presence of a mixture of trans-symmetrical, cis-symmetrical and unsymmetrical isomers in solution as shown by the possible structures.

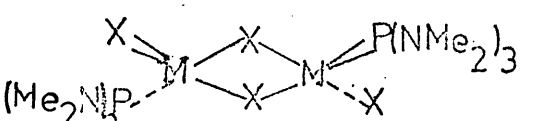

(1) trans-symmetrical

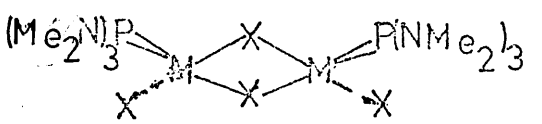

(2) Cis-symmetrical

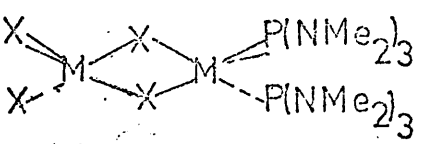

(3) Unsymmetrical

It is expected that the environments of the phosphines in the unsymmetrical isomer will be very different from those of the <u>cis</u> and the trans-symmetrical isomers. This will be considered further under ^{31}P chemical shifts of the complexes (Page 123).

^{1}H n.m.r. of 1:1 Complexes of $HgX_2P(NMe_2)_3$ (X = Cl, Br, I)

$HgCl_2P(NMe_2)_3$ and $HgBr_2P(NMe_2)_3$

60 MHz (298°K) ^{1}H n.m.r. spectra of $HgCl_2P(NMe_2)_3$ and $HgBr_2P(NMe_2)_3$ each consists of a 1:1 doublet as the major peak and four small ^{199}Hg satellites. The major peak arises from those molecules not containing ^{199}Hg while the four small satellites arise from those molecules containing ^{199}Hg (17% natural abundance, I = 1/2) and causes spin-spin coupling in the ^{1}H spectrum. The ^{199}Hg satellites were confirmed by double resonance experiments. The observation of a doublet of equal intensity as the major peak suggests the presence of one isomer in $CDCl_3$ solution of these complexes. In an earlier investigation[81] the presence of ^{199}Hg satellites seemed not to be considered. Fig.6 shows a 100 MHz (308°K) ^{1}H spectrum of $HgCl_2P(NMe_2)_3$. The ^{1}H n.m.r. parameters of $HgCl_2P(NMe_2)_3$ and $HgBr_2P(NMe_2)_3$ at 60 and 100 MHz are shown in the Table below.

Compound		$HgCl_2P(NMe_2)_3$	$HgBr_2P(NMe_2)_3$
60 MHz	δ_H ppm	2.80	2.82
	$^3J_{PH}$ (Hz)	12.3	11.9
	$^4J_{Hg-H}$ (Hz)	14.6	12.2
100 MHz	δ_H (ppm)	2.88	2.86
	$^3J_{PH}$ (Hz)	12.2	11.8
	$^4J_{Hg-H}$ (Hz)	14.5	12.0

100 MHz variable temperature ^{1}H n.m.r. of $HgCl_2P(NMe_2)_3$ and $HgBr_2P(NMe_2)_3$ from ambient temperature (308°K) to 213°K showed that the ^{1}H chemical shifts and ^{1}H - ^{31}P coupling constants are essentially

Fig. 6 : $HgCl_2 P(NMe_2)_3$ 100MHz (308 °K) ^1H NMR

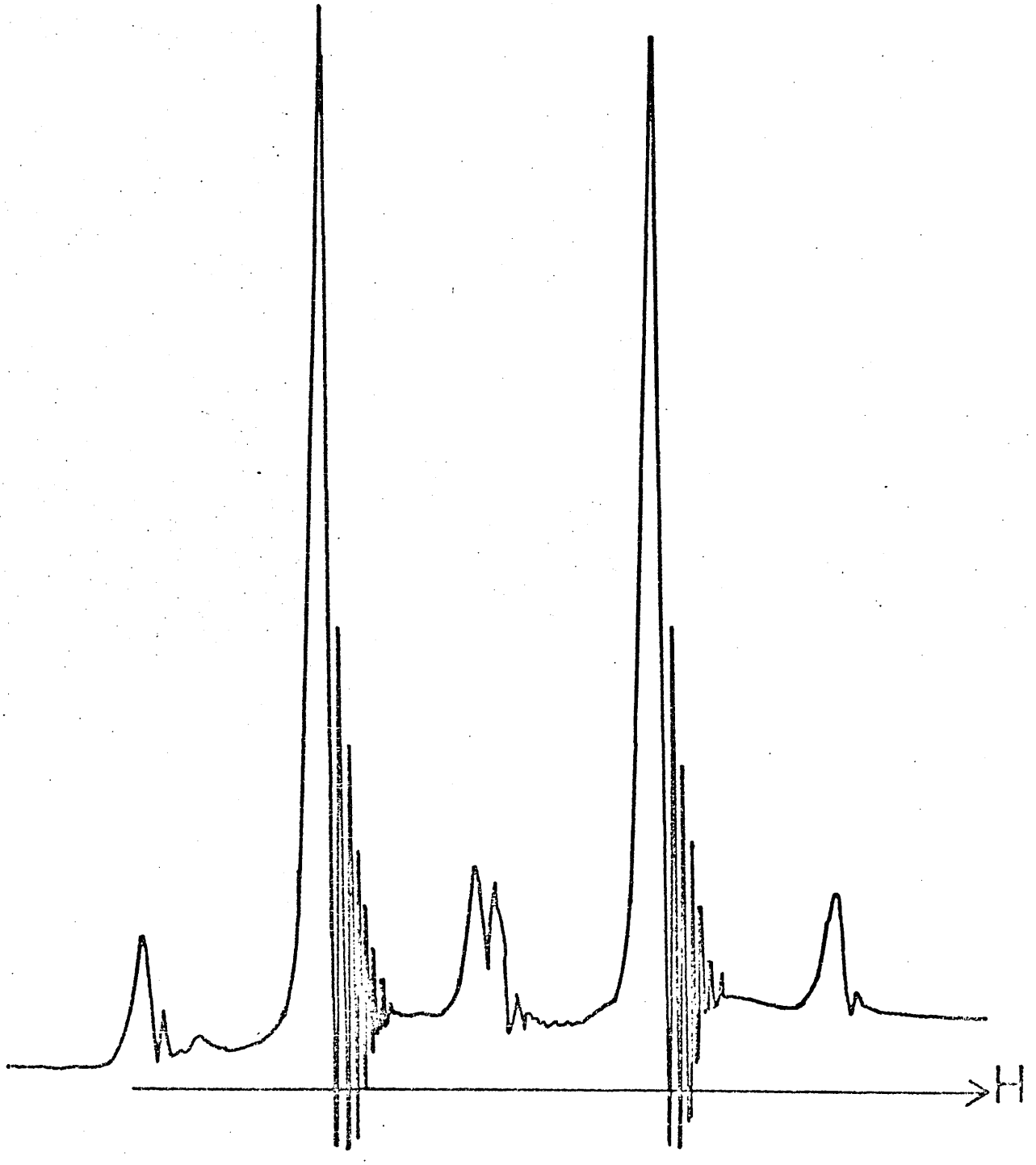

independent of temperature (Table 23).

A similar temperature independence of the ^{1}H n.m.r. parameters was observed at 343°K relative to 308°K. These indicate that either there are no ligand exchange processes involved at the experimental temperatures used or that the exchange processes are too slow to be detected on the n.m.r. time scale.

$HgCl_2PhP(NMe_2)_2$

The ^{1}H spectrum (298°K) in the methyl region showed two doublets of 1:1 intensity with four small ^{199}Hg satellites ($^{4}J_{H----Hg}$) = 14.5 Hz). The presence of the ^{199}Hg satellites were confirmed by double resonance experiments. The ^{1}H n.m.r. parameters are shown in Table 24.

^{1}H - ^{199}Hg INDOR Spectrum of $HgCl_2P(NMe_2)_3$

The ^{199}Hg INDOR spectrum of $HgCl_2P(NMe_2)_3$ (Fig. 7) showed two ^{199}Hg resonances of approximately equal peak heights and separation $^{1}J_{Hg-P}$= 11,264Hz. This indicates one phosphine ligand in the environment of each mercury, evidence that $HgCl_2P(NMe_2)_3$ is probably dimeric in $CDCl_3$ solution and therefore has either the trans-symmetrical structure

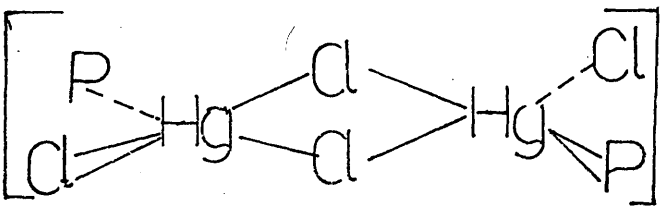

or the cis-symmetrical structure

Fig 7 $(Me_2N)_3PHgCl_2$ $^1H\{^{199}Hg\}$ INDOR

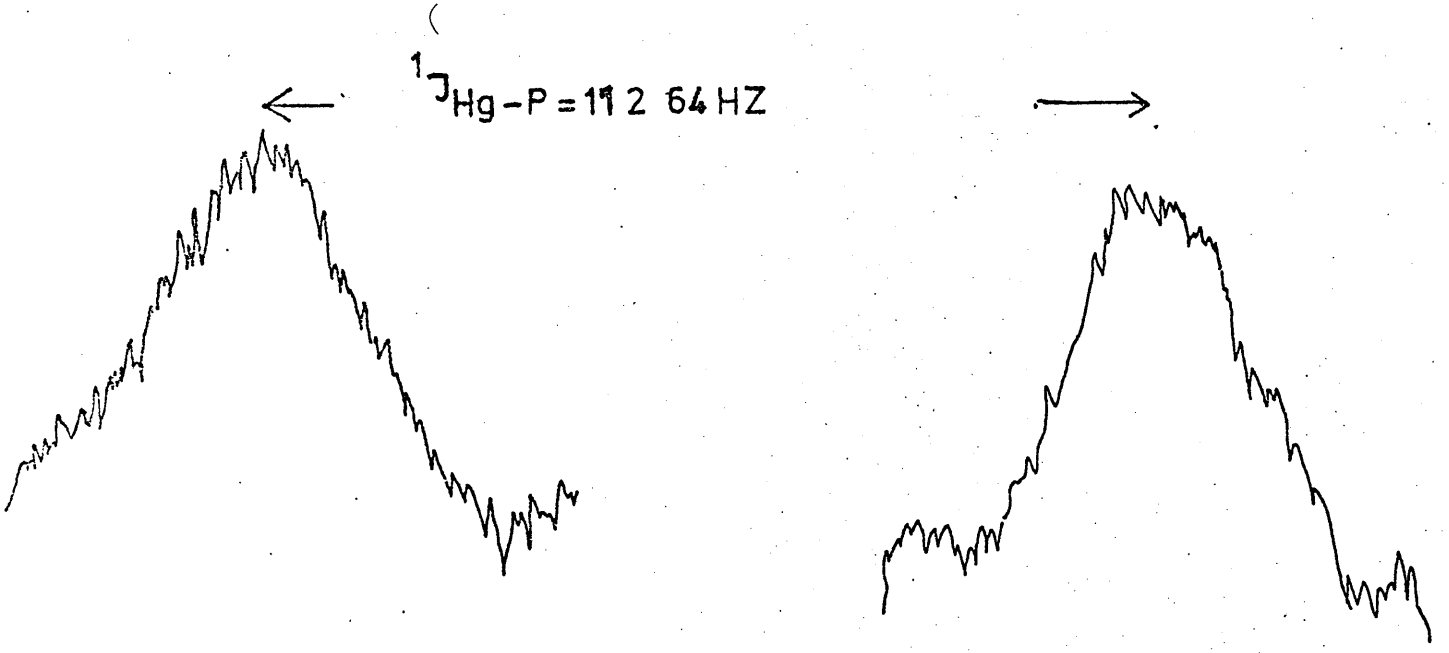

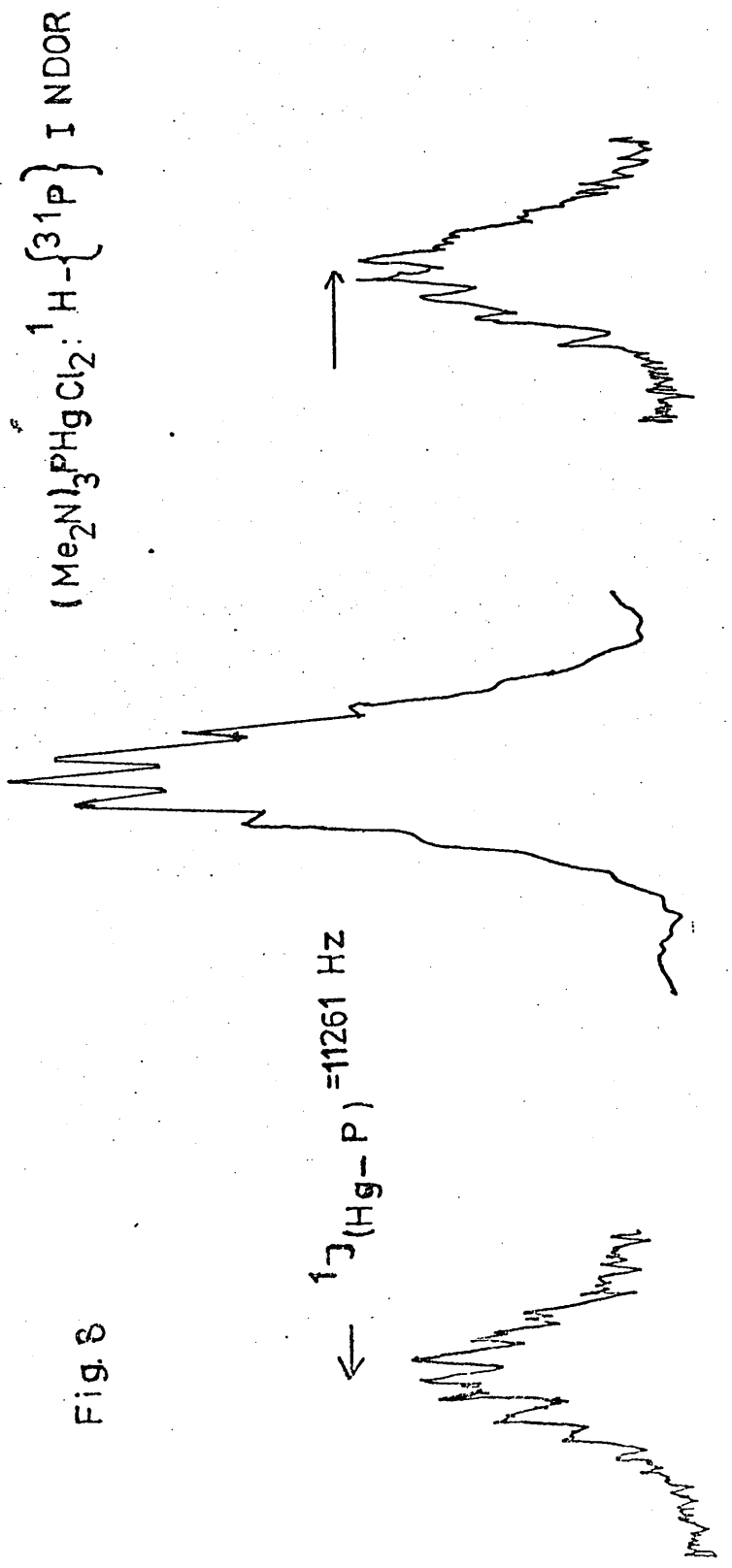

Fig. 8

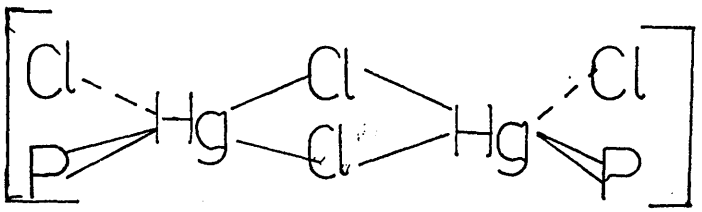

For the unsymmetrical structure

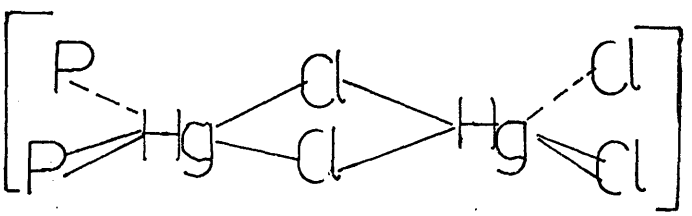

with two phosphine ligands in the environment of a mercury atom a triplet would be obtained in the ^{199}Hg INDOR spectrum.

Double resonance experiments on the ^{1}H spectrum of $HgCl_2 2P(NMe_2)_3$ (described on page 115) established a triplet of ^{199}Hg signals with J_{Hg-P} = 7167 Hz.

^{1}H - $\{^{31}P\}$ INDOR spectrum of $HgCl_2P(NMe_2)_3$ showed a central ^{31}P resonance not containing ^{199}Hg and two ^{199}Hg resonances of separation $^{1}J_{Hg-P}$= 11,261 Hz because of ^{31}P - ^{199}Hg nuclear spin coupling (Fig 8).

$\underline{HgI_2P(NMe_2)_3}$

100 MHz (308°K) ^{1}H n.m.r. spectrum of this complex showed a doublet of integrated peak intensity 1:1 but showed no ^{199}Hg satellites. This is probably because of a ligand dissociation equilibrium of the type

$$(HgI_2L)_2 \rightleftharpoons 2HgI_2 + 2L$$

where the $P(NMe_2)_3$ can exchange between the free state and the co-ordination

site of the mercury (II) ion. At slow rates of exchange at low temperatures it may be possible to observe the ^{199}Hg satellites. However, a variable temperature ^{1}H n.m.r. spectrum (308 to 213°K) failed to reveal the satellites. A similar phenomenon has been observed in the ^{31}P n.m.r. spectrum of di-iodobis (butyl diphenylphosphine) mercury (II)[137] where the ^{199}Hg satellites were not observed at room temperature.

The variable temperature data (Table 23) also indicate that the ^{1}H chemical shifts and the ^{1}H-^{31}P nuclear spin coupling constants are essentially independent of temperature.

$Hg(SCN)_2P(NMe_2)_3$[117]

The 100 MHz (298°K) ^{1}H spectrum showed a doublet of 1:1 intensity and four small ^{199}Hg satellites ($^{4}J_{(Hg-^{1}H)}$ = 14.0 Hz). The ^{1}H n.m.r. parameters are shown in Table 21.

1:2 Complexes of Zn(II),Cd(II) and Hg(II) with $P(NMe_2)_3$

The ^{1}H n.m.r. parameters of all 1:2 complexes are shown in Table 21. These will be discussed under

(i) ^{1}H chemical shifts (Page 121)

(ii) ^{1}H-^{31}P nuclear spin coupling constants (Page 132)

$ZnCl_2 2P(NMe_2)_3$

60 MHz (298°K) ^{1}H spectrum showed two doublets of unequal peak heights suggesting the presence of two components in $CDCl_3$ solution.

$CdCl_2 2P(NMe_2)_3$

60 MHz ^{1}H spectrum showed doublet of equal peak heights indicating the presence of one component in $CDCl_3$ solution.

Variable Temperature ^1H n.m.r. of $HgX_2 2P(NMe_2)_3$ Complexes

The variable temperature parameters are shown in Table 23.

$HgCl_2 2P(NMe_2)_3$

A deceptively 'simple' triplet with no ^{199}Hg satellites is obtained in the 100 MHz (308°K) ^1H spectrum with $^3J_{PH}$ = 11.2 Hz (Fig.9). At 273°K, a well resolved triplet is obtained ($^3J_{PH}$ = 11.9 Hz) the two outermost lines of the triplet (273°K) had a pair of ^{199}Hg satellites (J_{Hg-H} = 6.0 Hz). The third pair of ^{199}Hg satellites is probably hidden under the broad central resonance of the triplet (Fig.10).

$HgBr_2 2P(NMe_2)_3$

60 MHz (298°K) and 100 MHz (308°K) ^1H n.m.r. spectra of $HgBr_2 2P(NMe_2)_3$ showed a broad singlet (width at 1/2 height = 9.7 Hz), with a hyperfine structure which sharpened on ^{31}P decoupling. This showed that the hyperfine structure arose from ^{31}P-^1H coupling. A broad singlet instead of the expected doublet would be produced if there is intermolecular exchange of ligands.

At lower temperatures (273°K and 257°K) the rate of exchange slowed down and a 'triplet' with the ^{199}Hg satellites, $^4J_{(Hg-^1H)}$ = 5.3 Hz, was obtained with $^3J_{PH}$ = 11.8 Hz. A similar phenomenon is obtained in the cation $\left((MeO)_3P\right)_4 Cu^+$ (138).

$HgI_2 2P(NMe_2)_3$

100 MHz ^1H n.m.r. spectra at both 308°K and 274°K showed a broad singlet (width at 1/2 height = 10.6 Hz). At 253°K, a deceptively 'simple' triplet is obtained with $^3J_{PH}$ = 10.4 Hz. The ^{199}Hg satellites remained still unresolved at 213°K.

From the variable temperature ^1H n.m.r. studies the order of the rate of phosphorus-ligand exchange in the $HgX_2 2P(NMe_2)_3$ (X = Cl, Br, I) complexes

Fig 9 $HgCl_2$ 2 $P(NMe_2)_3$: 100MHz (308°K) ^1H NMR

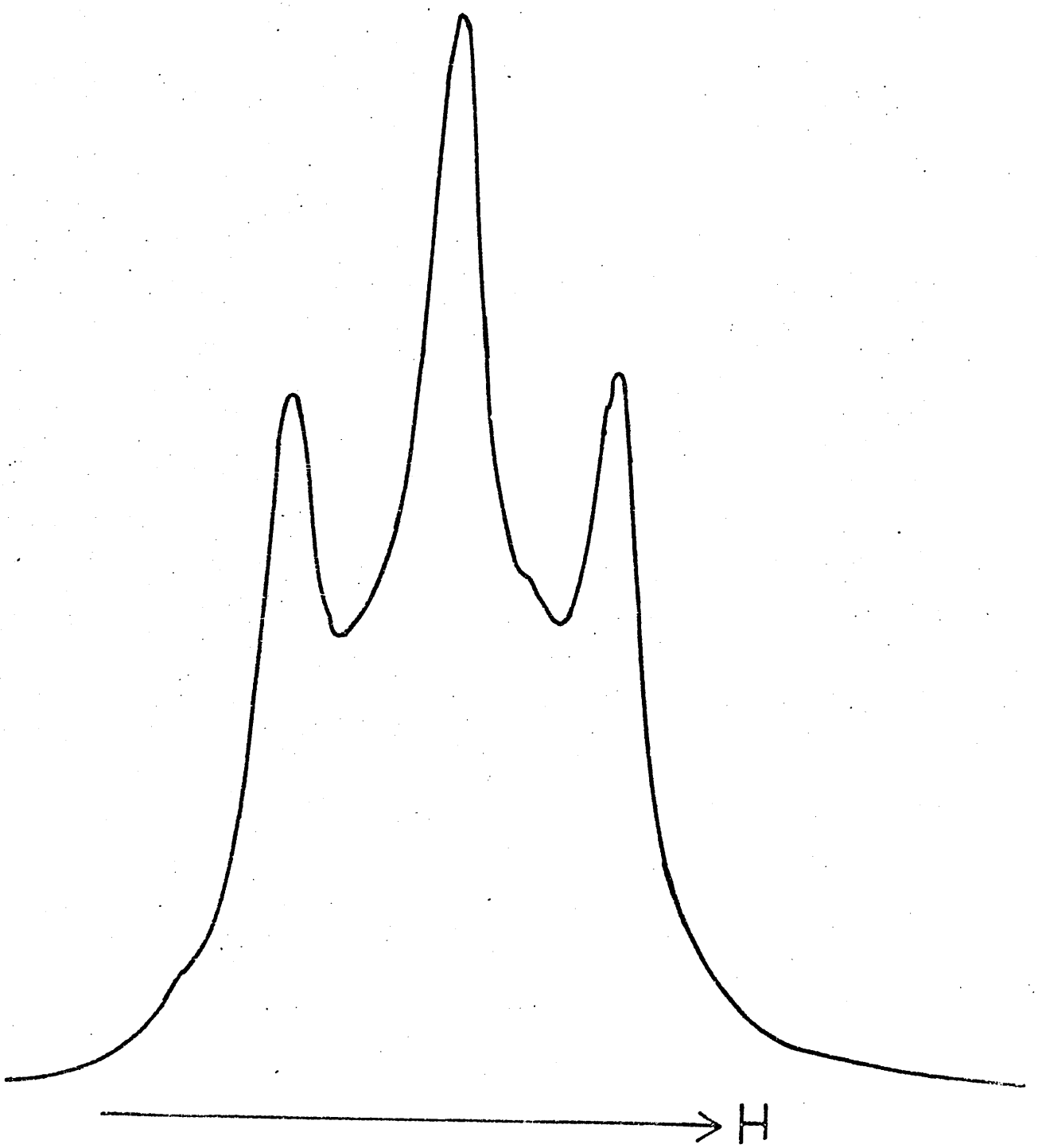

Fig 10 $HgCl_2$ 2: $P(NMe_2)_3$: 100 MHz(273°K) ^1H NMR

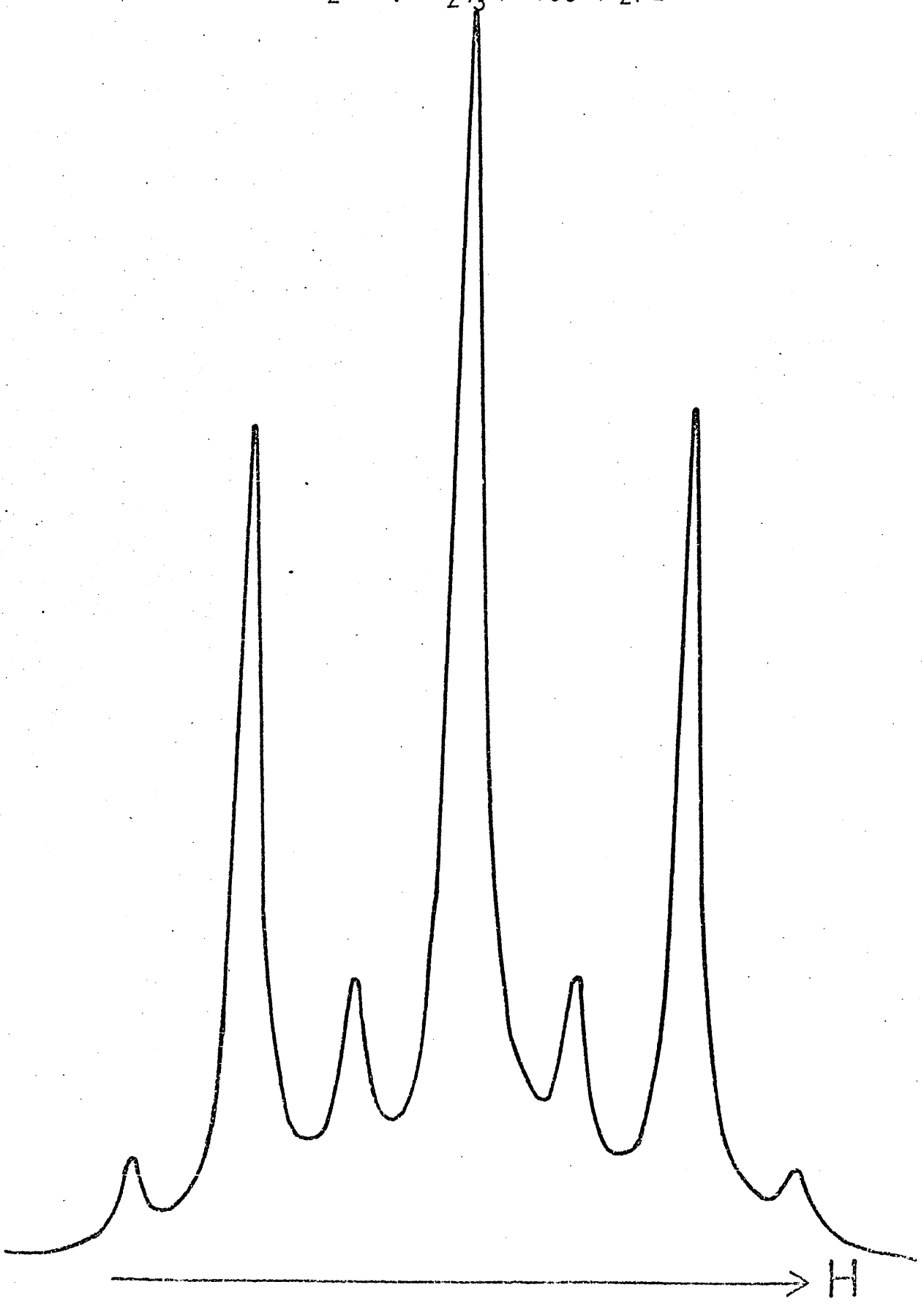

can be represented qualitatively by

$$I > Br > Cl.$$

^{13}C N.M.R. Spectra.

^{13}C n.m.r. parameters of the following complexes are shown in Table 25 $MX_2P(NMe_2)_3$, (M = Zn, X = Cl; M = Hg, X=Cl, Br, I) and $MX_2 2P(NMe_2)_3$ M = Zn, X = Cl; M = Hg, X = Cl, Br, I: M = Pt, X = Cl). The ^{13}C n.m.r. parameters will be discussed in detail on Page 130.

$ZnCl_2P(NMe_2)_3$

The ^{13}C spectrum (298^{o}K) showed a central doublet (E) of separation $^{2}J_{(^{13}C-^{31}P)}$, a highfield doublet (F) of separation $^{2}J_{(^{13}C-^{31}P)}$ and a low field singlet (G) consistent with three doublets obtained in the ^{1}H spectrum. The results indicate that three N-methyl carbons are in different chemical environments.

$HgX_2P(NMe_2)_3$

A doublet (E) of separation $^{2}J_{(^{13}C-^{31}P)}$ is obtained in the ^{13}C spectrum of each of these complexes consistent with the equivalence of all N-methyl carbons. This is consistent with the doublet observed in the ^{1}H spectrum which indicates that all N-methyl protons are equivalent.

$ZnCl_2 2P(NMe_2)_3$

A doublet (E) of separation $^{2}J_{(^{13}C-^{31}P)}$ and singlet (F) are obtained in the ^{13}C spectrum consistent with the two doublets obtained in the ^{1}H spectrum.

$CdCl_2 2P(NMe_2)_3$

The ^{13}C spectrum showed a broad singlet (E) (width at 1/2 height = 10.0 Hz) consistent with the doublet observed in the ^{1}H spectrum. On exposure of the sample solution to air for 10 min., there was no change in the ^{13}C spectrum

indicating that any possible hydrolysis of the product had no detectable effect on the spectrum.

$HgX_2 2P(NMe_2)_3$

A broad singlet (E) was obtained in all the ^{13}C spectra (widths at 1/2 height: 12.0 Hz, X = Cl; 10.0 Hz, X = Br; 5.0 Hz, X = I).

$PtCl_2 2P(NMe_2)_3$

The ^{13}C spectrum (298°K) is a deceptively simple triplet centred at 38.9 ppm. It has been demonstrated[139] that for transition metal phosphine complexes in which two mutually trans phosphine ligands containing α-methyl or methylene groups are co-ordinated to the same metal ion the $^{13}C-\{^1H\}$ multiplet of the α-methyl or methylene carbon can be a triplet depending on the phosphorus-phosphorus couplings. For such systems the spin system for the ^{13}C nuclei is AXX^1 (A = ^{13}C, X = ^{31}P) because of the very low natural abundance of ^{13}C as contrasted with the $A_nXX^1A_n^1$ spin system for the ^1H nuclei in such complexes. The condition for the observation of a triplet in the $^{13}C-\{^1H\}$ spectrum for the AXX^1 spin systems are either

(1) $|J_{AX} - J_{AX^1}|^2 < 8\, J_{XX^1}\, \Delta\nu_{1/2}$ where $\Delta\nu_{1/2}$ is the resolving power of the instrument or

(2) $|J_{PC} - J_{PC^1}|^2 < |J_{PH} - J_{PH^1}|^2$

Computer simulations[139] of an AXX^1 spin system where J_{AX} = 25 Hz, J_{AX^1} = 3 Hz and J_{XX^1} is varied from 0.0 Hz to 500 Hz indicated that for a $^{13}C-\{^1H\}$ spectrum of a complex a triplet should be observed only when $^2J_{PMP}$ is large (Ca 50 Hz).

This explains the observation of a 'triplet' in the $^{13}C-\{^1H\}$ spectrum of $PtCl_2 2P(NMe_2)_3$ ($^2J_{PMP}$ = 755 Hz).[113]

II. Chemical Shifts.

Introduction.

The three main contributions to the screening constant (σ) for a particular nucleus, N, has been expressed as [140]

$$\sigma_N = \sigma_N^{dia} + \sigma_N^{Para} + \sum_{B \neq N} \sigma_N^{NB}$$

The diamagnetic contribution (σ_N^{dia}) comes from the induced circulation of the inner electron cloud surrounding the nucleus in question which generates a magnetic field opposed to the applied field B. This results in shielding of the nucleus by the electrons from the field. It varies with change in chemical environment of the nucleus.

The paramagnetic contribution (σ_N^{Para}) comes from the induced circulation of the bonding electrons about the atom which generates a magnetic field in the same direction as the applied field B, the result of which is the deshielding of the nucleus, i.e. σ_N^{Para} always produces a shift to low field and is negative.

The σ_N^{NB} terms describe the magnetic field at the site of N produced by induced currents of electrons at neighbouring atoms or functional groups B, often called "neighbouring anisotropy effects". One source of neighbouring anisotropy effect in aromatic systems is the ring current anisotropy arising from the circulating electronic ring current in the conjugated pi bond on the aromatic system.

Other contributions to the chemical shifts may also come from solvent effects.

Results and Discussion.

^1H chemical shifts cover a narrow range (20 ppm). The diamagnetic term gives the major contribution to ^1H chemical shifts.

Table 28 [79] below shows the ^1H chemical shifts, δ_H, for some tris(dimethylamino)phosphine and tris(phenyl methylamino)phosphine complexes. An examination of the ^1H chemical shifts in Table 28 indicates that in general there is a deshielding of the N-methyl protons on co-ordination of phosphorus to a metal.

The ^1H chemical shifts of the tris(dimethylamino)phosphine complexes investigated here are shown in Table 21. The values for $ZnCl_2P(NMe_2)_3$, $ZnBr_2P(NMe_2)_3$ are obtained from the 220 MHz ^1H spectrum while that of $ZnI_2P(NMe_2)_3$ is obtained from the 100 MHz spectrum. This is because the ^1H spectra for $ZnCl_2P(NMe_2)_3$, $ZnBr_2P(NMe_2)_3$ are poorly resolved at 100 MHz. These results reveal that the ^1H chemical shifts for all the complexes shift to lower field relative to the free ligand value denoting deshielding of the N-methyl protons.

^1H n.m.r. of $P(NMe_2)_3$ in $CDCl_3$ indicates negligible change in the ^1H chemical shift compared to that of the neat $P(NMe_2)_3$. Therefore the observed deshielding of the N-methyl protons in the complexes is assumed not to be due to solvent effects and probably arises from an inductive change on co-ordination of phosphorus to a metal. The transmitted inductive effect causes a decrease in electron density about the N-methyl protons resulting in resonance at lower field.

Similarly in $PhP(NMe_2)_2HgCl_2$, δ_H is at 2.90 ppm compared to the free $PhP(NMe_2)_2$ value of 2.68 ppm (Table 24).

Table 28[79]

^1H n.m.r. Data for some Compounds of $P(NMe_2)_3$ and $P[N(CH_3)(C_6H_5)]_3$

Compound	$^3J_{PH}$ (Hz)	$\delta_{H(ppm)}$	Solvent
$P(NMe_2)_3$	8.8	2.42	neat
$P[N(CH_3)(C_6H_5)]_3$	2.8	2.67	$CDCl_3$
trans-$Cr(CO)_4 2P(NMe_2)_3$	9.84	2.65	C_6H_6
cis- $Mo(CO)_4 2P(NMe_2)_3$	10.9	2.60	C_6H_6
cis-$Mo(CO)_4 2P[N(CH_3)(C_6H_5)]_3$	9.2	3.10	$CDCl_3$
trans-$Mo(CO)_4 2P(NMe_2)_3$	10.1	2.67	C_6H_6
trans-$W(CO)_4 2P(NMe_2)_3$	10.4	2.56	C_6H_6
trans-$Fe(CO)_3 2P(NMe_2)_3$	9.6	2.67	C_6H_6
$Ni(CO)_4 2P(NMe_2)_3$	9.3	2.47	C_6H_6
cis-$PdCl_2 2P(NMe_2)_3$	9.7	2.63	C_6H_6
trans-$PdI_2 2P(NMe_2)_3$	10.3	2.40	C_6H_6
cis-$PtCl_2 2P(NMe_2)_3$	9.4	2.78	CH_2Cl_2
trans-$PtCl_2 2P(NMe_2)_3$	10.1	2.83	CH_2Cl_2
trans-$PtI_2 2P(NMe_2)_3$	10.0	2.81	CH_2Cl_2
$HgI_2 2P(NMe_2)_3$	Broad	2.83	$CDCl_3$
$OP(NMe_2)_3$	9.30	2.62	neat
$OP[N(CH_3)(C_6H_5)]_3$	11.0	2.62	

^{31}P Chemical Shifts.

Phosphorus chemical shifts cover a wide range (ca + 250 ppm e.g. Br_3P (+227 ppm) to ca 500 ppm e.g. P_4 molecule (- 450 ppm).

Various factors contribute to ^{31}P chemical shifts. These have made explanations of experimentally observed ^{31}P chemical shifts not simple, although theoretical treatments are available [141].

Meriwether and Leto [142] first studied in detail ^{31}P chemical shifts in co-ordination compounds. In order to rationalize the lower field shifts observed in complexes they considered several factors which included the following :

(a) the paramagnetic term

(b) the effect of sigma bond formation

(c) possible π-bonding between the substituent and phosphorus

(d) Aromatic ring currents in phenylphosphine complexes

(e) bond rehybridization effects because of changes in phosphorus bond angles on complex formation.

(f) electronegativity of atoms joined to phosphorus

(g) steric effects.

Some of their results are shown in Table 29.

For the tertiary phosphine complexes they [142] found the co-ordination shift, Δ, to be constant and therefore attributed the downfield co-ordination chemical shifts in the complexes compared to that of the free ligand to a strong donor sigma bond from phosphorus to nickel resulting in deshielding of the phosphorus nucleus.

For the trialkylphosphite complexes a much smaller low field shift was found (+ 20 ppm) and in phosphorus trichloride complexes high field shifts were observed. No definite conclusion was made as to the importance

Table 29

^{31}P Chemical Shifts[142] for some Nickel dicarbonyl di(phosphine) complexes.

Ligand	$\delta_{^{31}P\ ligand}$ (ppm)	$\delta_{^{31}P\ Ni(CO)_2P_2}$ (ppm)	Co-ordination Chemical Shift, $\Delta = \delta_{complex} - \delta_{ligand}$
$P(C_6H_5)_3$	-6.6	+ 32.6	+39.2
$P(C_6H_5)_2Et$	-12.0	+28.7	+40.7
$P(C_6H_5)Et_2$	-16.2	+23.2	+39.4
$P(Et)_3$	-19.1	+20.7	+39.8
$P(C_8H_{17})_3$	-31.8	+13.3	+45.1
$P(C_4H_9)_3$	-32.6	+12.1	+44.7
$PEt_2CH_2PEt_2$	-19.3	+29.9	+41.2
PCl_3	+215	+181	-34
PCl_2Ph	+164	-	
PF_3	+ 97	-	
$P(OEt)_3$	+140	+160	+20

of the paramagnetic contribution and the results in trialkylphosphite and phosphorus trichloride complexes were explained in terms of

(i) a weaker sigma bond from phosphorus to nickel

(ii) An increase in the back-donation from Ni to P, together with a strong drift of electrons from P to L where L is an alkyl or aryl substituent on phosphorus.

(iii) Variable changes in the LPL bond angles in forming the complexes resulting in large rehybridization effects.

The co-ordination chemical shift, Δ,

$$\Delta = \delta_{^{31}P\,complex} - \delta_{^{31}P\,ligand}$$

has been found generally useful in correlating the ^{31}P chemical shift of the free ligand to those of the complex[143][144]. From the correlation equation

$$\Delta = A\delta + B$$

Where A and B are constants, the various A and B values for a series of complexes of cis- and trans - L_2PdX_2 (X = Cl, N^-_3) were compared. The results indicated that the geometry of the complexes was more important than anion effects for phosphine complexes in general. Comparison of co-ordination chemical shifts where steric effects were held constant viz, for $(4 - ZC_6H_4)PMe_2$ (Z is a substituent) or varied viz, for R_2PBu^t or R_2PPh suggested that electronic effects are more important than steric effects in determining Δ[144]. It was concluded [144] that for phosphine complexes in general the co-ordination chemical shift is affected most by geometry followed by anion electronic effects and least by steric effects.

The ^{31}P chemical shifts obtained from double resonance experiments and the co-ordination chemical shifts, Δ, are shown in Table 26 for the compounds in the present study. It is seen that the co-ordination chemical

shifts of all the complexes except $HgCl_2 2P(NMe_2)_3$ are to high field indicating increased shielding of the ^{31}P nucleus.

The upfield Δ values observed may be attributed to some combination of the following factors :

(1) Increased nitrogen to phosphorus $p_\pi \longrightarrow d_\pi$ bonding resulting from increased positive charge on phosphorus on co-ordination of phosphorus to a metal ion.

(2) The paramagnetic contribution to the shielding constant.

This is given by an expression of the form (145)

$$\sigma^P = -\frac{1}{\Delta E}(Q_p + Q_d)$$

where ΔE is the average electronic excitation energy of states $p_x \longrightarrow p_y$ x and y being different p orbital directions and Q_p and Q_d depend on the electron imbalance in the various p and d orbitals centred on the ^{31}P nucleus.

(3) Bond rehybridization effects because of change in bond angles at ^{31}P on complex formation (146). However, since n.m.r. spectra are always run in solution bond angle changes in ligand on co-ordination always remain an unknown quantity, unless nematic n.m.r. is used.

(4) Steric effects arising from a bulky group on phosphorus depending on the size of the metal.

$HgX_2 2P(NMe_2)_3$ (X = Cl, I)

The low Δ value observed in $HgCl_2 2P(NMe_2)_3$ (Table 26) possibly indicate a reduction of previous upfield effect because the latter is shared between two phosphorus atoms.

No Δ value was obtained for $HgI_2 2P(NMe_2)_3$ because of instrumental difficulties at low temperature. ^{31}P decoupling experiment on the broad ^1H resonance of $HgI_2 2P(NMe_2)_3$ ($298^\circ K$, width at 1/2 height = 10.6 Hz)

indicated the absence of ^{1}H-^{31}P nuclear spin coupling.

$ZnX_2P(NMe_2)_3$, $CdCl_2P(NMe_2)_3$, and $HgCl_2PhP(NMe_2)_2$

By comparison of the Δ values for the $ZnX_2P(NMe_2)_3$ series (Table 26) the unsymmetrical structure is tentatively assigned to the component (A) with the smallest absolute value of Δ while the other absolute values of Δ are tentatively assigned to the cis - or trans - (B or C) symmetrical isomers. The percentages of the isomers have been calculated from the integrated areas in the ^{1}H n.m.r. It is rather surprising on account of the bulky nature of the ligand that the component (A) assigned to the unsymmetrical structure should be present in the highest percentage, since models of these complexes show that there is a high steric crowding among the N-methyl groups. It is relevant that the absolute value of Δ for the main doublet (A) in $ZnCl_2P(NMe_2)_3$ ($|\Delta|$= 29.3 ppm) determined from the ^{1}H spectrum by double resonance is very close to the value for component (A) in $ZnCl_2P(NMe_2)_3$ ($|\Delta|$ = 32.9 ppm).

Grim et al [137] observed two peaks ($\delta_{^{31}P}$ =+7.3 and + 19.4 ppm) of unequal intensities (60 : 40) with the corresponding ^{199}Hg satellites in methylene chloride solution in the ^{31}P n.m.r. of $(Bu_3P)_2Hg_2I_4$. This result was interpreted to indicate the existence of two structures in equilibrium. The upfield peak in the ^{31}P spectrum was tentatively assigned to the cis-symmetrical isomer or the unsymmetrical isomer while the low field peak was assigned to the trans-symmetrical structure. However, no evidence was given for the assignments.

The ^{31}P ^{1}H n.m.r. spectra of the $ZnX_2P(NMe_2)_3$ complexes each showed a single broad resonance possibly because of broadening by the ^{14}N quadrupole and no separate resolved resonances. The results are as follows :

Compound	$\delta^{31}P$ ppm	width at 1/2 height (Hz)
$ZnCl_2P(NMe_2)_3$	88.7	20
$ZnI_2P(NMe_2)_3$	71.2	60

It is noted that the ^{31}P chemical shifts of the major components in $ZnX_2P(NMe_2)_3$ (X = Cl, I) complexes (Table 26) are the same (within experimental error) as those obtained directly from the ^{31}P spectrum. It is interesting that Δ value for the B species in $ZnCl_2 2P(NMe_2)_3$ (Δ = - 94.8 ppm) is very close to the value for the B component in $ZnCl_2P(NMe_2)_3$ (Δ = - 93.9 ppm) This will be discussed further under

(1) $^1H-^{31}P$ nuclear spin coupling constants (Page 132)

(2) ^{13}C chemical shifts (Page 130)

(3) $^{13}C-^{31}P$ coupling constants. (Page 136)

For $CdCl_2P(NMe_2)_3$ the co-ordination chemical shifts of the two species are 92.5 and 109.5 ppm to high field which are in the same range as the values observed for the B and C isomers respectively in $ZnX_2P(NMe_2)_3$ complexes.

For $HgCl_2PhP(NMe_2)_2$, Δ is 10 ppm downfield of the free $PhP(NMe_2)_2$.

^{199}Hg Chemical Shifts.

^{199}Hg chemical shifts vary over a large range. Some selected examples are given in the Table below[95].

Compound	^{199}Hg Chemical Shift* ppm
$(CH_3)_2Hg$ (neat liquid in 5% benzene)	2,437
$HgCl_4^{2-}$ (sat'd, H_2O)	1,144
$HgBr_4^{2-}$ (sat'd, H_2O)	553
HgI_4^{2-} (0.5M, H_2O)	-920
$HgCl_2$ (0.25M, ethanol)	895

* Chemical shifts with respect to a 0.5 M solution of $Hg(OCO\,CH_3)_2$ in 1.05M CH_3CO_2H.

Increasing positive values correspond to decreasing shielding.

^{199}Hg chemical shifts are very much dependent on the solvent and the temperature. However, little is known about the relationships between structure and ^{199}Hg chemical shifts.

The mercury chemical shifts measured in this work are shown in Table 27. Because of the limited data no further discussions on these will be made.

^{13}C Chemical Shifts.

^{13}C chemical shifts vary over a large range of ca 200 ppm e.g. for trans (CO) group in $Ph_3PMo(CO)_5$ $\delta_{(^{13}C)}$ is at 211.0 ppm and for cis (CO) it is at 206.5 ppm [147]

Like ^{31}P chemical shifts, the dominant contribution to most ^{13}C chemical shifts is the paramagnetic term. The paramagnetic contribution to the shielding constant, σ, is given by [148]

$$\sigma_N^{Para} = \frac{-e^2h^2}{2m^2c^2}\left(\Delta E\right)^{-1} \left\langle r^{-3}\right\rangle_{2p} \left[Q_{NN} + \sum_{B\neq N} Q_{NB}\right]$$

where (i)e is the electronic charge, h Planck's constant m mass of the electron, c velocity of light.

(ii) Δ E is the mean electronic excitation energy of states $P_x \longrightarrow P_y$ (x and y being different p-orbital directions). A low value for Δ E causes deshielding.

(iii) $\left\langle r^{-3}\right\rangle_{2p}$, the mean value of the inverse cube of the distance between a 2P electron and the nucleus (r is the distance of a p electron from the ^{13}C nucleus). This term depends primarily on the effective nuclear charge at ^{13}C. Increase in effective nuclear charge at the

N-methyl carbons will contract the 2p orbitals, with accompanying decrease in r. The associated increase in $\langle r^{-3} \rangle_{2p}$ factor will result in deshielding of the N-methyl carbons.

(iv) Q_{NN}, the imbalance of electron densities in the various p orbitals centred on the carbon atom. For an atom or ion in a symmetrical environment Q_{NN} has a minimum value of zero. The maximum value of Q_{NN} ($Q_{NN\ max} = 2$) occurs when two p orbitals are filled and one is empty or one filled and two empty.

(v) ΣQ_{NB} measures the relative importance of sigma vrs pi bond character in the molecular orbital description of the unexcited molecule and is zero if pi bond order is zero.

^{13}C chemical shifts also depend on the inductive effect of substituents. Table 25 shows ^{13}C chemical shifts of the complexes.

It can be seen that there are two distinct ^{13}C chemical shift ranges :

(1) ^{13}C shifts to high field (ca 37.0 to 37.9 and 34.9 ppm) relative to the free $P(NMe_2)_3$ value [149] ($\delta_{(^{13}C)}$ = 38.3 ppm)

^{13}C shifts to low field (ca 38.6 ppm)

The observed shifts cannot be easily rationalized since the magnitude of the various factors outlined earlier are not known.

$ZnCl_2P(NMe_2)_3$, $ZnCl_2 2P(NMe_2)_3$ and trans-$PtCl_2 2P(NMe_2)_3$

The values for $ZnCl_2P(NMe_2)_3$, component (E) ($\delta_{(^{13}C)}$ = 37.0 ppm) and $ZnCl_2 2P(NMe_2)_3$, component (E) ($\delta_{(^{13}C)}$ = 37.5 ppm) suggest species in solution in which $P(NMe_2)_3$ is bonded to the metal ions since these values are close to the range 37.4 to 37.9 ppm observed in $HgX_2P(NMe_2)_3$ and $HgX_2 2P(NMe_2)_3$. The latter complexes have been shown in this work to contain metal-phosphorus bonds.

The resonance at 38.6 ppm for $ZnCl_2P(NMe_2)_3$ (Component G) corresponds to a species in solution with probably a metal-phosphorus bond since trans-$PtCl_2 2P(NMe_2)_3$ ($\delta_{(^{13}C)}$ = 38.9 ppm) has been shown here and elsewhere[113] to contain a platinum-phosphorus bond.

The similarity of the ^{13}C shifts in $ZnCl_2P(NMe_2)_3$, component (F) ($\delta_{(^{13}C)}$ = 34.8 ppm) and $ZnCl_2 2P(NMe_2)_3$, component (F), ($\delta_{(^{13}C)}$ = 34.9 ppm) indicate that they are probably similar species in solution. These will be discussed further under ^{13}C - ^{31}P nuclear spin coupling constants (page 136)

III. Nuclear Spin Coupling Constants.

The Fermi contact interaction is considered to be the main factor determining the magnitude of the nuclear spin coupling constant between interacting nuclei [150]. The magnitude of this coupling, among other factors, is proportional to the product of the electron densities in the S valence orbitals of the interacting nuclei.

^1H - ^{31}P Nuclear Spin Coupling Constants.

The results obtained in this work are shown in Table 21. The range of ^1H - ^{31}P nuclear spin coupling constants in some phosphorus compounds are summarised in the Table below.

Type of Compound	Example	$J_{(PH)}$ Hz			
		$^1J_{(PH)}$	$^2J_{(PH)}$	$^3J_{(PH)}$	Ref
P^{III} - H		180 to 225			
	PH_3	179			100
P^{III} - CH_3			1-5		
	$P(CH)_3$		2.7		100
P^{III} - O - CH_3				6-15	
	$CH_3OP(CH_3)_2$			10.9	100
P^{III} - N-CH	$P(NMe_2)_3$			8.8	70
$OP^{(V)}$ - N-C-H	$OP(NMe_2)_3$			9.3	70

Phosphorus co-ordination to groups more electronegative than nitrogen introduces a net positive charge on to the phosphorus. The increase in nitrogen to phosphorus $2p_\pi \longrightarrow 3d_\pi$ bonding results in a net positive charge on the nitrogen atom which polarizes the electron cloud in the C-H bond. Thus the effective nuclear charge on the proton is increased and the C-H bond acquires more S-character. Alternatively, since the S-character of an atom tends to concentrate in orbitals that the atom uses towards more electropositive groups[151] the S-character in the P-N bond is expected to increase on phosphorus co-ordination to a metal. Therefore, if phosphorus co-ordination occurs, $^3J_{(P-N-C-H)}$ is expected to increase in all the complexes. It is seen (Table 21) that $^3J_{(P-N-C-H)}$ essentially increases in all the complexes. The observed increase probably indicates that there is no nitrogen co-ordination in the complexes as this would make $^3J_{(PH)}$ small (cf $^3J_{(PH)}$ = 0 in $Me_2NPMe_2AlEt_3$[72]). However, other factors

may also be involved.

In $P(NMe_2)_3$ and $P(N(Me)(C_6H_5))_3$ complexes (Table 28) in which the phosphorus is co-ordinated to metals increased values of $^3J_{(PH)}$ of between 0.3 and 10.1 Hz relative to the free ligand values of 8.8 and 2.8 are also observed.

$ZnX_2P(NMe_2)_3$ (X = Cl, Br,I)

The observed increase in $^3J_{(PH)}$ values for A,B,C components (Table 24) indicate that these species probably contain metal-phosphorus bonds based on the earlier arguments for phosphorus co-ordination.

In a control experiment for $ZnI_2P(NMe_2)_3$ previously described (page 102) the two doublets had $^3J_{(PH)}$ values of 9.5 and 11.3 Hz indicating two complexes in solution with metal-phosphorus bonds.

$ZnCl_22P(NMe_2)_3$.

In a previous study [81] a broad resonance in the ^1H spectrum was reported for $ZnCl_22P(NMe_2)_3$ but the spectral width was not given. The low $^3J_{(PH)}$ value (8.6Hz) observed in the present work cannot be accounted for.

The increased $^3J_{(PH)}$ values observed for the other tris(dimethylamino)-phosphine complexes (Table 21) are in the range of those observed earlier[81] for these complexes ($^3J_{(PH)}$, 9.5 to 11.6 Hz).

$HgCl_2PhP(NMe_2)_2$

$^3J_{(PH)}$ is 12.5 Hz (Table 24) compared with the free ligand value of $^3J_{(PH)}$ = 6.0 Hz.

Metal-phosphorus coupling Constants.

The metal-phosphorus coupling constants of the complexes are shown in Table 27.

I.r. studies and molecular weight measurements[152] indicated that mercury salts of the type

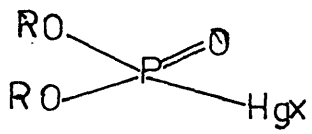

(R = Et, X=Cl, R=Pr^i, C=Cl, and Br, R=Bu^n, X=Cl, and Br) have the dimeric structure

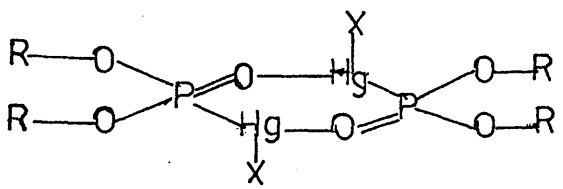

For these series of compound the directly bonded ^{31}P - ^{199}Hg coupling constants[153] are given in Table 30 below;

Table 30

$^{1}J_{(Hg-P)}$ Values for $HgX(EtO)_2PO$ Complexes[153]

X	$^{1}J_{(Hg-P)}$ Hz
$MeCO_2$	12,970
Cl	12.670
Br	12,240
I	1,180
$(EtO)_2PO$	7,500

The observed ^{199}Hg-^{31}P coupling constants for the mercury complexes in this work (Table 27) are also in the range of directly bonded ^{199}Hg-^{31}P

coupling constants observed[137] for L_2HgX_2 and $L_2Hg_2X_4$ ($L = Bu_3P$, Bu_2PhP, $BuPh_2P$, etc. X=Cl,Br,I) complexes $^1J_{(^{199}Hg-^{3}P)}$ = 3,726 to 6,627 Hz).

Although $^1J_{(Hg-^{31}P)}$ has not been measured in $HgBr_2 2P(NMe_2)_3$ it is expected to be in the same range as for $HgCl_2 2P(NMe_2)_3$. These results (Table 27) indicate that $HgX_2P(NMe_2)_3$ (X = Cl, Br,), $HgX_2 2P(NMe_2)_3$ (X = Cl,Br) contain metal-phosphorus bonds.

In <u>trans</u> - $PtCl_2 2P(NMe_2)_3$ $^1J_{(^{195}Pt-^{31}P)}$ is 3,188 Hz in agreement with previous measurements[113] (3,190 Hz).

$^{13}C - ^{31}P$ Coupling Constants $^2J_{(^{13}C-^{31}P)}$

The results are shown in Table 25.

$^2J_{(^{13}C-^{31}P)}$ values in all the complexes show a decrease. It is relevant that $^2J_{(^{13}C-^{31}P)}$ decreases in $OP(NMe_2)_3$ ($^2J_{(PC)}$ = + 2.2 Hz) relative to the free $P(NMe_2)_3$ value ($^2J_{(PC)}$ = + 19.4 Hz).[79]. The decrease observed in all the complexes implies that the mean electronic excitation energy approximation, ΔE, in the expression for nuclear spin coupling between bonded atoms does not apply to $^2J_{(^{13}C-^{31}P)}$ in these compounds. Therefore detailed discussion on the observed decrease cannot be made.

$HgX_2P(NMe_2)_3$

The observed $^2J_{(^{13}C-^{31}P)}$ values in $HgX_2P(NMe_2)_3$ complexes ($^2J_{(^{13}C-^{31}P)}$ = + 8.3 to + 7.4 Hz, Table 25) are greater than the observed values in the phosphorus (IV) compounds $OP(NMe_2)_3$ ($^2J_{^{13}C-^{31}P}$ = +2.2 Hz) and trans-$PtCl_2 2P(NMe_2)_3$ ($^2J_{^{13}C-^{31}P}$ = + 3.5 Hz, Table 25) indicating that

$HgI_2P(NMe_2)_3$ also contains a Hg-P bond. From the INDOR spectra (page 110) these complexes have the skeletal structures

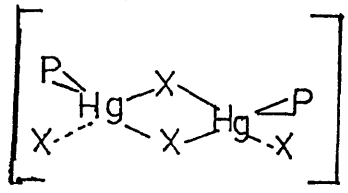

or

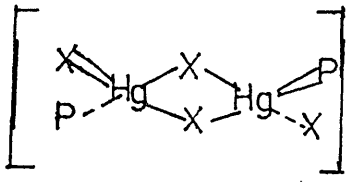

$HgX_2 2P(NMe_2)_3$ and $CdCl_2 2P(NMe_2)_3$

The spectral width at 1/2 height in the ^{13}C spectrum of each complex is shown below:

Compound	Width at 1/2 height (Hz)
$HgCl_2 2P(NMe_2)_3$	12.0
$HgBr_2 2P(NMe_2)_3$	10.0
$HgI_2 2P(NMe_2)_3$	5.0
$CdCl_2 2P(NMe_2)_3$	10.0

The broad ^{13}C resonance in each of these compounds is probably due to ligand exchange. The $^2J_{(^{13}C-^{31}P)}$ values are expected in the range 8.3 to 2.2 Hz. However, because of the width of the resonances the $^{13}C-^{31}P$ nuclear spin couplings are not resolved. (ie $^2J_{^{13}C-^{31}P}$ is less than 1/2 the measured line width).

$ZnX_2P(NMe_2)_3$

The $^2J_{(^{13}C-^{31}P)}$ value of 8.2 Hz in the ^{13}C spectrum of $ZnCl_2P(NMe_2)_3$ is in the range of values observed in $HgX_2P(NMe_2)_3$ complexes (Table 25). Therefore this component is tentatively assigned either the trans-symmetrical or the cis-symmetrical structure. Similarly, the $^2J_{(^{13}C-^{31}P)}$ value of 6.2 Hz may also be tentatively assigned either structure. The resonance at 38.6 ppm for $ZnCl_2P(NMe_2)_3$ (width at 1/2 height = 4.9 Hz) may be tentatively assigned the unsymmetrical structure.

$ZnCl_2 2P(NMe_2)_3$

The $^2J_{(^{13}C-^{31}P)}$ value of 6.4 Hz ($\delta_{(^{13}C)}$ = 34.9 ppm) is close to one value in $ZnCl_2P(NMe_2)_3$ ($\delta_{(^{13}C)}$ = 34.8 ppm, $(^2J_{(^{13}C-^{31}P)}$ = 6.2 Hz) and therefore both species possibly have similar structure. It is not possible to make any structural assignment for the resonance at $\delta_{^{13}C}$ = 37.5 ppm (width at 1/2 height = 10.1 Hz).

No evidence is obtained in the ^{13}C spectrum as to the presence of free $P(NMe_2)_3$ in $CDCl_3$ solution of $ZnCl_2 2P(NMe_2)_3$.

The tentative structural assignments from n.m.r. studies are summarized in Table 31.

Table 31

Tentative Structural assignments from n.m.r. studies for some $P(NMe_2)_3$ Complexes.

Complex	$\delta_{(^{13}C)}$ ppm	$^2J_{(^{13}C-^{31}P)}$ Hz	Tentative structural assignments
$MX_2P(NMe_2)_3$ M = Hg X= Cl, Br, I.	37.4 to 37.6	8.3 to 7.4	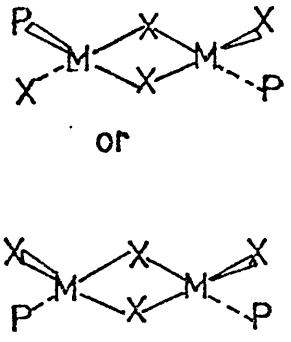
$HgX_2 2P(NMe_2)_3$ X= Cl, Br, I	37.6 to 37.9	< 6.0 to 2.5	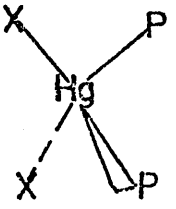
$CdX_2 2P(NMe_2)_3$ X = Cl	37.5	<5.0	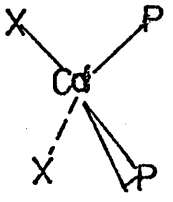

Table 31 (Cont)

Tentative Structural assignments from n.m.r. studies for some $P(NMe_2)_3$ Complexes.

Complex	$\sigma_{(^{13}C)ppm}$	$^2J_{(^{13}C-^{31}P)}$ Hz	Tentative structural assignments
$MX_2P(NMe_2)_3$ M = Zn; X = Cl	38.6		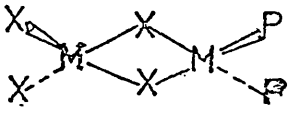
	37.0 and 34.8	8.2 and 6.2	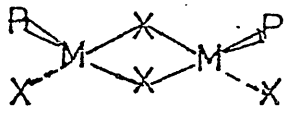 and 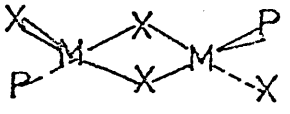
$MX_22P(NMe_2)_3$ M = Zn X = Cl	37.5		unassigned
	34.9	6.4	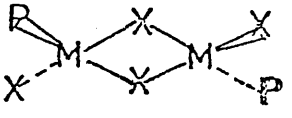 or 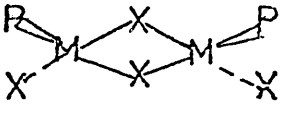

CHAPTER FOUR

COMPLEXES OF TRIS(2-PYRIDYL)PHOSPHINE AND TRIS(2-PYRIDYL)PHOSPHINE SULPHIDE.

I. EXPERIMENTAL

Experimental methods are the same as in Chapter 1 except the following :

Preparation of tris(2-pyridyl)phosphine (154)(155)

The synthesis of n-butyl lithium from n-butyl chloride and metallic lithium did not proceed at room temperature as described by Wibaut and Collegues(154).

A three-necked round-bottomed flask was fitted with a reflux condenser, a quick-fit dropping funnel, and a nitrogen inlet and outlet. The reaction vessel was protected from moisture by calcium chloride tubes. Dry anhydrous ether (50 ml) and finely divided lithium (1 gm, 0.15 gm atom) were introduced into the reaction vessel. While stirring magnetically under nitrogen, a solution of n-butyl chloride (7 gm, 0.076 mole), previously dried with calcium chloride and redistilled, in dry ether (20 ml) was added. The reaction was heated gently from the start over a water bath and after ca 3 hrs. the reaction was virtually complete when all the lithium had dissolved.

The reaction mixture was cooled to room temperature, then to - 40°C (acetone drikold-bath). A solution of 2-bromopyridine (8 gm, 0.05 mole) in ether (20 ml), Cooled to - 40°, was added slowly dropwise to the reaction mixture with stirring (15-20 min.) to yield a dark-red coloured 2-lithio pyridine.

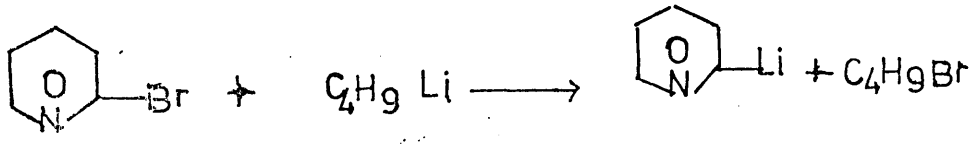

The reaction mixture was cooled to - 70° phosphorus trichloride (2.3 gm) in dry anhydrous ether (20 ml), kept at room temperature, was added from a dropping funnel (30 min.) with stirring under nitrogen. After the addition, the temperature was maintained at - 70° for a further 15 minutes.

The reaction mixture was warmed slowly to room temperature. The product was extracted with sulphuric acid (100 ml., 2M) to give a dark red product. This was made alkaline with sodium hydroxide (2M) which on repeated vigorous shaking and cooling under the tap yielded brown crystals. These when allowed to settle overnight in a refrigerator were filtered off, washed with distilled water and recrystallized from 1 : 1 MeOH : H_2O to give tris(2-pyridyl)phosphine, which was dried over silica gel in a desiccator kept at atmospheric pressure. Yield 1.0 gm. Because of the low yield repeated syntheses have to be made.

The analytical results are shown in Table 32.

The P⟶O stretch in Ph_3PO is at 1195 cm^{-1} (156). No absorption band is observed in this region in tris(2-pyridyl)phosphine which could indicate the presence of phosphine oxide as an impurity in the ligand prepared.

Tris(2-pyridyl)phosphine Sulphide (157)

Tris(2-pyridyl)phosphine (0.85 gm, 0.0032 mole) and sulphur (0.01 gm, 0.0031 mole) in dry benzene (200 CC) were stirred under nitrogen in a 100 ml. three-necked flask until all the reactants were dissolved to give a straw-coloured solution. The flask was immersed in an oil bath and the solution refluxed at about 88° for 2 hrs, cooled to room temperature and stored overnight in a refrigerator when needle-like colourless crystals separated. These were filtered off, washed with ether and the washings added to the filtrate. This yielded further crystals when stored in a refrigerator for several days. Yield 0.43 gm. Analytical data are shown

in Table 33.

Preparation of 1 : 1 Complexes of tris(2-pyridyl)phosphine with Zn(II), Hg(II) Halides.[81]

In a typical reaction, anhydrous zinc chloride (0.3435, 0.0025 mole) and tris(2-pyridyl)phosphine (0.6643 gm, 0.0025 mole) were refluxed in anhydrous ethanol (750 ml) until all the reactants had dissolved (1 hr.) to give a clear solution. After refluxing for a further ½ hr. the solution became straw-coloured. Thus colour change during refluxing was used as a criterion for complex formation. The solution was concentrated and the complex allowed to crystallize slowly out of solution at room temperature. The crude product (1.0027 gm) was recrystallized from ethanol (Yield 0.6684 gm).

Preparation of 1 : 1 Complexes of tris(2-pyridyl)phosphine sulphide with Zn(II) and Hg(II) Halides.

In a typical reaction mercury (II) iodide (0.5456 gm, 0.0012 mole) and tris(2-pyridyl)phosphine sulphide (0.3506 gm, 0.0012 mole) were refluxed in anhydrous ethanol (750 ml) until all the reactants had dissolved to give a clear colourless solution (2 hrs.). The solution was filtered hot and allowed to cool at room temperature when white feather-like crystals separated. These were filtered off and dried over silica gel in a dessicator at atmospheric pressure. Yield 0.6926 gm.

Analytical data.

The elemental analyses (Tables 32 and 33) show the metal to ligand ratio in the complexes but do not indicate whether they are dimeric or monomeric.

Molecular Weights.

The tris(2-pyridyl)phosphine complexes with Hg(II) halides were soluble only in DMSO- d_6, but insoluble in all other solvents used.

It was not possible to obtain the molecular weight of the complexes by osmometry because of their low solubilities. Attempts to obtain the molecular weights by mass spectrometry were not successful since they gave no parent ions.

N.m.r. Spectra.

The ^{1}H n.m.r. spectrum of tris(2-pyridyl)phosphine was measured as a 5% solution in deuterated dimethyl sulphoxide (DMSO- d_6) on a Varian FT XL - 100 instrument operating at 100 MHz, using 10 mm sample tubes.

The ^{1}H chemical shifts are identical to that reported previously.[158] To check the effect of solvent and concentration on the ^{1}H chemical shifts the ^{1}H spectrum was also obtained in 21% $CDCl_3$. Negligible changes in ^{1}H chemical shifts were observed.

Because the Hg(II) and Pt(II) complexes are soluble only in DMSO-d_6, ^{1}H, ^{13}C, ^{31}P n.m.r. of the complexes were run as saturated solutions in DMSO-d_6 operating at 25.2 MHz for ^{13}C, 40.5 MHz for ^{31}P and 100 MHz for ^{1}H.

Yellow crystals separated from a saturated solution of $PtI_2(Py_3P)_2$ in DMSO-d_6 when allowed to stand at room temperature for ca two days. The crystals were filtered off, dried and analysed (Found:%C : 36.6, H : 2.4; N : 8.5; P : 6.4; Hal : 26.0; Calc : C : 36.8; H : 2.5; N : 8.6; P : 6.3; Hal : 25.9). The analytical data indicated that there is probably no DMSO-Complex with PtI_2.

No n.m.r. spectra were obtained for the tris(2-pyridyl)phosphine sulphide complexes since these were insoluble in all the solvents tested.

The ZnX_2Py_3P complexes are soluble only in DMSO-d_6, but the ^{1}H and ^{13}C Spectra are too complex to be interpretable at the moment.

Table 32

Analytical Data For tris(2-pyridyl)phosphine Complexes.

Compound	Found %					Calculated %				
	C	H	N	P	Hal	C	H	N	P	Hal.
Py_3P	67.5	4.6	15.6			67.9	4.5	15.8		
$ZnCl_2Py_3P$	44.5	3.7	10.0		17.2	44.6	3.7	10.4		17.6
$ZnBr_2Py_3P$	37.7	2.9	8.5	3.6	33.6	37.9	3.1	8.7	3.2	33.4
ZnI_2Py_3P	30.9	2.1	6.8		44.0	30.8	2.1	7.1		44.4
$HgCl_2Py_3P$	33.0	2.2	7.9		12.8	33.5	2.2	7.8		13.2
$HgBr_2Py_3P$	28.9	2.4	6.9	5.1		28.8	1.9	6.7	5.1	
HgI_2Py_3P	25.1	1.9	5.6	4.5	35.6	25.0	1.7	5.6	4.3	35.4
$PtCl_2(Py_3P)_2$	43.9	3.4	10.1		8.6	44.1	3.8	10.5		8.8
$PtI_2(Py_3P)_2$	36.8	2.9	8.2	6.5	26.1	36.8	2.5	8.6	6.3	25.9

Table 33

Analytical Data for tris(2-pyridyl)phosphine Sulphide Complexes.

	Found %					Calculated %				
	C	H	N	P	Hal	C	H	N	P	Hal
Py_3PS	60.3	4.3	14.4			60.5	4.0	14.1		
$ZnCl_2Py_3PS$	41.0	3.2	9.2		16.6	41.5	2.8	9.6		16.4
$ZnBr_2Py_3PS$	34.2	2.1	8.0		30.4	34.5	2.3	8.0		30.6
ZnI_2Py_3PS	29.3	2.3	6.6		41.5	29.1	2.4	6.8		41.0
$HgCl_2Py_3PS$	31.8	2.3	7.8			31.6	2.1	7.4		
$HgBr_2Py_3PS$	27.6	2.0	6.4		24.3	27.6	1.8	6.4		24.3
HgI_2Py_3PS	24.0	1.8	5.6			23.9	1.6	5.6		

Table 34

Infrared Spectra of tris(2-pyridyl)phosphine complexes (4000-400 cm^{-1}).

Vibration / Compound	C-H Stretch ν(C-H)		C-C Stretch ν(C-C)		C-C, C-N Stretch ν(C-C, C-N)				
Py_3P	3020 vs	2990 ms	1570	1568	1450 vs	1445 vs	1425 vs	1420 vs	1410 vs
$ZnCl_2Py_3P$	3045 w		1580 vs	1568 sh	1452 vs		1424 vs		
$ZnBr_2Py_3P$	3045 ms		1586 vs	1568 sh	1460 vs	1432 vs			
ZnI_2Py_3P	3040 vs		1584 vs	1570 sh	1456 vs		1428 vs		
$HgCl_2Py_3P$	3060 bw		1570 vs	1560 sh	1448 vs			1420 vs	
$HgBr_2Py_3P$	3060 ms		1576 vs	1564 vs	1448 vs			1422 vs	
HgI_2Py_3P	3040 w		1572 vs	1562 sh	1448 vs		1424 vs		

Table 34 (Cont)

Vibration Compound	C-H Stretch ν(C-H)	C-C Stretch ν(C-C)		C-C, C-N Stretch ν(C-C, C-N)		
$PtCl_2(Py_3P)_2$	3040 vs	1572 vs	1564 sh	1452 vs	1429 vs	
$PtI_2(Py_3P)_2$	3040 vs	1572 vs	1564 sh	1452 vs		1420 vs

Table 34 (Cont)

Vibration / Compound	In plane C-H deformation β(C-H)					X-Sensitive	β(C-H)		Ring	
Py_3P	1280 vs	1275 vs	1210 ms	1150 vs	1145 vs		1080 ms	1045 vs	990 vs	985 vs
$ZnCl_2Py_3P$	1280 vs		1236 w	1160 vs			1090 vs	1056 vs	1012 vs	
$ZnBr_2Py_3P$	-	1276 vs	1240 vs	1160 vs			1088 vs	1060 vs	1016 vs	
ZnI_2Py_3P	1280 vs			1164 ms			1090 ms	1060 ms	1016 vs	
$HgCl_2Py_3P$	1284 ms				1184 w		1080 w	1044 w	988 vs	
$HgBr_2Py_3P$	1288 w				1150 w		1086 ms	1048 ms	992 vs	
HgI_2Py_3P	1282 w				1156 w		1086 w	1044 w	990 vs	

Table 34 (Cont)

Vibration / Compound	In plane C-H deformation β(C-H)			X-Sensitive	β(C-H)		Ring
$PtCl_2(Py_3P)_2$	1280 w		1152 wb	1124 sh	1084 ms	1046 w	992 vs
$PtI_2(Py_3P)_2$	1286 vs	1278 sh	1154 vs	1126 ms	1084 vs	1048 vs	992 vs

Table 34 (Cont)

Vibration Compound	Out of plane ring deformation ϕ(C-C) and out of plane CH deformation, γ(C-H)			In plane ring deformation α(C-C-C)	X- Sensitive				ϕ (C-C)
Py_3P	772 vs	747 vs	720 ms	620 vs	550 vs			433 vs	405 vs
$ZnCl_2Py_3P$	776 vs	752 w	724 w	648 ms	512 vs			432 vs	
$ZnBr_2Py_3P$	776 vs	748 vs	719 vs	644 ms	510 vs			428 vs	
ZnI_2Py_3P	772 vs		726 w	648 ms	510 vs			432 vs	
$HgCl_2Py_3P$	772 vs	744 vs		624 w.	528 vs	512 vs	504 vs	452 w	401 vs
$HgBr_2Py_3P$	770 vs	764 vs		624 w	550 w	528 vs	514 vs	452 w	400 ms
HgI_2Py_3P	772 vs	744 vs		625 w		522 sh	514 vs	440 wb	400 ms

Table 34 (Cont)

Vibration / Compound	Out of plane ring deformation ϕ(C-C) and out of plane CH deformation, γ(C-H)		In plane ring deformation α(C-C-C)	X-Sensitive			ϕ (C-C)	
$PtCl_2(Py_3P)_2$	772 vs	724 sh	620 w	560 ms	524 vs		450 wb	400 w
$PtI_2\ Py_3P$	768 vs	735 vs	620 ms	554 vs	530 vs	520 vs	456 vs	400 ms

Table 35

Infrared (I.R) and Raman (R) Spectra (4000-400 cm^{-1}) of tris(2-pyridyl)phosphine Sulphide Complexes.

Vibration / Compound		C-H Stretch ν(C-H)		ν(C-C, C-N)			β(C-H)			X-Sensitive
Py_3PS	IR	3080 vs	2980 w	1572 vs	1448 vs	1420 vs	1280 vs	1164 vs	1152 vs	1132 vs
	R			1576 w						1138 w
$ZnCl_2Py_3PS$	IR	3060 ms		1584 vs	1452 vs	1432 vs	1280 vs		1156 sh	1136 vs
$ZnBr_2Py_3PS$	IR	3060 vs	2990 w	1584 vs	1458 vs	1432 vs	1286 vs			1136 vs
	R			1594 vs						
ZnI_2Py_3PS	IR	3050 w		1580 ms	1452 ms	1428 vs	1276 w		1156 ms	1132 ms
	R			1586 ms			1277 w		1158 ms	1133 w
$HgCl_2Py_3PS$	IR	3075 wb		1574 vs	1448 ms	1424 vs	1280 w	1164 w		1128 w
	R	3075 vs		1578 vs			1288 w	1161 w		1137 ms

Table 35 (Cont)

Vibration / Compound		ν C-H Stretch	ν (C-C, C-N)			β (C-H)				X-Sensitive
$HgBr_2Py_3PS$	IR	3060 wb	1572 vs	1448 vs	1422 vs	1284 w	1280 w	1148 w		1132 vs
	R		1580 vs	1442 w				1145 vs		
HgI_2Py_3PS	IR	3040 wb	1570 vs	1444 w	1424 vs	1288 sh	1284 ms	1164 ms	1156 ms	1130 vs
	R	3060 w	1568 vs	1450 vw	1427 w	1289 w		1160 ms		1130 vs

Table 35 (Cont)

Vibration / Compound		β(C-H)			Ring	φ(C-C) and γ(C-H)				
Py_3PS	IR	1086 vs	1044 vs		988 vs	776 vs			744 vs	
	R		1034 ms		977 vs					
$ZnCl_2Py_3PS$	IR	1088 vs	1050 vs		1012 vs	780 vs	760 vs	758 vs	748 vs	732 vs
$ZnBr_2Py_3PS$	IR	1090 vs	1060 vs		1016 vs	796 ms	776 vs			732 vs
	R		1064 w		1026 vs					
ZnI_2Py_3PS	IR	1080 vs	1056 vs		1012 vs	784 ssh	770	756	744 ssh	728 ssh
	R			1058 vs	1019 vs					
$HgCl_2Py_3PS$	IR	1084 w	1044 w		990 vs	777 vs			740 vs	
	R	1097 w	1056 vs		999 vs				745 w	

Table 35 (Cont)

Vibration / Compound		ν(C-H)			Ring	φ(C-C) and γ(C-H)					
$HgBr_2Py_3PS$	IR	1084 ms		1044 w	990 vs	780 vs	764 vs	744 vs	728 vs		
	R							746 wb			
HgI_2Py_3PS	IR	1088 sh	1082 vs	1040 vs	988 vs	780 vs	772 vs	766 sh	746 vs	740 vs	728 vs
	R	1090 w		1045 vs	990 vs						734 w

Table 35 (Cont)

Vibration Compound		ν_{PS}			α(C-C-C)	X-Sensitive		X-Sensitive			ϕ(C-C)
Py_3PS	IR	684 vs			616 vs	524 vs		476 vs	444 vs		404 vs
	R		648 w		616 w						
$ZnCl_2Py_3PS$	IR		676 vs	644 vs		524 vs			448 ms	418 ms	398 ms
$ZnBr_2Py_3PS$	IR		676 vs	644 vs		532 vs			444 vs	416 m	398 ms
	R		678 ms		608 w						
ZnI_2Py_3PS	IR		672 vs	640 vs		528 vs		450 ms	440 ms	416 ms	395 ms
	R		670 vs	638 vs							
$HgCl_2Py_3PS$	IR			644 vs	630 vs	618 vs	526 sh	520 vs	444 ms		395 ms
	R			651 vs	632 sh						

Table 35 (Cont)

Vibration / Compound		ν_{PS}			α(C-C-C)		X-Sensitive		X-Sensitive			ϕ(C-C)
$HgBr_2Py_3PS$	IR		640 vs	628 vs		616 vs	524 vs	516 vs	472 ms	460 ms	436 vs	400 vs
	R		649 vs	627 ms								
HgI_2Py_3PS	IR		644 vs	630 vs	620 vs	616 vs	524 vs	516 vs	470 ms		448 vs 442 vs	400 vs
	R		640 w			611 vs						

Table 36

Far infrared Spectra (400-40 cm^{-1}) of tris(2-pyridyl)phosphine Complexes.

Compound												
Py_3P	370 w	360 w	340 w	325 w			268 m	248 m	235 w		200 m	185 msh
$ZnCl_2Py_3P$						280 w	260 wb	252 wb			208 vbs	
$ZnBr_2Py_3P$						280 vs		240 vssh		216 vssh		196 vs
ZnI_2Py_3P						280 vs		238 vs				192 vs
$HgCl_2Py_3P$	396 ms	364 w	344 w	328 w	292 vs	272 ms	260 w	244 w	224 w			184 vw
$HgBr_2Py_3P$	355 sh		335 s			280 m	255 bm	245 sh	220 w			195 s
$HgI_2\ Py_3P$	396 ms					272 w						

Table 36 (Cont)

Compound							
(Py_3) P						92 m	
$ZnCl_2Py_3P$		164 vs		136 vs		88 sh	
$ZnBr_2Py_3P$				140 ms		96 vs	
ZnI_2Py_3P	170 vs	160 sh		136 ms		94 w	
$HgCl_2Py_3P$					100 ms		
$HgBr_2Py_3P$			150 s				70 s
HgI_2Py_3P			156 ms	136 sh		92 mb	

Table 36 (Cont)

Compound											
$PtCl_2(Py_3P)_2$	396 w			324 vs	300 vs				224 vs		
$PtI_2(Py_3P)_2$									228 vs	216 vs	200 w

Table 37

Far Infrared Spectra (400-40 cm^{-1}) of tris(2-pyridyl)phosphine Sulphide Complexes.

Compound											
Py_3PS	376 w	348 ms	288 s	256 s	230 vs				150 vs		76 vsb
$ZnCl_2Py_3PS$	396 ms	372 vs	284 vsb	260 vsb	220 vsb	194 vs		164 vs		136 v	88 w
$ZnBr_2Py_3PS$	396 vs		288 vs	252 vs	200 vsb	176 sh				128 w	96 ms
ZnI_2Py_3PS	392 vs		288 vs	250 vs		192 vs	172 vsb			120 w	72 ms
$HgCl_2Py_3PS$	396 w	350 vs	288 vs	276 sh	240 vsb	192 w	184 sh			116 ms	68 vs
$HgBr_2Py_3PS$	398 vs	344 vs	288 vs	266 vs	208 ssh	200 w	184 vs	164 sh	140 w	104 w	72 w
HgI_2Py_3PS	396 vs	348 ms	286 ms	268 w	248 vs	196 sh			142 vs	108 w	88 ms

II. Infrared Spectra of tris(2-pyridyl)phosphine and tris(2-pyridyl)phosphine Sulphide Complexes.

Introduction.

da Mota et al [159] studied the i.r. spectra (1650-1550 cm^{-1}) of Ni(II) complexes with pyridine derivatives of the type

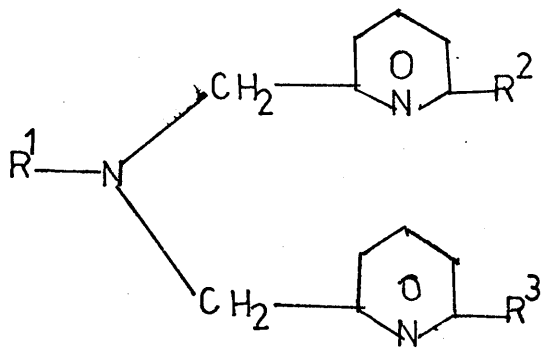

I

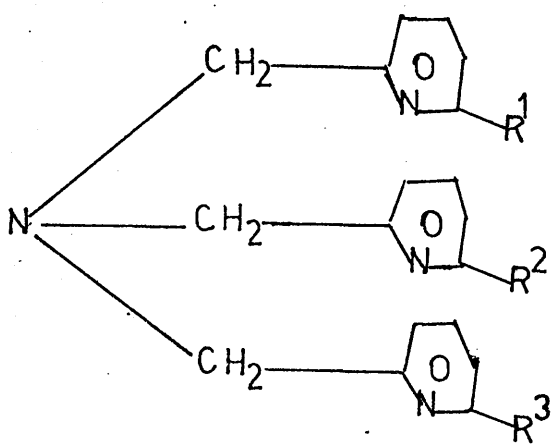

II

Where R^1, R^2, R^3 are protons or various alkyl groups.

Dalhoff et al [160] investigated i.r. spectra (1700-1400 cm^{-1}) of complexes of the type M (ligand) X_2 (M = Zn(II), Hg(II), X = Cl, Br,I) with the ligands

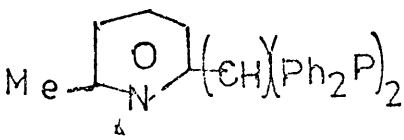

and

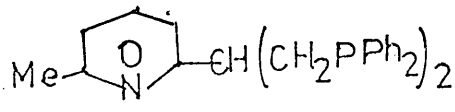

These workers [159][160] distinguished two absorption regions in the i.r. spectra (Nujol mulls) of the complexes and the free ligands. Band I corresponds to the highest energy pyridine ring deformation mode (1607-1587 cm^{-1}). Band II (1577-1567 cm^{-1}) the next highest frequency mode. They [159][160] noted that

(i) Complexes having all the constituent pyridyl nitrogen atoms co-ordinated showed two strong bands between 1650 and 1550 cm^{-1}. Band I showed an upward shift (Ca 10-20 cm^{-1}) in the complexes relative to the free ligands.

(ii) Complexes in which a pyridyl group is unco-ordinated exhibit three strong bands in the region 1650-1550 cm^{-1}, the middle one falling at the same frequency (within experimental error) as Band I in the free ligand.

Lever et al[161] described Zn(II), and Hg(II) Complexes of the types $Zn(LS)Cl_2$, Zn (LE) Cl_2, Hg_2 (LS)Cl_2, Hg_2 (LE) Cl_4, with 2-substituted pyridines

LS = 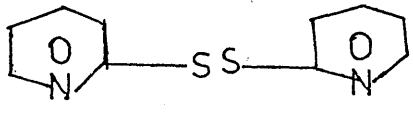 and

LE = 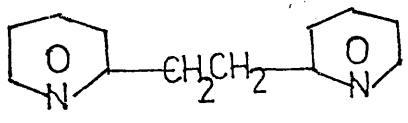

The observation [161] of two bands in the 400 cm^{-1} region both of which were shifted (Ca 5 to 36 cm^{-1}) to high frequencies relative to the free ligand values was interpreted to mean that the two pyridine residues were co-ordinated. A third class of complexes showed three or four bands in this region which were shifted (Ca 4-43 cm^{-1}) to high frequencies relative to the free ligand values and were considered [161] to arise from co-ordination by both pyridine residues but with a marked difference in the

chemical nature of the two metal-pyridine bonds.

In a previous study [81] of Zn(II) and Hg(II) halide complexes with tris(2-pyridyl)phosphine, the experimentally observed absorption bands were assigned by comparison with those of 2-Chloropyridine. Band I at 1571 cm^{-1} in the free tris(2-pyridyl)phosphine was observed to shift (Ca + 10 to + 19 cm^{-1}) to higher frequencies in the ZnX_2Py_3(X=Cl,Br,I) complexes. These were interpreted to indicate the co-ordination of all three pyridyl nitrogens. In the HgX_2Py_3P series shifts (Ca- 4 to 6 cm^{-1}) to lower frequencies were observed and were interpreted to indicate that all pyridyl nitrogens were unco-ordinated.

Triphenylphosphine Sulphide and trimethylphosphine Sulphide Complexes.

King et al [162] studied i.r. spectra (Nujol mulls) of triphenylphosphine sulphide and trimethylphosphine sulphide complexes with Pt(II), Hg(II) and Zn(II) halides. The P-S stretching frequencies in triphenylphosphine sulphide and trimethylphosphine sulphide fall by Ca - 45 to - 48 cm^{-1} and Ca - 27 to - 36 cm^{-1} relative to the free ligand values respectively on co-ordination to a metal ion. However, they [161] gave no evidence for the assigned P-S stretching frequencies (νP-S in Ph_3PS = 637 cm^{-1}; νP-S in Me_3PS = 565 cm^{-1}).

King et al [162] attributed the fall in the P-S stretching frequencies to a weakening of the secondary $3p_\pi \longrightarrow 3d_\pi$ bond between the sulphur and the phosphorus atoms by comparison with similar shifts to low frequencies (Ca - 38 to - 70 cm^{-1}) observed in triphenylphosphine oxide complexes on co-ordination of the phosphoryl oxygen to a metal [156] [163]. The decrease in νP-S could also be due to mass effects considering the S-Metal as a point mass [164]. Dalziel et al [164] assigned νP-S in triphenylphosphine sulphide at 639 cm^{-1} but gave no evidence for the assignment. Shifts (Ca - 40 to - 35 cm^{-1}) observed in the i.r. (Nujol mulls)

of HgX_2Ph_3PS (X = Cl, Br, I) complexes were used as diagnostic of a metal-sulphur bond.

Table 38

Summary of infrared spectra (4000-400 cm^{-1}) of tris(2-pyridyl)phosphine and tris(2-pyridyl)phosphine Sulphide complexes.

	C-C Stretch 1600 - 1570 cm^{-1}			P⟶S Stretch 684 cm^{-1}			Out of plane pyridine ring deformation (400 cm^{-1})		
Complex	Band in free ligand	Range of frequency shifts in Complexes relative to free ligand	Co-ordinated atom (s) Suggested by frequency shift.	Band in free ligand	Range of frequency shifts in Complexes relative to free ligand	Co-ordinated atom(s) suggested by frequency shift.	Band in free ligand	Range of frequency shifts in Complexes relative to free ligand	Co-ordinated atom(s) Suggested by frequency shift
ZnX_2Py_3P	1570	+14 to +20	3 pyridyl nitrogens				405	+23 to +28	3 pyridyl nitrogens
HgX_2Py_3P	1570	0 to +6	unco-ordinated pyridyl groups				405	0 to +1	unco-ordinated pyridyl nitrogens
$PtX_2(Py_3P)_2$	1570	+2	unco-ordinated pyridyl groups				405	0	unco-ordinated pyridyl nitrogens

Table 38 (Cont)

	C-C Stretch 1600-1570 cm^{-1}			P⟶S Stretch 684 cm^{-1}			Out of plane pyridine ring deformation (400 cm^{-1})		
Complex	Band in free ligand	Range of frequency shifts in Complexes relative to free ligand	Co-ordinated atom(s) Suggested by frequency shift.	Band in free ligand	Range of frequency shifts in Complexes relative to free ligand	Co-ordinated atom(s) suggested by frequency shift.	Band in free ligand	Range of frequency shifts in Complexes relative to free ligand	Co-ordinated atom(s) Suggested by frequency shift.
ZnX_2Py_3PS	1572	+8 to +12	3 pyridyl nitrogens	684	-8 to-12	unco-ordinated S atom	404	+10 to +14 and -6 to-9	inconclusive
HgX_2Py_3PS	1572	+2 to -2	unco-ordinated pyridyl groups	684	-50 to -56	Co-ordinated S atom	404	0 to -9	unco-ordinated pyridyl nitrogens

III. Summary of Results.

A summary of i.r. spectra (4000-400 cm^{-1}) of the complexes are shown in Table 38.

Summary of Far infrared (400-40 cm^{-1}) Spectra of tris(2-pyridyl)phosphine and tris(2-pyridyl)phosphine Sulphide complexes.

The criteria for the determination of bridging metal-halogen, ν_b(M-X and terminal metal halogen, ν_t(M-X), in the complexes are the same as those used for similar determinations in tris(dimethylamino)phosphine complexes (Chapter Two). A comparison of the ratios

$\frac{\nu_b(MX)(dimer)}{\nu_t(MX)(dimer)}$ (Table below) with

the values for the known dimeric compounds Zn_2Cl_4, $Hg_2Cl_4(PPh_3)_2$ and Al_2Cl_6 suggest that ZnX_2Py_3PS, HgX_2Py_3PS and ZnX_2Py_3P(X = Cl, Br, I) are dimeric with bridging halogens.

Compound	Range of $\frac{\nu_b(MX)dimer}{\nu_t(MX)dimer}$	Ref.
ZnX_2Py_3P	0.68 0.82	
ZnX_2Py_3PS	0.70 to 0.73	
HgX_2Py_3PS	0.60 to 0.62	
Zn_2Cl_4	0.71	128
Al_2Cl_6	0.68	128
$Hg_2X_4(PPh_3)_2$	0.62 to 0.70	22

It has not been possible to make similar assignments for HgX_2Py_3P(X = Cl, Br,I) complexes because of interference from ligand absorptions. However, from the similarity of their i.r. spectra in the regions 1580-1560 cm^{-1} and 400 cm^{-1} with those of HgX_2Py_3PS it can be inferred that HgX_2Py_3P complexes are also probably dimeric with bridging halogens.

Two very strong absorptions at 324 cm^{-1} and 300 cm^{-1} in $PtCl_2(Py_3P)_2$ with Pt-X stretches for a <u>cis</u> Pt(II) halide complex[165].

Table 39

Fundamental Vibration frequencies, cm^{-1} for Pyridine and 2-Substituted Pyridine.[166]

Assignment	Pyridine	2-Chloro Pyridine
C-H stretch,	3080	3080
ν_{CH}	3054	3057
	3036	3080
C-C stretching	1583	1577
ν(C-C)	1572	1568
C-C, C-N stretching	1482	1452
ν(C-C,C-N)	1439	1420
	1375	1363
C-H in plane	1288	1288
deformation β(CH)	1218	1150
X Sensitive	1148	1120
β(CH)	1085	1083
	1068	1048
X Sensitive	1030	727
Out of plane CH		
deformation γ(CH)	986	
Ring	992	994
Out-of-plane CH	942	960
deformation γ(CH)	891	881
	886	935

Table 39 (Cont)

Assignment	Pyridine	2-Chloro Pyridine
In plane ring deformation α(C-C-C)	652	620
X Sensitive	605	313
	405	190
Out of plane ring deformation Φ(C-C)	748,600	724,480

Discussion of Results.

Infrared and Raman Spectra (4000-400 cm^{-1}) of tris(2-pyridyl)phosphine and tris(2-pyridyl)phosphine sulphide complexes.

It has not been possible to obtain Raman spectra for tris(2-pyridyl)phosphine and complexes because the samples burnt up in the laser beam, though several attempts were made.

Green et al[166] proposed assignments for i.r. and Raman vibrational frequencies in pyridine and substituted pyridine by correlation of the observed absorption bands with the deuterated analogues and also by normal co-ordinate analysis (Table 39).

The assignment of the vibrational frequencies of a polyphenyl organometallic compound Ph_nM on the basis of assignments for the corresponding monohalogeno PhX (M and X have similar mass) is now well established.[167-171] Green et al[172] used the procedure to assign the vibrational frequencies in triphenylphosphine by comparison with those of chlorobenzene.

On this basis the correlation of the i.r. absorption bands in tris(2-pyridyl)phosphine, tris(2-pyridyl)phosphine sulphide and complexes (Tables 34 and 35) are made by comparison with the results of Green et al[166] (Table 39). However, which of the modes is symmetric or antisymmetric cannot be ascertained.

The most important regions in the i.r. spectra of the ligands and complexes from previous discussions[159][160][161][162][164] are

(1) Region 1600-1570 cm^{-1}

(2) Region 700-600 cm^{-1}

(3) Region 400 cm^{-1}

These will now be discussed.

Region 1600-1550 cm^{-1} C-C stretching modes.

For tris(2-pyridyl)phosphine the 'in phase' (C-C) stretching will produce a single mode for the highest energy pyridine ring vibration. However an 'out of phase' combination will produce a doubly degenerate mode. The magnitude of the ring-ring interaction is given by the separation (in cm^{-1}) between the single mode and the doubly degenerate mode. For tris(2-pyridyl)phosphine the highest energy pyridine ring stretching vibration is split into two components (1570 and 1568 cm^{-1}). For ZnX_2Py_3P (Table 34) and HgX_2Py_3P (Table 35) complexes, the highest energy mode is still split. This indicates that the pyridine rings are equivalent in the Zn(II) and Hg(II) complexes. Shifts (ca + 14 to + 20 cm^{-1}) in the free ligand band at 1570 cm^{-1} to higher frequencies in the ZnX_2Py_3P complexes (Table 34) are diagnostic of co-ordination of all pyridyl nitrogens to Zn(II) while that at 1568 cm^{-1} remains virtually unchanged consistent with previous investigations [81][159]. Shifts at 1570 cm^{-1} in the HgX_2Py_3P (ca 0 to 6 cm^{-1}) and $PtX_2(Py_3P)_2$ (ca + 2 cm^{-1}) compounds to higher frequencies are generally small compared with the corresponding shifts in ZnX_2Py_3P complexes (Table 34) while the 1568 cm^{-1} band shifts to lower frequencies (ca - 4 to - 8 cm^{-1}) consistent with the observation by Dalhoff et al [160]. These results indicate unco-ordinated pyridyl groups.

The i.r. spectrum of $HgCl_2Py_3P$ in DMSO-d_6 showed two strong bands at 1570 and 1560 cm^{-1} consistent with the solid state spectrum. However, the i.r. spectrum of $ZnCl_2Py_3P$ in DMSO-d_6 showed two strong bands at 1572 and 1560 cm^{-1} indicating unco-ordinated pyridyl groups.

The highest energy pyridine ring stretching mode ν(C-C) is not split in tris(2-pyridyl)phosphine sulphide. It is observed as a very strong band at 1572 cm^{-1}. It remains unsplit in ZnX_2Py_3PS and $HgCl_2Py_3PS$ complexes

(Table 35) indicating that the three pyridine rings remain equivalent in both the free ligand and the complexes. Shifts to higher frequencies (ca + 8 to + 12 and + 10 to + 18 cm^{-1}) in the i.r. and Raman spectra respectively of the bands at 1572 cm^{-1} (i.r.) and 1576 cm^{-1} (Raman) again indicate the co-ordination of all three pyridyl nitrogens (Table 35) while in the HgX_2Py_3PS negligible shifts (ca -2 to + 2 cm^{-1}) in the i.r. and Raman spectra indicate that the pyridyl nitrogens are not co-ordinated.

Region 700 - 600 cm^{-1}

Only one absorption band is observed in this region (648-620 cm^{-1}) in both the free tris(2-pyridyl)phosphine and all the complexes (Table 34).

It is expected that the P⟶S stretch in tris(2-pyridyl)phosphine sulphide will be in the same region as the P⟶S stretch in triphenylphosphine sulphide ($\nu_{P\rightarrow S}$ = 637 cm^{-1})(162). Two very strong i.r. bands (684 cm^{-1}, 616 cm^{-1}) and Raman bands (648 cm^{-1}, 616 cm^{-1}) are observed in tris(2-pyridyl)phosphine sulphide (Table 35). The band at 616 cm^{-1} is very close to the absorption at 620 cm^{-1} in tris(2-pyridyl)phosphine.

The very strong absorption at 684 cm^{-1} in tris(2-pyridyl)phosphine sulphide is absent in tris(2-pyridyl)phosphine and therefore this must be the P⟶S absorption band in tris(2-pyridyl)phosphine sulphide while the band at 616 cm^{-1} must be in the plane deformation mode, α(C-C-C), of the pyridine ring in tris(2-pyridyl)phosphine sulphide. Moreover, the band at 684 cm^{-1} moves to ca 630 cm^{-1} in the Hg(II) halide complexes (Table 35) while that at 616 cm^{-1} remains virtually unchanged in position (Table 35). However, the 616 cm^{-1} band moves to higher frequencies in ZnX_2Py_3PS complexes. The very large shifts in $\nu_{P\rightarrow S}$ (ca - 50 to 56 cm^{-1}) may be used as diagnostic of a metal-sulphur bond in the HgX_2Py_3PS complexes.

In ZnX_2Py_3PS complexes shifts (ca -8 to -12 cm^{-1}) relative to the absorption at 684 cm^{-1} were observed indicating the absence of metal-sulphur bonds.

Region 450-380 cm^{-1}

Out of plane pyridine ring deformations Φ(C-C).

Two strong i.r. absorptions 433 and 405 cm^{-1} are observed in tris(2-pyridyl)phosphine. The band at 405 cm^{-1} is often attributed to the out of plane pyridine ring deformation mode. Shifts (ca + 23 to + 28 cm^{-1}) to higher frequencies relative to the band at 405 cm^{-1} (Table 34) indicate co-ordination of all three pyridyl nitrogens in the ZnX_2Py_3P complexes. For $HgCl_2Py_3P$ and $PtX_2(Py_3P)_2$ complexes relatively no shift is observed in the position of the 400 cm^{-1} band, further indicating unco-ordinated pyridyl groups.

For tris(2-pyridyl)phosphine sulphide, Φ(C-C) is at 404 cm^{-1}. A splitting of this band into two medium strong absorptions one to a high and the other to a low frequency relative to the free ligand absorption is observed in all the ZnX_2Py_3PS (Table 35) complexes and no conclusion can be drawn as to nitrogen co-ordination in the Zn(II) complexes in this region. There is no significant change in the position of the 400 cm^{-1} band in the HgX_2Py_3PS complexes (Table 35) indicating further that the pyridyl nitrogens are unco-ordinated.

In conclusion the i.r. evidence discussed above suggests that

(1) tris(2-pyridyl)phosphine is a nitrogen donor with Class A metals and phosphorus donor with Class B metals.

(2) tris(2-pyridyl)phosphine sulphide is a nitrogen donor with Class A metals and sulphur donor with Class B metals (41)

Table 40

Tentative Assignments for metal-halogen Vibrations in tris(2-pyridyl)phosphine complexes (cm^{-1}).

Compound	$\nu_{t(M-X)}$	$\nu_{b(MX)}$	$\frac{\nu_{b(MX)}}{\nu_{t(MX)}}$
$ZnCl_2Py_3P$	164	136	0.82
$ZnBr_2Py_3P$	140	96	0.68
ZnI_2Py_3P	136	94	0.69
$HgCl_2Py_3P$	292		
$HgBr_2Py_3P$	195		
HgI_2Py_3P	156		
$PtCl_2(Py_3P)_2$	324,300		

Table 41

Tentative assignments for M-X, in tris(2-pyridyl)phosphine sulphide complexes (cm^{-1})

Compound	ν_{t} (M-X)	ν_{b} (MX)	$\frac{\nu_{b(MX)}\ (dimer)}{\nu_{t(MX)}\ (dimer)}$
$ZnCl_2Py_3PS$	220, 194	136	0.70
$ZnBr_2Py_3PS$	176	128	0.73
ZnI_2Py_3PS	172	120	0.70
$HgCl_2Py_3PS$	192, 184	116	0.60
$HgBr_2Py_3PS$	164	104	0.63
HgI_2Py_3PS	142	88	0.62

Table 42

Assignments for M-N, M-X, Vibrations in some Zn(II), Hg(II) halide complexes with pyridine, 2-substituted pyridine and terpyridine(cm^{-1})

Compound	ν_{MX}	ν_{M-N}	Co-ordination Number	Ref.
$ZnCl_2Py_2$	326	218		
	293		4	12
$ZnBr_2Py_2$	260	219	4	12
	254			
ZnI_2Py_2	210	222	4	12
$Zn(PySSPy)Cl_2$	323			161
$Hg(PySSPy)Cl_2$	328	225	4	161
$Hg_2(PyCH_2CH_2Py)Cl_4$	295	245	4	161
$Zn(terp)Cl_2$	287	244	5	173
	278			
$Zn(terp)Cl_2$	287	243	5	173
	278	222		
$Zn(terp)I_2$	187	245	5	173

IV. Far infrared spectra (400-40 cm^{-1}) of tris(2-pyridyl)phosphine and tris(2-pyridyl)phosphine sulphide complexes.

Results and Discussion.

Far i.r. spectra of tris(2-pyridyl)phosphine and tris(2-pyridyl)phosphine sulphide complexes are shown in Tables 36 and 37 respectively.

No Raman bands are observed in this region for tris(2-pyridyl)phosphine sulphide complexes. Probably they are very weak and hence not resolved.

Both tris(2-pyridyl)phosphine and tris(2-pyridyl)phosphine sulphide absorb very strongly in the region 400-40 cm^{-1}. Therefore the tentatively assigned metal-halogen vibrations are not 'pure' vibrations and probably contain some ligand vibrations.

Metal-halogen stretching Frequencies, ν_{M-X}.

The criteria for the assignment of the metal-halogen vibrations are the same as used for these assignments for tris(dimethylamino)phosphine complexes (Chapter 2). For the Zn(II) halide complexes with Py_3P and Py_3PS which have been shown in this study to be tridentate through the nitrogen atoms (hence Zn(II) is 5-co-ordinate for a monomeric complex and 6-co-ordinate for a dimeric complex) the metal-halogen stretching frequencies have been assigned on the principle that $\nu_{t(MX)}$ in 5- or 6-co-ordinate Zn(II) will be less than in the corresponding 4-co-ordinate complexes[173] if similar ligand types are involved (Tables 40, 41 and 42).

Two very strong absorptions at 324 cm^{-1} and 300 cm^{-1} in $PtCl_2(Py_3P)_2$ are correlated with Pt-Cl stretches for a square planar Pt(II) complex with cis-chlorides. For cis-$PtCl_2Py_2$, ν_{Pt-Cl} is at 343 and 329 cm^{-1}. For cis PtI_2 Py_2, ν_{Pt-I} is at 178 and 167 cm^{-1} [165]. The far i.r. spectrum of PtI_2 Py_2 is rather poor and no absorption is observed which could be correlated with Pt-I stretches. The weak absorption at 200 cm^{-1}

may be attributed to the free ligand.

The ratio of the terminal metal-halogen stretching vibration, $\nu_{t(MX)}$, to the bridging metal-halogen stretching vibration, $\nu_{b(MX)}$, for the complexes are shown in Tables 40 and 41. These are in the range for dimeric $Hg_2X_4(PPh_3)_2$ (X = Cl, Br,I) (0.62 to 0.70)[22] indicating that Zn(II) and Hg(II) complexes with tris(2-pyridyl)phosphine and tris(2-pyridyl)phosphine sulphide are dimeric with bridging halogens.

Metal-Nitrogen stretching Frequencies, ν_{M-N}.

Metal-nitrogen (pyridine) stretching frequencies with bond order of one occur in the range 300-200 cm^{-1} (128) Table 42 summarises the data for metal-nitrogen vibrations in some Zn(II) and Hg(II) complexes. However, it has not been possible to make assignments for ν_{M-N} here because of very strong absorptions by the ligands in the region (400-40 cm^{-1}) investigated.

Metal-phosphorus Vibrations ν_{M-P}.

No absorptions are observed in the spectra of the HgX_2Py_3P complexes which are independent of the mass of the halogen and which could be assigned to metal-phosphorus vibrations, probably they are too weak.

Other Bands.

Other bands in the i.r. (400-40 cm^{-1}) spectra of Py_3P and Py_3PS complexes for which no assignments have been made are shown in Tables 36 and 37 respectively.

Structure of Tris(2-pyridyl)phosphine and Tris(2-pyridyl)phosphine Sulphide Complexes.

In a previous study[81] the structure $\left[M(Py_3P)_2 \right]^{2+} \left[MX_4 \right]^{2-}$ was proposed for the ZnX_2Py_3P complexes on the basis of bands observed at 280, 128 cm^{-1} (X = Cl), 195 and 95 cm^{-1} (X = Br), 165 and 95 cm^{-1} (X = I) which were attributed to MX_4^{2-} ions. An absorption at 280 cm^{-1} is observed

in ZnX_2Py_3P (X = Cl, Br,I, Table 36) and $HgBr_2Py_3P$ (Table 36) complexes. For $MX_4^=$ ions the following absorptions are observed :

	ν_{MX} cm^{-1}	Ref
$ZnCl_4^=$	277, 130	174 - 179
$ZnBr_4^=$	200, 91	174 - 179
$ZnI_4^=$	165, 71	174 - 179

Therefore the absorptions at 280 cm^{-1} are not due to $ZnX_4^=$ ions. The absorptions observed[81] for ZnX_2Py_3P at 128 cm^{-1} (X=Cl), 95 cm^{-1} (X=Br), 165 and 65 cm^{-1} (X=I) were not observed in the present study. The very strong band at 196 cm^{-1} for $ZnBr_2Py_3P$ is also observed as very strong bands 192 cm^{-1} (ZnI_2Py_3P), and 195 cm^{-1} ($HgBr_2Py_3P$); therefore these are also not due to $ZnX_4^=$ ions.

I.r. spectra in the regions 1600-1550 cm^{-1}, 700-600 cm^{-1} and in the region 400 cm^{-1} discussed in this work indicate that

(1) For ZnX_2Py_3P and ZnX_2Py_3PS (region 1600-1560 cm^{-1} and 700-600 cm^{-1}) the three pyridyl nitrogen atoms are co-ordinated.

(2) For HgX_2Py_3P and HgX_2Py_3PS the phosphorus and sulphur atoms are co-ordinated respectively.

(3) The pyridyl rings are equivalent in all the complexes as in the free ligands (region 1600-1550 cm^{-1}).

(4) The pyridyl rings for $HgCl_2Py_3P$ are in the same environment in both the solid state and in DMSO-d_6 solution (region 1600-1550).

(5) The Zn(II) and Hg(II) complexes are probably dimeric with bridging halogens (region 400-40 cm^{-1})

Fig 11. Structure of tris(2-pyridyl) phosphine

and tris(2-pyridyl) phosphine sulphide

Complexes.

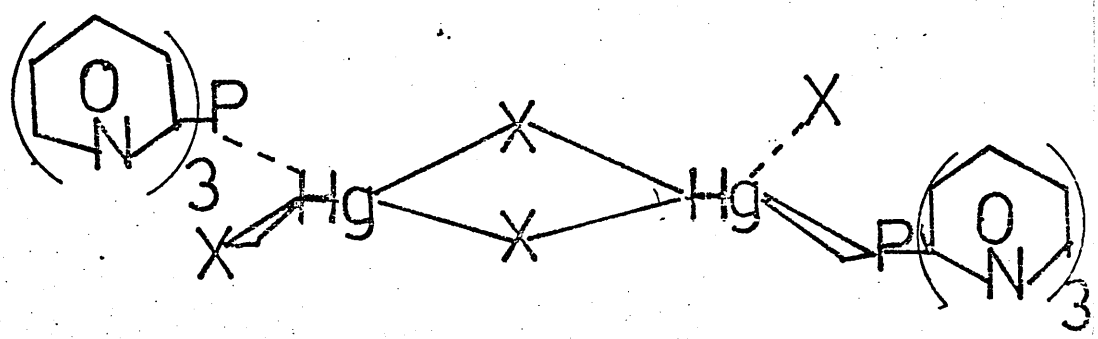

I (X= Cl, Br, I)

II

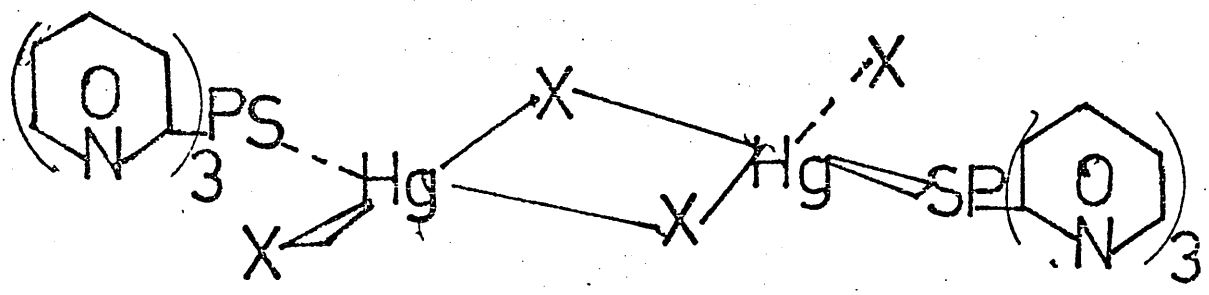

(X = Cl, Br, I)

Fig. 11a. Model of ZnX_2Py_3PS.

The aromatic pi clouds are not shown.

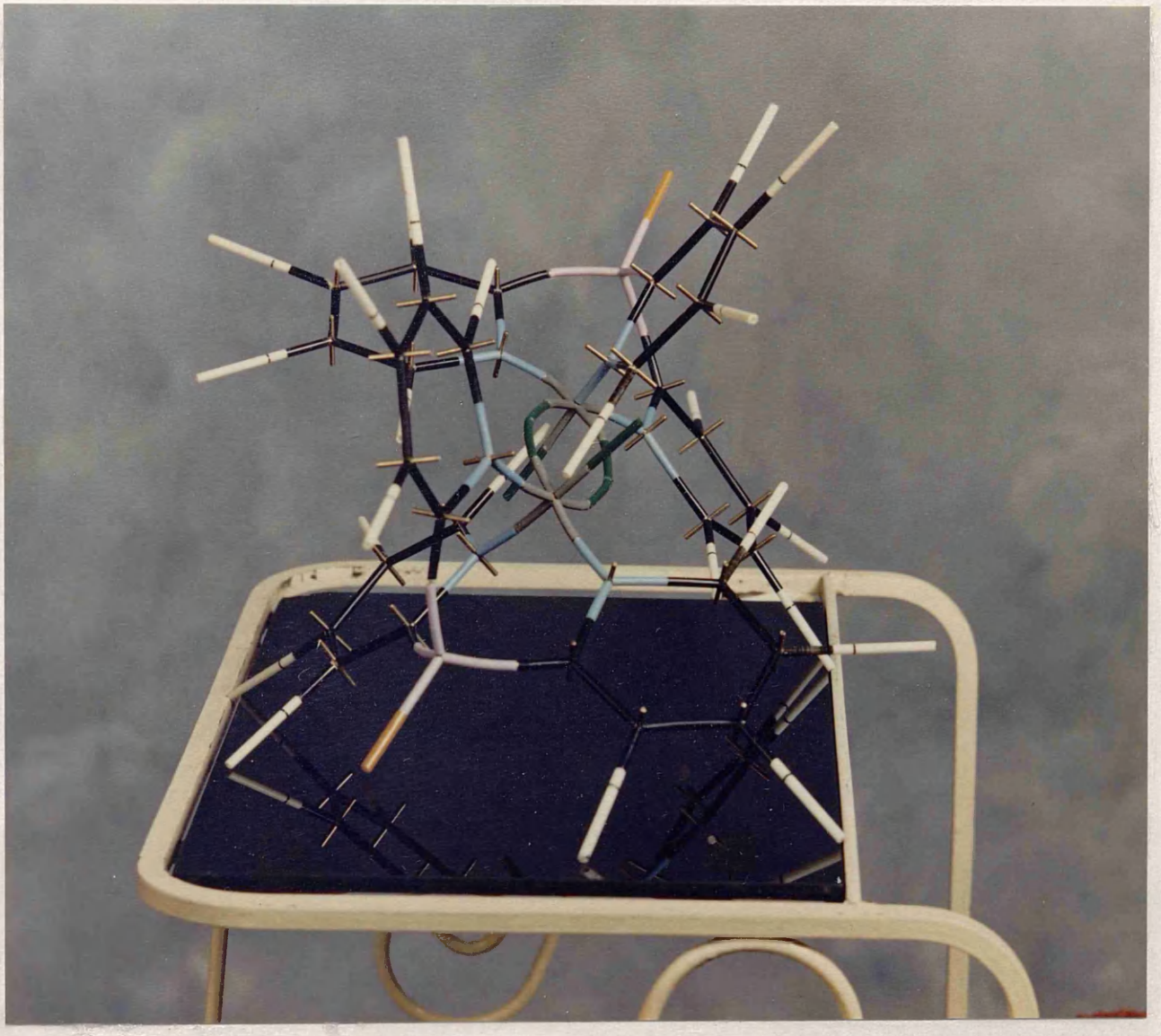

Colour	Code		
H	White	P	Violet
C	Black	S	Dark yellow
N	Blue	Zn	Gray
Cl	Dark green		

Assuming a trans-symmetrical structure for the complexes

(i) on steric grounds

(ii) by comparison with the crystal structure of $Ph_3PSeHgCl_2$[89]

the solid state structures (I, II and (III)) are proposed (Fig.11)

(I) is probably similar to Ph_3PHgCl_2 the crystal structure[24] of which was interpreted to indicate that the bridge is almost totally symmetrical.

(II) is probably similar to $Ph_3PSeHgCl_2$[89] the crystal structure[89] which was interpreted to indicate a less symmetrical arrangement of ligands about the mercury atoms.

It is not possible to infer from the Raman spectra of MX_2Py_3PS complexes whether the molecules have a centre of symmetry or not because of the possibility of existence of Raman bands too weak to be resolved.

CHAPTER FIVE

NUCLEAR MAGNETIC RESONANCE SPECTRA OF TRIS(2-PYRIDYL)PHOSPHINE COMPLEXES WITH Hg(II) AND Pt(II) HALIDES.

Table 43.

^{1}H n.m.r. parameters for tris(2-pyridyl)phosphine and derivatives. All chemical shifts are in ppm, coupling constants are in Hz.

Compound	Py_3P	Py_3PO (158)	Py_3PS	$HgCl_2$ Py_3P			
				Exp	Cal		
δ_{H_3}	7.44	8.19	8.23	7.93	7.94		
δ_{H_4}	7.78	7.78	7.73	7.98	7.98		
δ_{H_5}	7.28	7.35	7.28	7.58	7.58		
δ_{H_6}	8.74	8.75	8.65	8.71	8.71		
$^3J_{34}$	7.50	7.74	7.81	7.45	7.40		
$^4J_{35}$	1.30	1.29	1.23	1.40	1.20	1.45	1.38
$^5J_{36}$	1.00	0.99	0.97	0.90	0.85	1.00	0.81
$^3J_{45}$	7.50	7.73	7.71	7.30	7.30	7.62	7.95
$^4J_{46}$	1.80	1.72	1.76	1.80	1.70		
$^3J_{56}$	4.80	4.76	4.74	4.50	4.50	4.84	5.96
$^3J_{PH_3}$	1.73	5.56	6.36	4.50	4.60		
$^4J_{PH_4}$	2.07	4.22	4.54	4.20	3.90		
$^5J_{PH_5}$	1.18	2.40	2.95	2.85	2.80		
$^4J_{PH_6}$	-0.46	-0.43	-0.70	-0.80	-0.80		

Table 43 (a)

^{1}H Chemical shifts of Pt(II) complexes with tris(2-pyridyl)phosphine.

	δ_H (ppm)			
	δH_3	δH_4	δH_5	δH_6
$PtCl_2(Py_3P)_2$	7.75	8.07	7.31	8.75
$PtI_2(Py_3P)_2$	8.06	8.14	7.40	8.36

Table 44

^{13}C N.M.R. Parameters and Substituent effects.

	$\delta_{^{13}C}$*					Substituent effects					^{13}C-^{31}P coupling constants (Hz)				
Compound	C-2	C-3	C-4	C-5	C-6	C-2	C-3	C-4	C-5	C-6	$^{1}J_{C_2-31P}$	$^{2}J_{C_3-31P}$	$^{3}J_{C_4-31P}$	$^{4}J_{C_5-31P}$	$^{5}J_{C_6-31P}$
Pyridine	150.6	124.5	136.4	124.5	150.6										
Py_3P	161.4	128.6	136.1	123.1	150.1	-10.8	-4.1	+0.3	+1.4	+0.5	-4.7	17.0	3.4	< 0.6	12.8
Py_3PS	155.0	128.3	136.6	125.4	149.7	-4.4	-3.8	-0.2	-0.9	+0.9	115.0	24.7	9.8	3.3	19.4
$HgCl_2Py_3P$	150.1	131.1	137.2	126.2	150.9	-0.5	-6.6	-0.8	-1.7	-0.3	70.5	24.9	8.5	1.8	17.9
$HgBr_2Py_3P$	152.3	130.9	137.0	125.5	150.6	-1.7	-6.4	-0.6	-1.0	-0.3	58.6	23.9	5.8	< 0.5	16.5
HgI_2Py_3P	153.1	130.7	137.0	125.5	150.6	-2.5	-6.2	-0.6	-1.0	-0.3	53.7	23.0	7.2	< 0.5	16.3

Table 44 (Cont)

Compound	$\delta^{*}_{^{13}C}$					Substituent effects					^{13}C-^{31}P coupling constants (Hz)				
	C-2	C-3	C-4	C-5	C-6	C-2	C-3	C-4	C-5	C-6	$^{1}J_{C_2}$-^{31}P	$^{2}J_{C_3}$-^{31}P	$^{3}J_{C_4}$-^{31}P	$^{4}J_{C_5}$-^{31}P	$^{5}J_{C_6}$-^{31}P
$PtCl_2(Py_3P)_2$	-	131.3	136.1	124.7	149.9	-	-6.8	-0.3	-0.2	1.0	-	-	-	-	-
$PtI_2(Py_3P)_2$	-	131.1	137.5	126.5	149.6	-	-6.6	-1.1	-2.0	1.0	-	-	-	-	-

* The assignments were determined by selective ^{1}H decoupling experiments.

NUCLEAR MAGNETIC RESONANCE SPECTRA OF TRIS(2-PYRIDYL)PHOSPHINE COMPLEXES WITH Hg(II) and Pt(II) HALIDES.

Introduction.

Analysis[158] of the ^1H spectra of tris(2-pyridyl)phosphine derivatives of the type

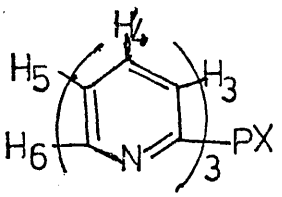

X= lone pair, O, S or Se

indicated that $^3J_{P-H_3}$, $^4J_{P-H_4}$ and $^5J_{P-H_5}$ have the same sign as those for the corresponding $^1H-^1H$ couplings in pyridine. $^3J_{^1H-^1H}$ in pyridine is absolutely positive[180]. But $^3J_{P-H_3}$, $^4J_{P-H_4}$, $^5J_{P-H_5}$ are of opposite sign to $^4J_{P-H_6}$, i.e. $^4J_{P-H_6}$ is negative. Small changes in $^1H-^1H$ coupling constants on co-ordination of phosphorus were observed an indication that the electron density in the aromatic ring changes little[181]. Therefore increases observed in ^{31}P --- H coupling constants were attributed to variations in phosphorus electron density and change in hybridization on co-ordination of phosphorus[181]. No ^{13}C spectra of tris(2-pyridyl)phosphine and derivatives have previously been determined. However, determination of the magnitudes of spin-spin coupling constants involving the aromatic ^{13}C atoms and ^{31}P in some hetero-aromatic phosphines such as tris-2-thienyl-phosphine (I) and dimethyl-2-thienylphosphine sulphide (II)

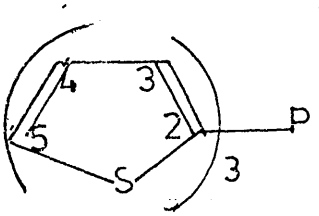

I

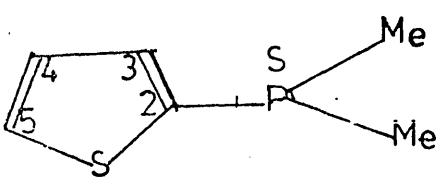

II

indicated that the one bond $^{13}C-^{31}P$ coupling constants $^{1}J_{C_2-31_P}$ in the phosphine is much smaller than in the P(IV) compound. This has been explained in terms of the changes in phosphorus hybridization.

I. Summary of Results.

$^{3}J_{PH_3}$, $^{4}J_{PH_4}$, $^{5}J_{PH_5}$ were larger in the complexes (Table 43) relative to the corresponding values in tris(2-pyridyl)phosphine consistent with phosphorus co-ordination.

31_P co-ordination chemical shifts of the complexes (ca + 38.6 to + 14.0 ppm, Table 45) are to low field indicating deshielding of the ^{31}P nuclei.

One bond $^{13}C-^{31}P$ nuclear spin coupling constants $^{1}J_{(C_2-31_P)}$ in the Hg(II) halide complexes with tris(2-pyridyl)phosphine (ca 70.5 to 53.7 Hz) increased relative to $^{1}J_{(C_2-31_P)}$ in the free ligand (-4.7 Hz) denoting a substantial change in hybridization at phosphorus on co-ordination and hence the presence of a Hg-P bond.

$^{1}J_{(195_{Pt}-31_P)}$ for dichlorobis (tris(2-pyridyl)phosphine)Pt(II) ($^{1}J_{(195_{Pt}-31_P)}$ = 3,870 Hz) is consistent with the presence of a Pt-P bond.

Results and Discussion.

The 100 MHz (343°K) ^{1}H spectrum of tris(2-pyridyl)phosphine complex with Hg(II) chloride was analysed as an ABC DX Spectrum where X = ^{31}P and D is H_6 using the n.m.r. simulation program SIMEQ II written for the Varian XL-100 FT system by Dr. C.W.F. Kort and Dr. M.J.A. de Bie (183).

The ^{1}H n.m.r. parameters are shown in Table 43. Fig. 12 shows the ^{1}H spectrum of dichloro(tris(2-pyridyl)phosphine) Hg(II).

It was not possible to obtain $^{1}H-^{1}H$ and $^{1}H-^{31}P$ nuclear spin coupling constant values for the Pt(II) complexes because of the poor resolution resulting

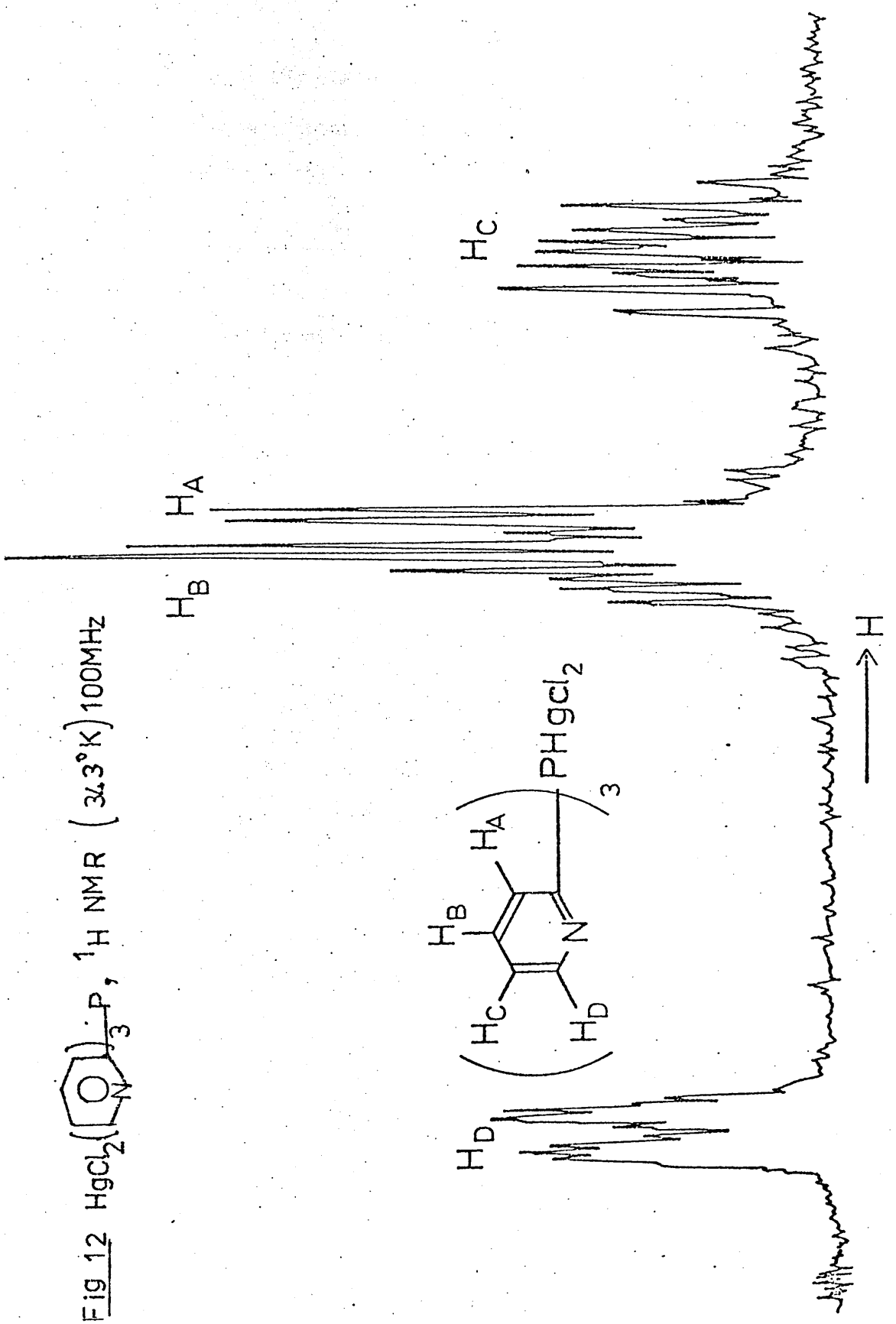

Fig 12 $HgCl_2$(O)$_3$P, ^1H NMR (343°K) 100MHz

from the low solubility of the complex in DMSO-$_{d6}$, the only solvent in which it is soluble to some extent. The ^{1}H chemical shifts for the Pt(II) complexes are shown in Table 43a.

^{1}H-^{1}H Coupling Constants

The signs of the ^{1}H-^{1}H nuclear spin coupling constants (Table 43) determined experimentally are all positive relative to positive $^{3}J_{(H----H)}$. The ^{1}H-^{1}H nuclear spin coupling constants in pyridine and protonated pyridine relevant to the discussion are shown in Table 43. The ring protons in pyridine (I) and tris(2-pyridyl)phosphine (II) are numbered conventionally as

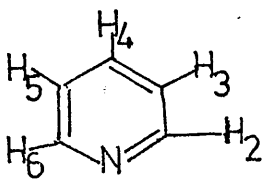

I

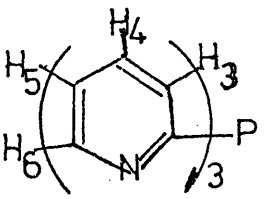

II

Merry and Goldstein[184] observed that the largest ^{1}H-^{1}H coupling constant changes occurs for J_{56} ($\Delta J_{56}=J_{56}$ protonated - J_{56} base) on protonation of the pyridyl nitrogen. Similar increases in J_{56} have been observed for other N-protonated heterocycles[185]. The conclusion has been that these changes in coupling constants are general for hetero-aromatic compounds and have been associated with the co-ordination of the nitrogen lone pair and development of positive charge on the nitrogen atom. In the Hg(II) chloride complex with tris(2-pyridyl)phosphine, J_{56} shows a small decrease rather than an increase (Table 43) suggesting that the nitrogen is not co-ordinated. It is relevant that J_{56} for tris(2-pyridyl)phosphine sulphide also shows a small decrease (Table 43)

^{1}H-^{31}P Nuclear Spin Coupling Constants.

An increase is observed in the magnitudes of $^{3}J_{PH_3}$, $^{4}J_{PH_4}$, and especially $^{5}J_{PH_5}$ in the dichloro- (tris(2-pyridyl)phosphine) Hg(II) relative to the corresponding values in the free ligand while $^{4}J_{PH_6}$ shows a small decrease (Table 43). This increase is consistent with the increase in the magnitudes of ^{1}H-^{31}P coupling constants for tris(2-pyridyl)phosphine oxide and sulphide(158 and the P(1V) derivatives of tris(2-thienyl)phosphine and tris(2-furyl)-phosphine(186)(187).

II. ^{31}P Chemicals Shifts.

The results are shown in Table 45. The value for $PtI_2(Py_3P)_2$ is obtained from double resonance experiments on the ^{1}H spectrum.

Table 45

^{31}P Chemical Shifts for some Py_3P Complexes

Compound	Width at 1/2 height Hz	$\delta_{^{31}P}$(PPM)	Co-ordination Chemical Shift Δ ppm
Py_3P	3.0	-2.8	
$HgCl_2Py_3P$	195.0	+ 35.8	+ 38.6
$HgBr_2Py_3P$	58.0	+ 28.8	+ 31.6
HgI_2Py_3P	59.0	+ 20.6	+ 23.4
$PtCl_2(Py_3P)_2$	20.0	+ 18.0	+ 20.8
$PtI_2(Py_3P)_2$		+ 11.2	+ 14.0

Some of the factors affecting ^{31}P chemical shifts and co-ordination chemical shifts have been discussed earlier (Chapter Three Page 123).

The ^{31}P spectrum in all the Hg(II) halide complexes with tris(2-pyridyl)-phosphine each showed a single broad resonance and no fine structure

probably because of broadening by the nitrogen quadrupole. Phosphorus co-ordination in tris(2-pyridyl)phosphine will decrease the s-character of the lone pair and increase the s-character in the phosphorus-pyridyl bond. This in turn will

(1) increase the magnitude of the RPR bond angles in the complexes (where R is the pyridyl ring) and hence the bond hybridization at phosphorus

(2) change the steric contribution to the ^{31}P co-ordination chemical shift depending on the size of the metal.

(3) the magnitude of the paramagnetic term.

The co-ordination chemical shift will also depend on the strength of the metal-phosphorus sigma bond (if sigma bonding alone is assumed, although no information is available about the involvement of Hg (II) and Pt (II) d orbitals in pi bonding with tris(2-pyridyl)phosphine). The downfield co-ordination chemical shift observed in these complexes, Table 45, probably arises from some combination of the factors described above.

^{31}P-^{199}Hg Coupling Constants

Neither the ^{1}H nor the ^{31}P spectrum of HgX_2Py_3P complexes showed any ^{199}Hg satellites probably because of some ligand exchange phenomena on the n.m.r. time scale and hence it has not been possible to determine the magnitude of the ^{199}Hg-^{31}P nuclear spin coupling constants.

III. ^{195}Pt-^{31}P Coupling Constants.

The ^{31}P spectrum of dichlorobis(tris(2-pyridyl)phosphine)Pt(II) consists of a broad ^{31}P resonance (width at 1/2 height=20 Hz) with two symmetrically placed ^{195}Pt satellites of separation $^{1}J_{(^{195}Pt-^{31}P)} = 3870$ Hz. This proves the presence of a Pt-P bond in the complex. This result can be compared with other ^{195}Pt-^{31}P coupling constants shown below

Complex	R	L	X	$^{1}J_{195_{Pt-}31_{P}}$ Hz	Ref
trans-$\left[PtX_2(Bu_3P)_2 \right]$			Cl	2380	188
			Br	2334	189
			I	2200	190
Cis- $\left[PtX_2(Bu_3P)_2\right]$			Cl	3508	
			Br	3479	189
			I	3379	190
Cis- $\left[PtPhCl(Et_3P)_2\right]$				4138	188
trans- $\left[Pt\left\{(RO)_2PO\right\}_2L_2\right]$	Ph	Py		3657	191
	Ph	Et_3P		3476	191
	Ph	Et_3AS		3336	191

From the $^{1}J_{(195_{Pt-}31_{P})}$ values in the above Table, no conclusion can be drawn as to whether $PtCl_2(Py_3P)_2$ is cis or trans in DMSO solution. It has not been possible to obtain a value for $^{1}J_{(195_{Pt-}31_{P})}$ in $PtI_2(Py_3P)_2$ because of the very low solubility of the complex and no ^{31}P resonance could be detected in the ^{31}P spectrum.

IV. ^{13}C Chemical Shifts.

The results are shown in Table 44. Some of the factors influencing ^{13}C chemical shifts have been discussed earlier (Chapter Three Page 130).

The ring carbons in tris(2-pyridyl)phosphine (I) and triphenylphosphine or monosubstituted benzene (II) are numbered as follows

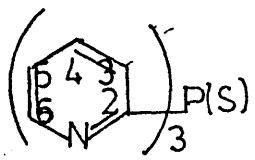

I

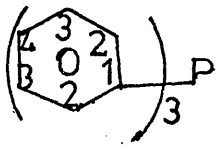

II

Each chemically distinct aromatic carbon in the tris(2-pyridyl)phosphine complex with Hg (II) chloride under conditions of complete ^{1}H decoupling gives a doublet (Fig.13). The C-5 carbon of tris(2-pyridyl)phosphine itself and that of Hg (II) bromide and iodide complexes showed single resonances, (thus showing $^{4}J_{C_5-^{31}P}$ to be small (less than 1/2 the measured linewidth).

Substituent effects at ring Carbons in 2-substituted pyridines.

The substituent effects at ring carbons relative to pyridine (Table 44) are the differences in chemical shifts (ppm) between the parent pyridine[158] and

(1) tris(2-pyridyl)phosphine

(2) tris(2-pyridyl)phosphine sulphide

(3) Hg(II) halide complexes with tris(2-pyridyl)phosphine.

In 2-substituted pyridines, the two positions C-4 and C-6 are meta to the substituents. In the present study the downfield shifts at C-4 and C-6 in both the free tris(2-pyridyl)phosphine and in all the P(IV) derivatives are very small (Table 44). The effect on carbon shieldings when the hydrogen atom in the 2-position in pyridine is replaced by a variety of substituents has been studied[192]. The most significant substituent effects have been found to be at the carbon atoms bearing the

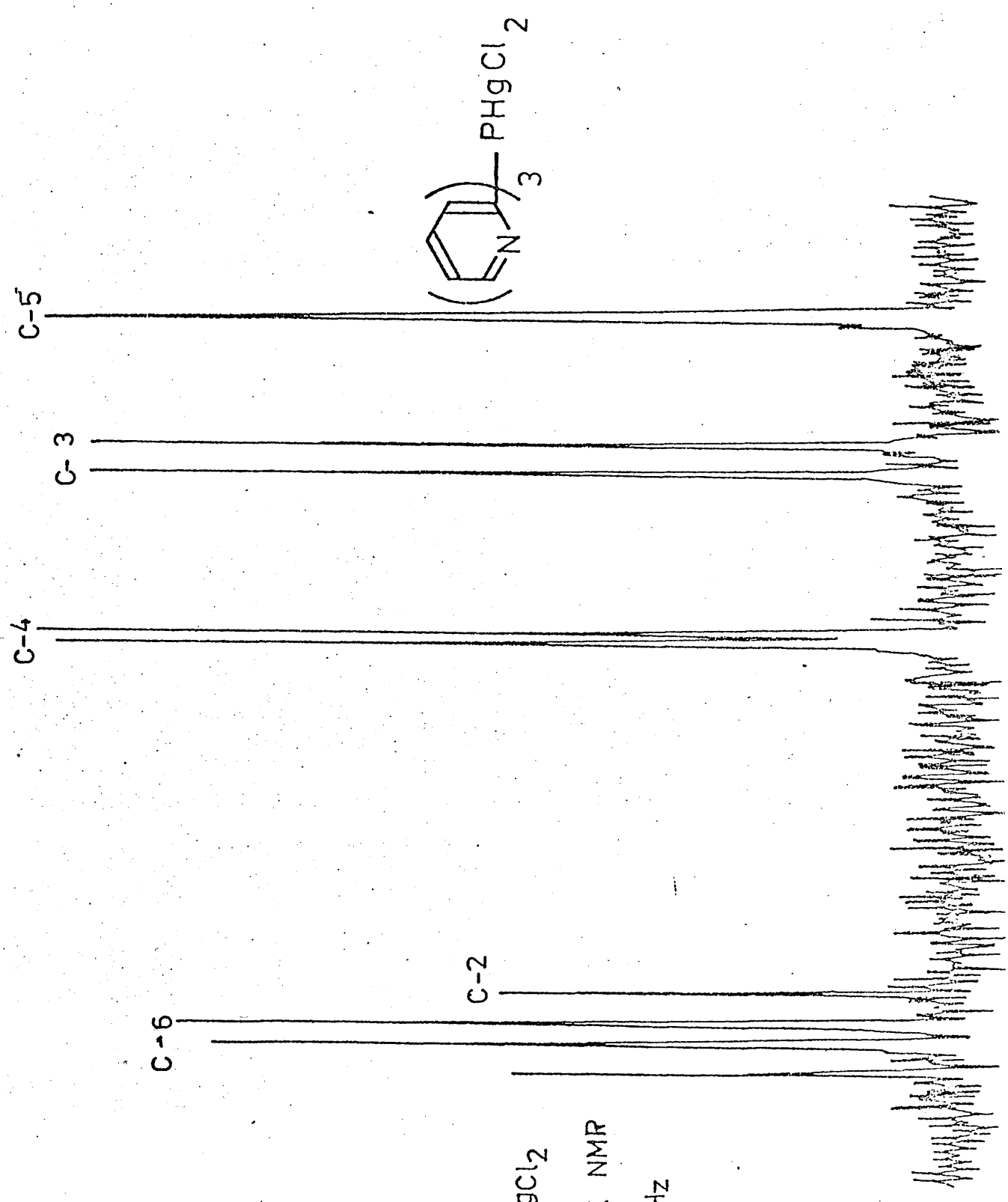

Fig 13

^{13}C 298°K NMR

25·2 MHz

Table 46

Substituent Effects on Ring Carbon Shieldings in 2-substituted Pyridines and Monosubstituted Benzenes.

As well as the Difference between the two sets of Data [192].

Substituent	Pyridine C-2	Benzene C-X	Diff	Pyridine C(H)-3	Benzene Ortho	Diff	Pyridine C(H)-4	Pyridine C(H)-6	Benzene meta	C(H)-4 Diff	C(H)-6 Diff	Pyridine	Benzene Para	Diff
F	-14.0	-35.1	21.1	14.0	14.0	-0.3	-5.4	2.3	-0.9	-4.5	3.2	2.4	4.4	-2.0
O CH_3	-14.2	-30.2	16.0	13.1	14.7	-1.6	-1.8	2.6	-0.9	-0.9	3.5	7.6	8.1	-0.5
NH_2	- 9.8	-19.2	9.4	15.0	12.4	2.6	-1.7	1.6	-1.3	-0.4	2.9	10.5	9.5	1.0
CH_O	-2.7	- 9.0	6.3	2.7	-1.2	3.9	-1.3	0.1	-1.2	-0.1	1.3	-3.8	-6.0	2.2
$COCH_3$	-3.7	- 9.3	5.6	3.0	-0.2	3.2	-1.0	2.1	-0.2	-0.8	2.3	-2.5	-4.2	1.7
Cl	-1.4	- 6.4	5.0	-0.3	-0.2	-0.1	-3.0	0	-1.0	-2.0	1.0	1.2	2.0	-0.8
CH_2CH_3	-13.3	-16.1	2.8	2.6	2.7	-0.1	0.1	0.8	-1.6	1.7	2.4	2.6	2.3	0.3

Table 46 (Cont)

Substituent	Pyridine C-2	Benzene C-X	Diff	Pyridine C(H)-3	Benzene Ortho	Diff	Pyridine C(H)-4	Pyridine C(H)-6	Benzene meta	C(H)-4 Diff	C(H)-6 Diff	Pyridine	Benzene Para	Diff
Br	7.4	5.4	2.0	-4.4	-3.3	-1.1	-3.3	-0.4	-2.2	-1.1	1.8	0.6	1.0	-0.4
CN	16.3	15.6	0.7	-4.7	-4.3	-0.4	-2.0	-1.1	-1.3	-0.7	0.2	-0.3	-4.3	1.0
CH_3	-9.3	-9.1	-0.2	1.1	-0.3	1.4	-0.8	0.8	-0.3	-0.5	1.1	2.5	2.8	-0.3

substituents, C-2 (Table 46).

Substituent effects at C-5, *para* to the 2-substituent have been found to be very small and have been explained as due to the decrease in inductive or magnetic anisotropic effects of substituents with distance from the *para*-carbons. The similarity of the trend in carbon shieldings at *para*-carbons in mono-substituted benzenes and C-5 carbons in 2-substituted pyridines has been noted (Table 46). It is useful to compare carbon shieldings in Group V triphenyls [193] (Table 47) with those observed in the present work (Table 44).

Table 47

^{13}C n.m.r. of Group V Triphenyls[193].

(^{13}C shifts relative to external TMS).

Substituent Effects relative to Benzene.

Compound	C_1 C-X	Subst. Effect	C-2 ortho	Subst. Effect	C-3 meta	Subst. Effect	C-4 *para*	Subst. Effect
C_6H_6	128.7							
$Ph_3PMo(CO)_5$	136.4	-7.7	133.7	-5.0	129.3	-0.6	130.7	-2.0
Ph_3P	138.3	-9.6	134.4	-5.7	129.2	-0.5	129.3	-0.6
Ph_3As	140.5	-11.8	134.3	-5.6	129.3	-0.6	129.0	-0.3
Ph_3Sb	139.3	-10.6	136.8	-8.1	129.4	-0.7	129.2	-0.5
Ph_3Bi	131.1	-2.4	138.1	-9.4	131.0	-2.3	128.3	+0.4

As in tris(2-pyridyl) phosphine, the greatest substituent effect in Group V triphenyls is at the carbon atoms bearing the substituents. The substituent effects relative to the free pyridine (Table 44) in tris(2-pyridyl)-phosphine, tris(2-pyridyl)phosphine sulphide and in the Hg(II) and Pt(II) halide complexes with Py_3P at C-4 and C-6 are very small giving a similar

situation to the meta substituent effects in Group V triphenyls relative to benzene (Table 47). Also for Py_3P and its complexes the next greater substituent effect is found at C-3 (ortho-carbon) (Table 44) as in the Group V triphenyls (Table 47).

As presented in Chapter Three the paramagnetic term has been shown to be dominant for most ^{13}C chemical shifts[194]. The principal factors affecting this term are the charge polarization, variation in bond order, and average excitation energy. For all the Hg(II) halide complexes the C-2 resonance moves markedly upfield (ca 8 to 10 ppm) (Table 44) compared to that of the free ligand while that of the C-5 resonance moves downfield by ca 2 to 3 ppm. An upfield shift (ca 5 ppm)is also observed for the C-2 carbon for tris(2-pyridyl)phosphine sulphide (Table 44). An upfield shift (ca 2 ppm) for the C-1 carbon is also observed in the triphenyl-phosphine complex with molybdenum penta carbonyl[193] (Table 47). Since the hybridization at C-2 in the Py_3P complexes is assumed invariant the observed upfield shift at C-2 could be attributed to several factors which include the following

(i) A higher mean electronic excitation energy, ΔE

(ii) the imbalance of electron densities in the various p orbitals centred on the carbon atom

(iii) An increase in the Carbon-phosphorus bond order resulting from increased s character in the carbon-phosphorus bond due to reduction in s-character of old lone pair.

However the relative contributionsof these factors resulting in the upfield shifts are not known.

In the case of Pt(II) complexes weak resonances were obtained because of the very low solubility in DMSO. Hence the resonance for C-2 carbons were not observed.

Increased electron density in aromatic rings due to electron releasing substituents is known to effect an upfield shift in carbons para to the substituents while electron with drawing substituents effect decreased shielding[193]. The small downfield shift of the C-5 carbons indicates that there is probably no significant pi bonding between the metal and the aromatic orbitals.

V. ^{13}C-^{31}P Coupling Constants.

The one bond ^{13}C-^{31}P coupling constant $^{1}J_{(C_2-^{31}P)}$ for Py_3P is small (< 0.6 Hz). $^{1}J_{(P-C)}$ increases from a small negative value in the free ligand to large positive values in the complexes (Table 44). This parallels a similar result in $Ph_3PMo(CO)_5$ where an increase in $^{1}J_{(^{13}C-^{31}P)}$ (36 Hz, probably positive) in the complex is observed compared to the value ($^{1}J_{^{13}C-^{31}P}$ = 21 Hz (probably negative) in the free ligand[193]. An increase in $^{1}J_{(^{13}C-^{31}P)}$ is also observed for all other long range ^{13}C-^{31}P couplings (Table 44). A similar change has been observed for $^{1}J_{(^{13}C-^{31}P)}$ in alkylphosphine derivatives[195][196][197-199]. The changes have been attributed to the co-ordination of the phosphorus lone pair [200].

In conclusion $^{1}H_5$-^{31}P and ^{13}C-^{31}P nuclear spin coupling constants, in particular $^{5}J_{H_5-^{31}P}$ and $^{1}J_{(CP)}$, indicate that for Py_3P complexes with Hg(II) halides the phosphorus atom is co-ordinated to the metal.

The $^{1}J_{(^{195}Pt-^{31}P)}$ value of 3,870 Hz obtained for $PtCl_2(Py_3P)_2$ indicates the presence of a Pt-P bond.

REFERENCES.

(1) M.C. Sneed, R.C. Brasted, "Comprehensive Inorganic Chemistry", Van Nostrand Co, New York, 1955. Vol. 4.

(2) J.J. Dulka and T.H. Risby, Anal. Chem. 1976, 48, 640A.

(3) J.R. Musgrave In "The Encyclopedia of Chemistry", (Ed. C.A. Hampel and G.G. Hawley), Van Nostrand Co. New York, 1973, page 168.

(4) C.A. Hampel "The Encyclopedia of the Chemical Elements", Reinhold Book Corp., New York, 1968, page 401.

(5) N. Irving Sax, "Dangerous Properties of Industrial Materials", Third Edition, Van Nostrand Co, New York (1968).

(6) B.J. Leonard, Nature 1971 234, 43.

(7) R.S. Nyholm, Proc. Chem. Soc. 1961, 273.

(8) F.A. Cotton and G. Wilkinson, "Advanced Inorganic Chemistry", Interscience, London, Third Edition 1972, page 503.

(9) J.W. Thompson, F.J. Wagstaffe Trans. Far. Soc., 1940, 36, 797.

(10) A.F. Wells "Structural Inorganic Chemistry" Claredon Press, Oxford. Third Edition (1962) Page 890.

(11) D.P. Graddon, K.B. Heng and E.C. Walton, Aust. J. Chem. 1966, 19, 1801.

(12) R.J.H. Clark and C.S. Williams, Inorg. Chem. 1965, 4, 350.

(13) H.P. Klug and L. Alexander, J. Am. Chem. Soc. 1944, 66, 295.

(14) J.G. White, Acta Cryst. 1963, 16, 397.

(15) N.R. Kunchur and M.R. Trunter J. Chem. Soc. 1958, 3478.

(16) V.K. Brodersen, Acta Cryst. 1955, 8, 723.

(17) R.L. Carlin, J. Roitman, M. Dankeff and J.O. Edwards, Inorg.Chem. 1962, 1, 182.

(18) F.G. Mann, H.S. Peiser and D. Purdue, J. Chem. Soc, 1940, 1209.

(19) R.C. Cass, G.E. Coates and R.G. Hayter, J. Chem. Soc. 1955, 4067.

(20) I.S. Ahuja, D.H. Brown, R.H. Nuttall and D.W.A. Sharp, J. Inorg.Nucl. Chem. 1965, 27, 1625.

(21) I.S. Ahuja, D.H. Brown, R.H. Nuttall and D.W.A. Sharp, J. Inorg.Nucl. Chem, 1965, 27, 1105.

(22) G.B. Deacon and J.H.S. Green, D.J. Harrison, Spectrochim Acta, 1968. 24A, 1921.

(23) G.B. Deacon and J.H. Green, Chem. Ind., 1965, 1031.

(24) N.A. Bell, M. Goldstein, T. Jones and I.W. Nowell, J. Chem. Soc, Chem. Comm., 1976, 1039.

(25) G.A. Calson, J.P. McReynolds and F.H. Verhoek, J. Am. Chem. Soc., 1945, 67, 1334.

(26) D. Grdenic, Quart. Rev. 1965, 19, 303.

(27) J.R. Allan, D.H. Brown, R.H. Nuttall and D.W.A. Sharp, J.Chem.Soc.A, 1966, 1031.

(28) N.S. Gill and H.J. Kingdom, Aust. J. Chem. 1966, 19, 2197.

(29) G. Morgan and F.H. Burstall, J. Chem. Soc. 1938, 1672.

(30) B.B. Emelius and A.G. Charpe, "Advances in Inorganic Chemistry and Radiochemistry", by J.R. Miller, "Recent Advances in the Stereochemistry of Nickel, Palladium and Platinum". Academic Press, New York, 1962, Vol.4.

(31) S.E. Livingstone and B. Wheelan, Aust. J. Chem, 1964, 17, 219.

(32) R.A. Shunn, Inorg. Chem. 1970, 9, 394.

(33) L. Porri, M.C. Gallazzi, and G. Vitulli. Chem. Comm. 1967, 228.

(34) P.M. Boorman and A.J. Carty, Inorg. Nucl. Chem. Letts. 1968, 4, 101.

(35) L.M. Venanzi; J. Chem.Soc. 1958, 719.

(36) G.A. Mair, H.M. Powell and D.E. Henn, Proc. Chem. Soc., 1960, 415.

(37) M.K. Deh, S.K. Amasa, U.S.T. Kumasi, Ghana, Unpublished Work.

(38) J.K. Stalik and J.A. Ibers, Inorg. Chem, 1970, 9, 453.

(39) D.S. Payne, J.A.O. Mokuolu and J.C. Speakman, J. Chem. Soc. Chem. Comm. 1965, 599.

(40) A.D.Allen, and T. Theophanides, Can.J.Chem, 1964, 42, 1551.

(41) S.Arland, J. Chatt and N.R. Davies, Quart.Rev. 1958, 12, 265.

(42) R.G. Pearson, J.Am.Chem.Soc., 1963, 85, 3533.

(43) R.S. Drago, and B.B. Wayland, J.Am.Chem.Soc.,1965, 87, 3571.

(44) Chem. Abstr. 71, 22, 766x.

(45) Chem. Abstr. 81, 171, 280t.

(46) L.V. Vilkov, L.S. Khaikin, Zh. Strukt, Khim, 1969, 10, 1101, quoted in Russ. Chem. Rev. 1971, 40, 1014.

(47) A.H.Cowley, M.J.S. Dewar, D.W. Goodman, J.R. Schweiger, J.Amer.Chem. Soc., 1973, 95, 6506.

(48) H.V. Sidgewick and H.M. Powell, Proc.Roy. Soc.,A, London, 1940, 176, 153.

(49) J.G. Verkade in "Co-ord. Chem. Rev. (Ed. A.B.P. Lever, Elsevier, Amsterdam, 1972/73, 9, 1

(50) E.D. Morris and C.E. Nordman, Inorg. Chem. 1969, 8, 1673.

(51) R. Dorschner and G. Kaufmann, Inorganica.Chim.Acta, 1975, 15, 71.

(52) J.H. Hargis, S.D. Worley and W.B. Jennings, Auburn University, Private Communication.

(53) A. Albert and E.P. Serjeant "Determination of Ionization Constants of Acids and bases", Chapman and Hall, London, (1962).

(54) J.J. Donoghue and R.S. Drago, Inorg. Chem, 1962, 1, 866.

(55) M.G.W. de Bolster, "The Co-ordination Chemistry of Aminophosphine Oxides and Related Compounds", Ph.D. Thesis (1972).

(56) D.W.J. Cruickshank, J. Chem. Soc., 1961, 5486.

(57) J. Emsley and D. Hall "The Chemistry of Phosphorus" Chap. 2. Harper and Row Ltd. London (1976). Chap. 2.

(58) A.P. Lane, D.S. Payne, J. Chem. Soc., 1963, 4004.

(59) G. Ewart, D.S. Payne, A.L. Porte and A.P. Lane, J.Chem.Soc., 1962, 3984.

(60) D.W.J. Cruickshank, Acta. Cryst. 1964, 17, 671.

(61) D.F. Clemens and H.H. Sisler, Inorg.Chem. 1965, 4, 1222.

(62) A.H. Britain, J.E. Smith, P.L. Lee, K. Cohn and R.H. Schwendeman. J.Am.Chem.Soc., 1971, 93, 6772.

(63) R.L. Kuczkowski, H,W. Schiller and R.W. Rudolph, Inorg.Chem, 1971, 10, 2205.

(64) B.B. Beagley, A.G. Robiette and G.M. Sheldrick, J.Chem.Soc.,A, 1968, 3002, 3061.

(65) K. Hedberg, J. Am. Chem. Soc., 1955, 77, 6491.

(66) J.M. Jenkins and J.G. Verkade, Inorg.Chem, 1967, 12, 2250.

(67) R.L. Keiter and J.G. Verkade, Inorg. Chem, 1969, 8, 2115.

(68) R.B. King, Inorg. Chem, 1963, 2, 936.

(69) R.B. King and T.F. Korenowski, J. Organometal. Chem. 1969, 17, 95.

(70) R.D. Bertrand, F.B. Ogilvie and J.G. Verkade. J.Am.Chem.Soc., 1970, 92, 1908.

(71) M.D. La Prade and C.E. Nordman, Inorg.Chem. 1969, 8, 1669.

(72) D.F. Clemens, H.H. Sisler and W.S. Brey Jnr., Inorg.Chem. 1966, 5, 527.

(73) J.P. Laurent, J. Gerard, C. Gerard, J. Inorg.Nucl.Chem., 1969, 31, 1353.

(74) J. Gerard, J.P. Laurent, C. Gerard, Bull.Soc. Chim. France, 1970, 3, 838.

(75) R.R. Holmes and R.P. Wagner, J.Am. Chem. Soc., 1962, 84, 357.

(76) H. Nörth and H.J. Vetter, Ber. 1963, 96, 1298.

(77) C.W. Schultz and R.W. Parry, Inorg.Chem., 1976, 15, 3046.

(78) H.North and H.J. Vetter, Chem. Ber., 1963, 96, 1479.

(79) F.B. Ogilvie, J.M. Jenkins and J.G. Verkade, J.Am.Chem.Soc., 1970, 92, 1916.

(80) L.W. Houk, R. Dobson, J. Chem. Soc., A., 1968, 1846.

(81) H.W. Cruickshank, Ph.D. Thesis, Paisley College of Technology, 1973.

(82)
(a) R.K. Boggess and D.A. Zatko, Inorg.Chem. 1976, 15, 626

(b) R.K. Boggess and D.A. Zatko, Inorg. Nucl. Chem. Letts., 1976,12,7.

(83) W.F. Dahlhoff, T.R. Dick, G.H. Ford and S.M. Nelson.
J. Inorg. Nucl. Chem, 1971, 33, 1799.

(84) W.R. McWhinnie and G.C. Kulasingam and J.C. Draper, J. Chem. Soc. A., 1966, 1199.

(85) J.C. Lancaster and W.R. McWhinnie, J. Chem. Soc. (A)., 1967, 1253.

(86) W.R. McWhinnie, R.C. Poller and M. Therverasa, J. Chem. Soc. A., 1967, 167

(87) G.C. Kulasingam and W.R. McWhinnie, J. Chem. Soc., A., 1967, 1253.

(88) G. Dyer and D.W. Meek, J. Am. Chem. Soc., 1967, 89, 3983.

(89) L.S. Glasser, L. Ingram, M.G. King, and G.P. McQuillan,
J. Chem. Soc., A., 1969, 2501.

(90) D. Chapman, D. Chaoman and P.D. Magnus,
"Introduction to Practical High Resolution N.M.R. Spectroscopy",
Academic Press, London (1962).

(91) V.J. Kowalesky, Prog. N.M.R. Spectroscopy, (Ed. J. Feeney, L.H. Sutcliffe, J.W. Emsley), Pergamon Press, London (1969). Vol.5, Chap.1.

(92) R.F.M. White, Chem. Brit. 1968, 4, 20.

(93) W. McFarlane, Ann. Rev. N.M.R. Spectrosc. Academic Press, London (1968) Vol. 1 page 135.

(94) R.J. Abraham, "The Analysis of High Resolution N.M.R. Spectra", Elsevier, Amsterdam (1971), page 9.

(95) T. Axenrod and A. Webb, "Nuclear Magnetic Resonance Spectroscopy of Nuclei other than Protons", John Wiley, New York (1974).

(96) L.F. Johnson, Anal. Chem. 1972, 5A, 557.

(97) G.E. Hall, Ann.Rev. N.M.R. Spectrosc. 1968, 1, 227.

(98) R.S. Tobias, J.Chem.Educ., 1967, 44, 2, 1967, 44, 70.

(99) R.S.Drago, "Physical Methods in Inorganic Chemistry", Rheinhold, New York, 1965.

(100) A.J. Gordon, R.A. Ford, "The Chemists Companion", John Wiley, New York (1972).

(101) L. Friedman and W.P. Wetter, J.Chem. Soc. A, 1967, 36.

(102) R.N. Keller and H.D. Wycoff, Inorg.Syn. 1946, 2,1.

(103) G.W. Watt and W.A. Cude, Inorg.Chem.,1968, 7, 335.

(104) A.B. Burg and P.J. Slota, J.Am.Chem.Soc.,1958, 80, 1107.

(105) R.A. Chittenden and L.C. Thomas, Spectrochim,Acta., 1966, 22, 1449.

(106) D.S. Payne and A.P.Walker, J.Chem.Soc.(C), 1966, 498.

(107) L. Larsson, Acta. Chem. Scand, 1952, 6, 1470.

(108) R. Burganda, Ann-Chim. 1963, 347

(109) R. Mathis, La Faille, R. Burganda, Spectrochim. Acta, 1974, 30A, 357.

(110) J.L. Vidal and G.E. Ryschkewitsch, J. Inorg. Nucl. Chem. 1976, 38, 1933.

(111) J.L. Vidal and G.E. Ryschkewitsch, J. Inorg. Nucl. Chem. 1976, 38, 1937.

(112) J.T. Donoghue and R.S. Drago, Inorg.Chem. 1963, 2, 1158.

(113) W. McFarlane and D.S. Rycroft, J. Chem. Soc. Far. Trans., II, 1974, 70, 37.

(114) R.D. Hill and G.D. Meakis, J. Chem.Soc., 1958, 760.

(115) J.T. Braunholtz, E.A.V. Ebsworth, F.G. Mann and N. Sheppard, J.Chem. Soc., 1958, 2780.

(116) S. Fleming, R.W. Parry, Inorg. Chem., 1972, 1, 11.

(117) J.G. Wright, Chemistry Dept., University of Glasgow, Private Communication.

(118) A.R. Davies, C.J. Murphy and R.A. Plane, Inorg.Chem., 1970, 9, 423.

(119) J.R.Barcelo and J. Bellanato, Spectrochim Acta, 1956, 8, 27.

(120) W.G. De Bolster and W.L. Groeneveld, Rec. Trav. Chim., 1971, 90, 477.

(121) L.J. Bellamy, "Advances in Infrared Group Frequencies", Chapman and Hall, London (1975).

(122) N.B. Colthup, L.H. Daly and S.E. Wiberley, "Introduction to Infrared and Raman Spectroscopy", Academic Press, New York, (1975).

(123) J.E. Mayhood, R.B. Harvey, Can. J. Chem., 1955, 33, 1552.

(124) A.B. Burg and A.J. Sarkis, J. Am. Chem. Soc., 1965, 87, 238.

(125) M.A. Fleming, R.J. Wyma, R.C. Taylor, Spectrochim. Acta. 1965, 27, 1189.

(126) L.W. Daasch and D.C. Smith, Anal. Chem, 1951, 23, 853.

(127) D.E.C. Corbridge, "The Infrared Spectra of Organophosphorus Compounds". In Topics in Phosphorus Chemistry, ... (Eds. M. Grayson and M. Griffith), John Wiley, London (1969). Vol. 6.

(128) J.R. Ferraro, "Low-frequency Vibrations of Inorganic and Co-ordination Compounds", Plenum Press, New York, (1971).

(129) R.J.H. Clark, Spectrochim Acta, 1965, 21, 1955.

(130) G.E. Coates and C. Parkin, J. Chem. Soc., 1963, 421.

(131) R.J.H. Clark and C.S. Williams, J. Chem. Soc. (A), 1966, 1425.

(132) D.M. Adams, "Metal-Ligand and Related Vibrations", Arnold, London (1967).

(133) L. Sacconi, A. Sabatini and P. Gans, Inorg. Chem., 1964, 3, 1772.

(134) J. Hiraishi, I. Nakagawa and T. Shimanouchi, Spectrochim. Acta., 1968, 24A, 819.

(135) A.F. Cameron, K.P. Forest and G. Ferguson, J. Chem. Soc., A, 1971, 1286.

(136) J.W. Emsley, J. Feeney and L.H. Sutcliffe, "High Resolution Nuclear Magnetic Resonance Spectroscopy, Pergamon Press, London (1966). Vol. 2 page 115.

(137) S.O. Grim, Pui Jun Lui and R.L. Keiter, Inorg. Chem. 1974, 13, 342.

(138) W. McFarlane and D.S. Rycroft, J. Magn. Res. 1976, 24, 95.

(139) D.A. Redfield, J.H. Nelson, L.W. Carry, Inorg-Nucl. Chem. Letts 1074, 10, 727.

(140) S. Saika and C.D. Slichter, J. Chem. Phys., 1966, 45, 2916.

(141) J.H. Letcher and J.R. Van Wazer, J. Chem. Phys., 1966, 45, 2916.

(142) L.S. Meriwether and J.R. Leto, J. Am. Chem. Soc., 1961, 83, 3192.

(143) B.E. Mann, C. Masters, B.L. Shaw, R.M. Slade and R.E. Stainbank, Inorg. Nucl. Chem. Letts., 1971, 7, 881.

(144) A.W. Verstuyft and J.H. Nelson, Inorg. Nucl. Chem. Letts, 1976, 12, 53

(145) B.E. Mann, J. Chem. Soc., Perkin II, 1972, 30.

(146) W. McFarlane, D.S. Rycroft, J. Chem. Soc., Dalton, 1974, 249.

(147) G.C. Levy, "Topics in Carbon-13 N.M.R. Spectroscopy, John Wiley & Sons, New York (1976), Vol. 2.

(148) F.W. Wehrli and T.W. Wirthlin, "Interpretation of ^{13}C N.M.R. Spectra", Heyden (1976).

(149) R. Keat, Chem. Dept. Glasgow University, Private Communication.

(150) J.A. Pople and D.P. Santry, Mol. Physics, 1964, 8, 1.

(151) H.A. Bent, J. Inorg. Nucl. Chem., 1961, 19, 43.

(152) F.K. Butcher, B.E. Deuters, W. Gerrard, E.F. Mooney, R.A. Rothenbury and H.A. Willis, Spectrochim. Acta., 1964, 20, 759.

(153) J. Bennet, A. Pidcock, C.R. Waterhouse, P. Coggan, A.T. McPhail and P.M. Gross, J. Chem. Soc. (A), 1970, 2094.

(154) J.B. Wibaut, A.P. De Jonge, H.G.P. Van Der Voort, P.Ph.H.L. Otto, Rec. Trav. Chim., 1951, 70, 1054.

(155) Chem. Abs. 52, 201, 56C.

(156) F.A. Cotton, R. Barnes and E. Bannister, J. Chem. Soc., 1960, 2199.

(157) F.G. Mann and J. Watson, J. Org. Chem., 1948, 13, 502.

(158) H.J. Jakobsen, J. Mol. Spectrosc., 1970, 34, 245.

(159) M. de Mota, J. Rodgers and S.M. Nelson, J. Chem. Soc., (A), 1969, 2036.

(160) W.V. Dalhoff, T.R. Dick, G.H. Ford, W.S.J. Kelly and S.M. Nelson, J. Chem. Soc., (A), 1971, 3495.

(161) D.A. Baldwin, A.B.P. Lever and R.V. Parish, Inorg. Chem., 1969, 8, 107.

(162) M.G. King and G.D. McQuillan, J. Chem. Soc., (A), 1967, 898.

(163) P. Gans, Vibrating Molecules: An Introduction to the Interpretation of Infrared and Raman Spectra, Chapman and Hall, London, (1971), page 190.

(164) J.A.W. Dalziel, A.F. Le C. Holding and B.E. Watts, J. Chem. Soc., A., 1967, 359.

(165) R.A. Walton, J. Chem., Soc., (A)., 1969, 61.

(166) J.H.S. Green, W. Kynaston and H.M. Paisley, Spectrochim Acta., 1963, 19, 549.

(167) G.B. Deacon, R.A. Jones and P.E. Rogasch, Aust. J. Chem., 1963, 16, 360.

(168) G.B. Deacon, R.A. Jones, Aust. J. Chem., 1963, 16, 499.

(169) D.H. Brown, A. Mohammed, D.W.A. Sharp, Spectrochim. Acta., 1965, 21, 659.

(170) W.R. Cullen, G.B. Deacon and J.H.S. Green, Can. J. Chem., 1969, 44, 717.

(171) L.A. Harrah, M.T. Ryan and C. Tamorski, Spectrochim. Acta., 1962, 18, 21.

(172) G.B. Deacon and J.H.S. Green, Spectrochim. Acta, 1968, 24A, 845.

(173) C. Postmus, J.R. Ferraro and W. Wozniak, Inorg. Chem., 1967, 6, 2030.

(174) G.B. Deacon, J.H.S. Green and F.B. Taylor, Aust. J. Chem., 1967, 20, 2069.

(175) R.J.H. Clark and T. Dunn, J. Chem. Soc., 1963, 1198.

(176) D.M. Adams, J. Chatt, J.M. Davidson and J. Garret, J. Chem. Soc., 1963, 2198.

(177) J.A. Rolfe, D.E. Sheppard and L.A. Woodward, Trans. Far., Soc., 1954, 50, 1275.

(178) D.A. Long and J.Y.H. Chau, Trans. Far. Soc., 1962, 58, 2325.

(179) G.B. Deacon, J.H.S. Green and W. Kynaston, Aust. J. Chem., 1966, 19, 1603.

(180) A. Saupe, Z. Naturforsch., 1965, 20a, 572.

(181) W. McFarlane, Org. Magn. Res., 1969, 1, 3.

(182) H.J. Jakobsen and O. Manscher, Acta. Chem., Scan., 1971, 25, 680.

(183) C.W.F. Kort and M.J.A. de Bie, Unpublished Work.

(184) J.B. Merry and J.H. Goldstein, J. Am. Chem. Soc., 1966, 88, 5560.

(185) M.H. Palmer and B. Semple, Chem. Ind. (London), 1965, 1766.

(186) H.J. Jakobsen and J.A. Nielsen, J. Mol. Spectrosc., 1969, 31, 230.

(187) H.J. Jakobsen and J.A. Nielsen, J. Mol. Spectrosc., 1970, 33, 474.

(188) J.F. Nixon and A. Pidcock, In Ann. Rev. NMR Spectrosc., (Ed. E.F. Mooney), Academic Press, London (1969, Vol.2, page 345.

(189) A. Pidcock, R.E. Richards and L.M. Venanzi, J. Chem., Soc., A., 1966 1707.

(190) L.M. Venanzi, Chem. Brit., 1968, 4, 162.

(191) F.H. Allen, A. Pidcock, C.R. Waterhouse, J. Chem. Soc., A., 1970, 12, 2087.

(192) H.L. Retcofsky, R.A. Friedel, J. Phys. Chem., 1968, 72, 2619.

(193) O.A. Gansow and B.Y. Kimura, Chem. Commun., 1970, 1621.

(194) M. Karplus and J.A. Pople, J. Chem. Phys., 1963, 38, 2803.

(195) C.J. Jameson, J. Am. Chem. Soc., 1969, 91, 6232

(196) W. McFarlane, Chem. Commun. 1967, 58.

(197) W. McFarlane, Proc. Roy. Soc., (London) A, 1968, 306, 165.

(198) G. Mavel and M. Green, J. Chem. Soc., Chem. Commun., 1968, 742.

(199) F.J. Weigert and J.D. Roberts, J. Am. Chem. Soc., 1969, 91, 4940.

(200) G. Mavel, In J.W. Emsley, J. Feeney and L.H. Sutcliffe, Progress in N.M.R. Spectroscopy, Pergamon, Oxford (1966), Vol. 1 page 261.